Hunger Games: on the Role of Endocannabinoids in Food Reward and Emotional Regulation in Mice

Dissertation der Fakultät für Biologie
der Ludwig-Maximilians-Universität München

Daniel E. Heinz

München 2021

Hunger Games: on the Role of Endocannabinoids in Food Reward and Emotional Regulation in Mice

Dissertation der Fakultät für Biologie
der Ludwig-Maximilians-Universität München

Daniel E. Heinz

Eingereicht am 30. August 2021
Tag der mündlichen Prüfung: 04. Mai 2022

Diese Dissertation wurde am Max-Planck-Institut für Psychiatrie unter Leitung meines Doktorvaters, PD Dr. rer. nat. Carsten T. Wotjak, angefertigt.

Erstgutachter: PD Dr. rer. nat. Carsten T. Wotjak

Zweitgutachter: Prof. Dr. Laura Busse

#PassionForScience

Eidesstattliche Erklärung

Ich versichere hiermit an Eides statt, dass die vorgelegte Dissertation von mir selbständig und ohne unerlaubte Hilfe angefertigt ist.

München, den 14. Juli 2022 Daniel Heinz

(Unterschrift)

Erklärung

Hiermit erkläre ich, *

☒ dass die Dissertation nicht ganz oder in wesentlichen Teilen einer anderen Prüfungskommission vorgelegt worden ist.

☒ dass ich mich anderweitig einer Doktorprüfung ohne Erfolg **nicht** unterzogen habe.

☐ dass ich mich mit Erfolg der Doktorprüfung im Hauptfach .....

und in den Nebenfächern .....

bei der Fakultät für ..... der .....

(Hochschule/Universität)

unterzogen habe.

☐ dass ich ohne Erfolg versucht habe, eine Dissertation einzureichen oder mich der Doktorprüfung zu unterziehen.

München, den 14. Juli 2022 Daniel Heinz

(Unterschrift)

*) Nichtzutreffendes streichen

CONTENTS

ABBREVIATIONS

2-AG	2-Arachidonyl Glycerol
5-CSRTT	5-Choice Serial Reaction Time Task
AA	Arachidonic Acid
AAV	Adeno Associated Virus
ABHD	Alpha/Beta-Hydrolase Domain
ABPP	Activity Based Protein Profiling
ACSF	Artificial Cerebrospinal Fluid
AEA	Arachidonylethanolamide, Anandamide
AgRP	Agouti Related Protein (or Peptide)
ANOVA	Analysis Of Variance
AP	Anterior-Posterior
Arc	Arcuate Nucleus
b.c.	Before Christ
base	Baseline
BCA	Bicinchoninic acid Assay
BLA	Basolateral Amygdala
BMBF	German Ministry of Research and Education/ Bundesministerium für Bildung und Forschung
BMT	Beetle Mania Task
BP	Breaking Point
cAMP	Cyclic Adenosine Monophosphate
CB1/2	Cannabinoid Receptor Type 1 (or 2)
CBN	Cannabinoid Null Mutant, $CB1^{-/-}$
CCK	Cholecystokinin
CES	Carboxylesterase
CNO	Clozapine N-Oxide
CPu	Caudate Putamen
Cre	Cre-Recombinase

Ctx	Cortex
DAG	Diacylglycerol
DAGL	Diacylglycerol Lipase
DaLi	Dark Light Box
Dex	Dexamethason
DMEM	Dulbecco's Modified Essential Medium
DMSO	Dimethylsulfoxide
DNA	Desoxyribonucleic Acid
DREADD	Designer Receptor Exclusively Activated by Designer Drugs
DSI/E	Depolarization-induced Suppression of Inhibition/ Excitation
DTT	Dithiothreitol
DV	Dorsal-Ventral
e.g.,	Exempli Gratia
eCBS	Endocannabinoid System, or Endocannabinoids
EDTA	Ethylenediaminetetraacetic Acid
EPM	Elevated Plus Maze
ERK	Extracellular-signal Regulated Kinases
EtOH	Ethanol
FAAH	Fatty Acid Amide Hydrolase
FDA	Food and Drug Administration
FDR	False Discovery Rate
FELASA	Federation for Laboratory Animal Science Associations
Fig.	Figure
FR-	Food Restriction (no)/ ad libitum diet
FR+	Food Restriction (yes)
G.	Ghrelin
GPCR	G-Protein Coupled Receptor

GR	Glucocorticoid Receptor
GV-SOLAS	Society of Laboratory Animal Sciences
HEK293	Human Embryonic Kidney 293 cells
HEPES	4-(2-hydroxyethyl)-1-piperazineethanesulfonic acid
hiFCS	Heat Inactivated Fetal Calf Serum
Hip	Hippocampus
HYP/Hy	Hypothalamus
IMDM	Isove's Modified Dulbecco's Medium
ISH	*In Situ* Hybridization
ITT	Inter Trial Interval
IVC	Individually Ventilated Cage(s)
ko	Knockout
LFQ	Label Free Quantification
LH	Limited Hold
LS	Lateral Septum
LS MS/MS	Liquid Spectrometry / Mass Spectrometry
MAGL	Monoacylglycerol Lipase
MAPK	Mitogen-Activated Protein Kinase
ML	Mediolateral
NaCl	Sodiumchloride
NAPE	N-Acylphosphatidylethalonamide
NTS	Nucleus Tractus Solitarii
OFT	Open Field Test
PBS	Phosphate Buffered Saline
PCA	Principal Component Analysis
PI	Protease Inhibitor
PKA	Protein Kinase A
PLC	Phospholipase C
POMC	Pro-Opiomelanocortin

PR/ PR4	Progressive Ratio (4)
PTSD	Posttraumatic Stress Disorder
PVC	Polyvinyl Chloride
RDoC	Research Domain Criteria
RIA	Radio-Immune Assay
Rim	Rimonabant/ SR141716A / SR
RIPA	Radioimmunoprecipitation Assay buffer
RNA	Ribonucleic Acid
RT	Room Temperature
SC	Superior Colliculus
SD	Stimulus Duration
SEM/s.e.m.	Standard Error of Mean
SEP	Super Ecliptic green fluorescent Protein
sEPSC	Spontaneous Excitatory Postsynaptic Currents
SF1	Steroidogenic Factor 1
SNr	Substania Nigra (pars reticularis)
SR	SR141716A/ Rimonabant / Rim
SSC	Standard Saline Citrate
Tes.	Testosterone
THC	Δ9-Tetrahydrocannabinol
TRPV1	Transient Receptor Potential cation channel V1
US	United States (of America)
VH	Ventral Hippocampus
Vhc	Vehicle
vmH	Ventromedial Hypothalamus
WHO	World Health Organization
wt	Wildtype

ABSTRACT

Since millennia, cannabis has been used for recreational and medical purposes, such as relief of chronic pain, emotional relaxation and regulation of appetite. A central role within the signaling cascade comes to the G-protein coupled cannabinoid receptor 1 (CB1) and its two endogenous ligands 2-arachidonoylglycerol (2-AG) and anandamide (AEA).

The present work explored the involvement of CB1 signaling in regulation of the positive valence system in food restricted mice by using the progressive ratio (PR) touchscreen task to assess the motivation to work for food. I could demonstrate that not only exogenous Δ^9-tetrahydrocannabinol (THC), but also elevation of 2-AG levels by pharmacological blockage of its main degrading enzyme, monoacylglycerol lipase (MAGL), enhanced the willingness to work for food. Pharmacological enhancement of AEA, in contrast, had no effects. I further substantiated the selective involvement of 2-AG by verifying the specificity of the pharmacological interventions, using enzymatic activity measurements. In combination with subsequent pharmacological interventions, I could rule out that other potential degrading enzymes of 2-AG (CES1, ABDH6) play a similar role as MAGL. Moreover, blockade of the rate-limiting enzyme of 2-AG synthesis, DAGLα, completely abolished the increase in motivation to work for food triggered by MAGL inhibition.

In the next set of experiments, I dissected the brain circuits and neuronal populations responsible for the effects of 2-AG on food intake. Using conditional CB1-deficient mice, I could rule out a contribution of CB1 expressed on GABAergic neurons of the forebrain (Dlx-CB1-KO) or cortical glutamatergic neurons (Nex-CB1-KO). In contrast, the stimulating effects of 2-AG were completely abolished in mice with deletion of CB1 from cortical and subcortical projection neurons (CaMK-CB1-KO). Given my finding of increased 2-AG levels within the hypothalamus following inhibition of MAGL, that were even further enhanced in food restricted as compared to ad libitum fed mice, I focused my further investigations on that brain structure. Indeed, restriction

of CB1 deletion to the hypothalamus by local injection of AAV-CaMK-Cre into CB1f/f mice fully resembled the phenotype of the CaMK-CB1-KO. Also, mimicking the effects of 2-AG action via CB1 by using chemogenetic interventions limited to the hypothalamus caused the animals to work more for food. The deletion of CB1 from selected subpopulations of the hypothalamus had either only a marginal (SF1-CB1-KO) or no effect at all (POMC-CB1-KO). In contrast, restriction of CB1 deletion to the arcuate nucleus completely abolished 2-AG action, thus demonstrating the crucial involvement of that brain structure.

Pharmacological enhancement of 2-AG signaling affected the willingness to work for food in food restricted animals only. This suggested that the altered physiological state has direct impact on 2-AG synthesis. Since food restriction led to increased plasma levels of corticosterone, I blocked the glucocorticoid receptor shortly before testing and, thereby, abolished the effects of enhanced 2-AG signaling. Thus, corticosterone seemed to stimulate the 2-AG system in a non-genomic manner.

Interestingly, pharmacological blockade of CB1 receptors failed to affect the willingness of food restricted animals to work for food, but blocked the effects of pharmacologically enhanced 2-AG signaling. This implies that the levels of 2-AG are efficiently constraint by the degrading enzyme MAGL. To explore whether corticosterone is engaged not only in the activation but also the termination of 2-AG signaling, I treated brain slices with the synthetic glucocorticoid dexamethasone and provided first evidence for alterations in compartmentalization and dimerization of the enzyme, which likely affect its efficacy. This finding suggests that corticosterone exerts yin-yang effects on 2-AG signaling by activating both the endocannabinoid system (2-AG) and its main degrading enzyme MAGL.

The question remained as to the reasons for the tight control of 2-AG signaling. To shine light on this topic, I performed two closely related satellite projects, which studied (i) the consequences of food restriction with or without

pharmacological blockage of MAGL on the negative valence system. In addition (ii) I disentangled the neuronal signature of CB1-controlled fear responses to a threatening stimulus. In the first satellite study, I observed an interaction between feeding state and MAGL inhibition with decreased exploratory behavior (in particular vertical exploration) in food restricted mice. This indicates that enzymatic constraints of 2-AG signaling in food restricted animals ensures undisturbed exploration which is needed to forage for food. Thus, MAGL seems to act as an interface between the positive and the negative valence system.

In the second satellite study, dissection of the neuronal basis of CB1-controlled threat responding revealed increased active fear in Dlx-CB1-KO, whereas CaMK-CB1-KO showed the opposite phenotype (i.e., decreased active fear), with no alterations in total-CB1-KO and Nex-CB1-KO. By means of local recombination of CB1 expression I could restrict the decrease in active fear to CB1 deletion from the hypothalamus, specifically SF1-positive neurons. Thus, CB1 signaling affects both positive and negative valence systems by involving different hypothalamic neuronal populations.

Taken together, I discovered a so far unrecognized homeostatic principle of simultaneous activation and dampening of 2-AG signaling by corticosterone that tightly controls the motivation of food restricted mice to work for food. I could localize its neuronal basis within the arcuate nucleus of the hypothalamus and demonstrate that – despite evidence for mutual interactions – the control of the positive and the negative valence systems involves independent hypothalamic neuronal populations.

ZUSAMMENFASSUNG

Seit geraumer Zeit wird Cannabis für berauschende und medizinische Zwecke verwendet. Hierzu zählen die Linderung von chronischen Schmerzen, emotionale Entspannung und die Regulation von Appetit. Der G-Protein gekoppelte Cannabinoid Rezeptor Typ 1 (CB1) mit seinen endogenen Liganden 2-arachidonylglycerol (2-AG) und Anandamid (AEA) stehen dabei im Mittelpunkt der Signalkaskaden.

Meine Arbeit beschäftigt sich mit der Beteiligung von CB1 vermittelten Signalen in der Regulation des positiven Valenzsystems in futterreduzierten Mäusen. Über die Progressive Ratio (PR) Touchscreen Aufgabe wurde die Motivation zum Arbeiten für Futter bestimmt. Ich konnte zeigen, dass nicht nur exogenes Δ^9-Tetrahydrocannabinol (THC), sondern auch erhöhte Level von 2-AG, vermittelt durch die Blockade des haupt-abbauenden Enzyms, Monoacylglycerol Lipase (MAGL), in einer erhöhten Bereitschaft zum Arbeiten für Futter resultieren. Dagegen blieb die pharmakologische Erhöhung von AEA ohne Effekt. Um die selektive Beteiligung von 2-AG nachzuweisen, untersuchte ich die Spezifität der pharmakologischen Interventionen durch Messung von Enzymaktivitäten. Kombiniert mit sich daran anschließenden pharmakologischen Interventionen, konnte ich die Beteiligung anderer abbauender Enzyme von 2-AG (CES1, ABHD6) ausschließen. Des Weiteren verhindert die Blockade des geschwindigkeitsbestimmenden Enzyms in der Synthese von 2-AG, DAGLα, die durch die Blockade von MAGL induzierte Zunahme der Bereitschaft, für Futter zu arbeiten.

Der darauffolgenden Experimentalblock beschäftigte sich mit der Dissektion von neuronalen Netzwerken und Populationen, die für den 2-AG Effekt auf die Futteraufnahme verantwortlich sind. Mit der Verwendung von konditionalen, CB1-defizitären Mäusen konnte ich eine Rolle von CB1 auf GABAergen Neuronen im Vorderhirn (Dlx-CB1-KO) oder kortikalen glutamatergen Neuronen (Nex-CB1-KO) ausschließen. In Kontrast dazu blieben die stimulierenden Effekte von 2-AG bei Abwesenheit von CB1 auf kortikalen und

subkortikalen Projektionsneuronen (CaMK-CB1-KO) aus. In Abwesenheit der erhöhten 2-AG Level im Hypothalamus nach Blockade von MAGL und deren weiterer Erhöhung durch Futterreduktion, konzentrierte ich mich bei meinen weiteren Untersuchungen auf diese Gehirnstruktur. Tatsächlich erbrachte die selektive Deletion von CB1 im Hypothalamus durch lokale Verabreichung von AAV-CaMK-Cre in CB1f/f Mäusen den gleichen Phänotyp wie die CaMK-CB1-KO. Auch das Nachahmen der Effekte von 2-AG über CB1 durch chemogenetische Interventionen im Hypothalamus führt zu einer erhöhten Bereitschaft, für Futter zu arbeiten. Die Deletion von CB1 in ausgewählten Subpopulationen des Hypothalamus hatte nur einen marginalen (SF1-CB1-KO) oder gar keinen Effekt (POMC-CB1-KO). Die Deletion von CB1 im Nucleus Arcuatus hingegen hob den 2-AG Effekt auf und stellte somit die essenzielle Bedeutung dieser Gehirnstruktur unter Beweis.

Auf der Suche nach möglichen endogenen Aktivitäten von 2-AG konnte ich zeigen, dass Futterreduktion zu erhöhten Plasmakonzentrationen von Corticosteron führt und der 2-AG Effekt durch die Blockade des Glukokortikoidrezeptors kurz bevor der Testung aufgehoben wird. Demnach scheint Corticosteron das 2-AG System auf nicht-genomische Weise zu beeinflussen.

Interessanterweise blieb die pharmakologische Blockade des CB1 Rezeptors *per se* ohne Wirkung auf die Bereitschaft zum Arbeiten für Futter. Die Effekte von pharmakologisch erhöhtem 2-AG konnten allerdings aufgehoben werden. Dies impliziert, dass die Level von 2-AG effizient durch das degradierende Enzym MAGL limitiert werden. Zum Überprüfen, ob Corticosteron nicht nur an der Aktivierung, sondern auch an der Terminierung von 2-AG beteiligt ist, wurden Hirnschnitte mit dem synthetischen Glucocorticoid Dexamethason behandelt. Dadurch konnten sich erste Hinweise auf die Veränderung in der Kompartimentierung, Dimerisierung und damit Effizienz bilden. Die Ergebnisse legen den Schluss nahe, dass Corticosteron gegensätzliche Effekte auf 2-AG und dessen degradierendes Enzyms MAGL vermittelt.

Es bleibt die Frage für die Gründe der strengen Kontrolle der 2-AG Signalgebung. Um das Thema zu beleuchten, führte ich zwei Satelittenprojekte durch, die (i) die Konsequenzen von Futterreduktion mit oder ohne pharmakologische Blockade von MAGL auf das negative Valenzsystem untersuchen. Außerdem habe ich (ii) die neuronale Signatur von CB1-kontrollierten Furchtreaktionen auf einen furchteinflößenden Stimulus untersucht.

In der ersten Satelittenstudie konnte ich eine Wechselwirkung zwischen dem Fresszustand und der MAGL Inhibition mit reduziertem Explorationsverhalten (insbesondere vertikale Exploration) in futterreduzierten Mäusen feststellen. Dies weist darauf hin, dass enzymatische Einschränkungen der 2-AG-Signalgebung bei Tieren mit eingeschränkter Nahrungsaufnahme eine ungestörte Exploration gewährleisten, welche für die Nahrungssuche erforderlich ist. Demnach scheint MAGL als Schnittstelle zwischen dem positiven und negativen Valenzsystem zu fungieren

In der zweiten Satellitenstudie, der Suche nach der neuronalen Verschaltung von CB1-kontrollierter Furchtantwort zeigten Dlx-CB1-KO erhöhtes, aktives Furchtverhalten, wohingegen CaMK-CB1-KO den gegenteiligen Phänotypen aufweisen (verminderte aktive Furcht). Totale-CB1-KO und Nex-CB1-KO blieben ohne Effekt. Mit Hilfe von lokaler CB1 Rekombination konnte ich die Verminderung von aktiver Furcht der Deletion im Hypothalamus, genauer SF1-Neuronen zuordnen. Somit beeinflusst die CB1-Signalgebung sowohl das positive als auch das negative Valenzsystem, wobei unterschiedliche neuronale Populationen des Hypothalamus einbezogen sind.

Zusammenfassend entdeckte ich ein bisher unbeachtetes homöostatisches Prinzip von simultaner Aktivierung und Dämpfung von 2-AG Signalwegen mittels Corticosteron, welches die Motivation von futterreduzierten Mäusen für Futter zu arbeiten streng reguliert. Ich konnte die Effekte auf neuronale Populationen im Nucleus Arcuatus und Hypothalamus zurückführen. Zudem konnte ich zeigen, dass die Kontrolle des positiven und negativen

Valenzsystems – trotz Evidenz für gegenseitige Wechselwirkungen – auf eigenständigen neuronalen Populationen im Hypothalamus beruht.

1. INTRODUCTION

The cannabinoid system holds an impressive history across the world. The first evidence of therapeutic use of *Cannabis sativa* is described about 3000 b.c. in China. In a mixture with wine, *Ma-jo* was used as an anesthetic in year 200 (Grotenhermen and Brenneisen, n.d.; Guy et al., 2004). Records of the ancient world describe an aphrodisiac effect while provoking appetite (Mathre, 1997).

Later in history, the roman empire imported the plant to England. There, the first analgetic description occurred.

> *„For wounds take this plant which one calls chamepithys and another name hemp, pound it and lay it onto the wound; if the wound be very deep then take the sap and wring it into the wound. For pain of the innards take the same plant, give it to drink, it takes away the pain" [The Old English Herbarium Manuscript V,* (Pollington, 2000; Guy et al., 2004) adapted from (Simon, 2012)*].*

After the distribution in the Arabic and African regions, the description in the medieval times followed. Among them were various, well known authors of herbals and pharmacopoeia. For instance, Hildegard von Bingen (about 1150) and Paracelsus (1493 – 1541) wrote down the effect of hemp. Subsequent brisk medical, but also dope psychoactive use, first bans followed. In 1484, Pope Innocent VIII (1432 – 1492) labeled cannabis as unholy. The psychoactive potential of hemp, however, was described and distributed in Europe only in 1563.

Scientific interest constantly increased within the 18th century. As an important step, the botanical classification as two separate species named *Cannabis sativa* (1753, Linné) and *Cannabis indica* (1783, Lamarck) took place.

Decades later, the first description for the use of hemp in the dysfunctional nervous system followed by the botanist Theodor Friedrich Ludwig Nees von Esenbeck (1787 – 1837) in 1830 (von Esenbeck et al., 1830). The first described psychiatric case study with Hemp was published 1845 by Jacques Joseph Moreau (1804 – 1884). The following years, German, British and American pharmaceutical companies developed and marketed diverse hemp products, among others, soporific, asthma cigarettes, narcotics and analgesics. This boom was followed by a closer, pharmacological interest in the early 20th century. The major aim was to identify the major (psychoactive) ingredients. With the identification of pure chemical substances unrelated to cannabis, which targeted various symptoms and diseases, the interest in medicinal cannabis had dropped. With a statement by the world health organization (WHO) of the lack of therapeutic effect and the prohibition of hemp use in the US in the 1920s the boom ended.

The renaissance of cannabinoids, however, started in the 1960s of the last century. Raphael Mechoulam and colleagues established a new research field by the first description of "an active constituent of hashish", Δ^9-tetrahydrocannabinol (THC; Gaoni and Mechoulam, 1964). Enormous scientific interest led to discoveries and theories of the exogenous and, especially, endogenous cannabinoid system.

It was clear from an early stage that dealing with highly lipophilic substances requires features in handling that resulted in some difficulties. Nonetheless, the complex search for receptors and additional ligands attained its peak in the late 1980s, resulting in the first description of ligand binding localization (Herkenham et al., 1990) and the cloning of the later called cannabinoid receptor type 1 (CB1; Matsuda et al., 1990). Next to the strong interest in the central nervous system, a second type of receptor was found mainly in the periphery (Bouaboula et al., 1993). The later called

cannabinoid receptor type 2 (CB2; Munro et al., 1993) will chaperone the field of immune system for decades.

The link of CB1 to a G-protein (Glass and Felder, 1997) followed and we learned a lot about potential co-transmitters such as glutamate, GABA and the panicogenic cholecystokinin (CCK; Marsicano and Lutz, 1999). At the same time, the laboratory of Raphael Mechoulam successfully searched for endogenous ligands. With the discovery of arachidonylethanolamide (anandamide, AEA; Devane et al., 1992) and 2-arachidonyl glycerol (2-AG; Mechoulam et al., 1995; Sugiura et al., 1995a) the endogenous Cannabinoid System (eCBS) was founded. With the discovery of pharmacological tools as an antagonist of CB1 (SR141716A, inverse agonist; (Rinaldi-Carmona et al., 1994), or genetically modified mouse mutants (as $CB1^{-/-}$; Zimmer et al., 1999; Azad et al., 2001; Marsicano et al., 2002), the young research field "exploded". With CB1, as the most abundantly expressed G-protein coupled receptor (GPCR) in the brain, the endocannabinoid system's role in psychiatric research constantly gained importance.

Until now, an impressive amount of scientific literature appeared. The present work makes a small contribution. I investigated the yin and yang effects of the eCBS. Three major topics are covered. As a part of the metabolic system, the impact of food intake and physiological changes introduced by hunger outline a central part. The animal's defensive system including anxiety, fear and panic, but also motivational processes represent additional topics.

1.1 The Endocannabinoid System of the Brain

Among different signaling systems in the body's physiological function, the endogenous cannabinoid system is one of the most colorful and powerful systems. Its suggested homeostatic principle bears a variety of physiological functions including embryonal development (Paria et al., 1995), skin and wound healing (Correia-Sá et al., 2020), immune reactions (Munro et al., 1993; Cabral et al., 1995) up to described roles in the central nervous system such as neuronal developments (Harkany et al., 2004), in pain mediation and regulation (Calignano et al., 1998). Malfunctions, such as metabolic (e.g., diabetes) or psychiatric diseases (e.g., Schizophrenia, mood disorders, post-traumatic stress disorder (PTSD)) frequently coincided with alterations in endocannabinoid signaling cascades, while highlighting its therapeutic potential (Schneider et al., 1998; Lastres-Becker et al., 2003; Monteleone et al., 2005; Laviolette and Grace, 2006; Jesudason and Wittert, 2008; Micale et al., 2013; Volk and Lewis, 2016). Our overall knowledge of the complex endocannabinoid system with its two ligands and their ways of action, however, is still limited.

Primarily two endogenous ligands of CB1 maintain the physiological homeostasis. Whereas brain levels of AEA (Devane et al., 1992) are about 10-fold lower (pmol/g) than those of 2-AG (Mechoulam et al., 1995; Sugiura et al., 1995b; Buczynski and Parsons, 2010), its binding affinities were found to be vice versa (Sugiura et al., 1995b, 1999).

While both bind to the most highly expressed G-protein coupled receptor (GPCR) in the central nervous system (Herkenham et al., 1991; Marsicano and Kuner, 2008), the cannabinoid receptor 1, its conformation changes and GPCR related signaling cascades are activated. Recruited $G\alpha_i$ (not s or q; Mukhopadhyay et al., 2002; Howlett, 2004) leads to the inhibition of adenylyl cyclase resulting in decreased production of cAMP (Eldeeb et al., 2016) or the activation of the mitogen-activated kinase (MAPK) cascade

(Hwang et al., 2017) regulating nuclear transcription factors. By binding of ß-arrestin in the second wave, the extracellular signal-regulated kinase (ERK) pathway is activated (Delgado-Peraza et al., 2016), followed by the desensitization and internalization of the receptor in the final wave (Nogueras-Ortiz and Yudowski, 2016).

One characteristic of presynaptic CB1 activation is its neuromodulatory role of restraining presynaptic transmission (Felder et al., 1995; Shen et al., 1996; Lévénès et al., 1998). Less free cAMP results in less active phosphokinase A (PKA) and therewith in the net dephosphorylation of potassium channels. The axon's hyperpolarization and, in the response of depolarizing stimuli, depression are consequences of activated potassium currents (Deadwyler et al., 1995; Hampson et al., 1995; Childers and Deadwyler, 1996). Therewith, the distinguished consequence of the activation of CB1 depends on the nature of participating cells. Vice versa, however, it had been hypothesized that CB1 activation indirectly enhances cAMP levels (Maneuf and Brotchie, 1997) upon enhanced synthesis of prostaglandins (Hillard and Bloom, 1983; Burstein et al., 1986).

In a way of feedback regulation, Ca^{2+} and cAMP stimulate the *de novo* synthesis of *N*-acylphosphatidylethalonamide (NAPE), a precursor of anandamide (Cadas et al., 1996) and mediate a postsynaptic "on demand" synthesis (Piomelli, 2003; Alger and Kim, 2011, Fig. 1).

Brain CB1 can be found in non-neuronal cells as well. Among those, astroglial and mitochondrial CB1 were described to be essential for energy homeostasis, memory formation or the regulation of leptin signaling, among others, and had been investigated in the past years (Bénard et al., 2012; Bosier et al., 2013; Hebert-Chatelain et al., 2016; Robin et al., 2018).

Although both AEA and 2-AG share the same major receptor, they, nonetheless may mediate opposing effects. The reasons for this phenomenon are still unknown. Different mechanistical observations, however, support our understanding of this fundamental question.

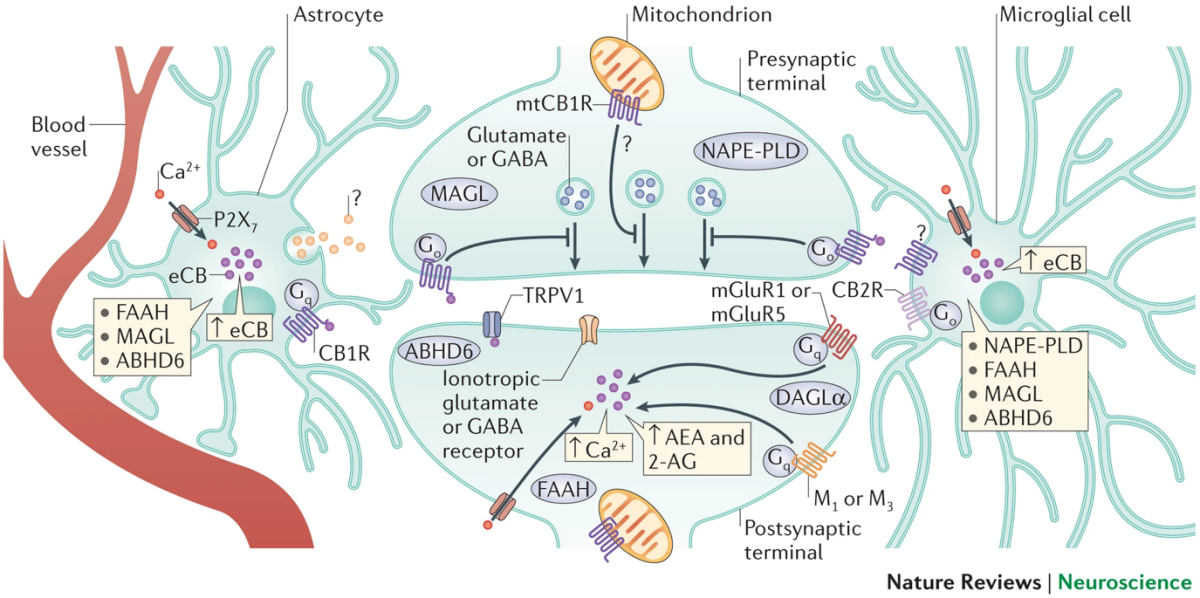

Figure 1: The endocannabinoid system and its compartments. The G-protein coupled CB1 receptor gets activated by the endocannabinoids (eCB) 2-AG and AEA. In neurons, release of synaptic vesicles is reduced upon activation of CB1. 2-AG and AEA are produced on demand (enzymes: DAGLα or NAPE-PLD) or by increased intracellular Ca^{2+} levels. The lipophilic molecules are degraded in a specific manner by MAGL, ABHD6 (2-AG) and FAAH (AEA). The authors of the underlying review (Lutz et al., 2015) further speculate about the involvement of different receptors as CB2, TRPV1, mGluR1 or mGluR5. Adapted from Lutz et al., 2015; permission granted by Springer Nature; license number: 5295811198533.

In contrast to AEA, which regulates long-term depression by additional binding to the postsynaptic transient receptor potential cation channel V1 (TRPV1; Chávez et al., 2010), 2-AG is implicated in depolarization-induced suppression of inhibition (DSI) and excitation (DSE; Kano et al., 2009). A potential explanation for this mechanism comes from its pharmacodynamic properties, as the signaling of AEA is more "tonic-like", whereas 2-AG subserve more of a phasic, "burst-like" mechanism for the activation of

CB1 (Ahn et al., 2008; Gorzalka et al., 2008; Hill et al., 2010b). Not surprisingly, a tonic activation by long-term agonist exposure may lead to a G-Protein subunit-independent desensitization and irreversible CB1 internalization (Hsieh et al., 2002; Wu et al., 2008).

The mechanistic toolbox, essential for the search of the Janus-faced role of both ligands, tremendously improved over decades. Beside the acute pharmacological antagonism of receptors (CB1: inverse agonist rimonabant, SR141716A; TRPV1: SB-366791), constitutive null-mutations (CB1 knockout mice, CBN, $CB1^{-/-}$) allow the investigation of a chronic lack of receptors. With the use of specific Cre-deleter mice or viral constructs combined with receptor floxed mice, specific (neuronal) cell populations (e.g., glutamatergic or GABAergic neurons) can be targeted.

Once the system is activated, pharmacological means allow the inhibition of endocannabinoid's synthesis (→ reduced levels) or, post-release, of their degradation (→ elevated levels).

The major biosynthesis of 2-AG is mediated by two enzymes: Phosphatidylinositol 4,5-bisphosphate (PIP_2) is hydrolyzed by phospholipase Cß (PLCß) to diacylglycerol (DAG), which is subsequently converted to 2-AG by diacylglycerol lipases (DAGLα and DAGLß; DAGLα as main synthesizing enzyme; Kano et al., 2009).

Free lipophilic ligands will be removed by fatty acid amide hydrolase (FAAH), specific for anandamide, and monoacylglycerol lipase (MAGL), specific for 2-AG. Whereas MAGL is responsible for about 85 % of 2-AG's hydrolysis, alpha/beta-Hydrolase containing 6 and 12 (ABHD6 and ABHD12) are responsible for about 4 % and 9 %. Targeted inhibition of FAAH or MAGL result in enhanced brain levels of the respective endocannabinoid upon prior synthesis. With an enormous clinical potential (Patel et al., 2017; Sartori and Singewald, 2019; Piomelli, 2020), both

mechanistic tools are frequently used in preclinical and clinical research again.

A special interest comes to the understanding of endocannabinoid signaling in regulation of motivation and emotions in the context of psychiatric diseases. For instance, there is a broad body of literature on the regulation of anxiety and fear processes in physiological and pathological (e.g., PTSD or stress exposure) conditions (Gorzalka et al., 2008; Hill et al., 2010b; Lutz et al., 2015; Genewsky and Wotjak, 2017; Lange et al., 2017; Patel et al., 2017; Sbarski and Akirav, 2018; Sartori and Singewald, 2019; Chadwick et al., 2020). Anandamide is described as anxiolytic and facilitating acute fear relief (Dincheva et al., 2015; Heinz et al., 2017; Morena et al., 2019; Mayo et al., 2020), whereas 2-AG enhances fear reactions (Llorente-Berzal et al., 2015; Heinz et al., 2017; Segev et al., 2018) despite anxiolytic consequences (Busquets-Garcia et al., 2011). The exact mechanism of action, however, remains unknown and needs to be validated by further studies. In particular, the role of endogenous constrains of endocannabinoid signaling by the degrading enzymes requires further investigation. The impact of the endocannabinoid system is by far not limited to the negative valence system, but also prominently involved in the positive valence system.

1.2 Cannabinoids in Metabolic Processes

Whereas food shortage and malnutrition remain a tremendous, worldwide problem, the Western societies must deal with the opposite problem. Obesity is a widespread disease with several underlying environmental as well as genetic risk factors. Food is nearly unlimited and easily available. Additionally, it is highly enriched in calories, whereas caloric requirement is steadily decreased (less physical activity, clothes and well temperate

housing). From an evolutionary perspective, animals are not used to ad libitum availability of food. Industrialized agriculture, possibility of refrigeration and the ongoing globalization, as examples, however, enable the potential availability in various regions.

Exposure to unlimited palatable, attractive food to animals may result in overeating (Bernstein et al., 1975). The imbalance between appetite (*I like/want to eat*) and hunger (*I must eat*) in favor of the first, lead to increased food intake followed by overweight and obesity.

With increasing effort and limited availability of food, different states can be defined. Whereas liking requires no or low effort at most, wanting leads animals to work for food (e.g., hunting). The willingness to work for food can be assessed in experimental settings where the animals have to spend more effort to obtain food. Two key features are the physiological base as the hunger state of animals, and the type of food (e.g., palatable, or attractive food). Operant conditioning of food restricted rodents enables to assess the willingness to work for food. Food restricted animals form stimulus-response associations (e.g., to touch a highlighted square on a touchscreen in order to obtain a food reward). With the Progressive Ratio (PR) protocol, the number of target touches to receive one reward increases by a defined number. For instance, PR4 requires 1 touch in the first trial, 5 (1 + 4) in the second trial, 9 (5 + 4) in the third trial and so on. The point when animals stop working for food is defined as breaking point (BP). Given the small amount of reward gained per trial, lack of motivation rather than satiety might be the reason to further participate in the task.

Starting with descriptions by marijuana consumers, CB1’s role in food intake and appetite got more and more evident in the recent past.

Stimulation of the CB1 receptor is coupled to eating and working for food harder, and more frequently than normal (Kirkham and Williams, 2001). With the development of rimonabant by Sanofi (Rinaldi-Carmona et al., 1994), the therapeutic potential of attenuated CB1 signaling has raised expectations and hopes (van Gaal et al., 2005; Tucci et al., 2006). As a major drawback, after two years, Acomplia® (rimonabant) was suspended from the European marked in 2008 (EMEA, 2008), while the FDA refused the marketing approval for the US in 2007 due to serious psychiatric side effects.

More than a decade later, the (clinical) interest in CB1 related research resurgences (clinicaltrials.org) and antagonizing CB1 remains a potential option for body weight control (Lopez Trinidad et al., 2021), in particular if peripheric reactions are triggered (Quarta and Cota, 2020).

Piazza et al. (Piazza et al., 2017) propose the theoretical framework according to which activation of CB1 results in two physiological states (Brown et al., 1977; Koch and Matthews, 2001): increased appetite, as the "sensitivity to appetitive properties of food" and the increased willingness to work for food (or "stimulation of food intake beyond satiety" (Piazza et al., 2017). The role of the hypothalamus as a key region of action was described early (Trojniar and Wise, 1991), and with it the Arcuate Nucleus (Arc), a structure near to the median eminence and 3rd ventricle. Due to the close proximity between the Arc and the median eminence, a structure described for exchange of systemic (blood) signal peptides such as hormones, the Arc has a role in coordination and reacting to peripheral signals (Rodríguez et al., 2010; Myers and Olson, 2012). Accordingly, orexigenic (appetite stimulating) and anorexigenic (loss of appetite, producing anorexia) neuronal populations were described within the Arc: the appetite stimulating AgRP- (agouti-related peptide) and the satiety-

mediating POMC- (pro-opiomelanocortin) positive neurons (Waterson and Horvath, 2015). As summarized recently by Timper and Brüning, POMC neurons were described to project to the paraventricular hypothalamic nucleus (PVN, important structure in sympathetic, peripheral output; Kannan et al., 1989), dorsomedial- (dmH), lateral-, and ventromedial- (vmH) hypothalamus (Kleinridders et al., 2009; Waterson and Horvath, 2015; Timper and Brüning, 2017). Deletion experiments demonstrated the overall role of the distinct regions. Whereas PVN-destruction results in overeating, vmH-destruction results in hyperphagia and obesity (Leibowitz et al., 1981; Shimizu et al., 1987). CB1's role on POMC-positive neurons was discussed previously as an essential promotor of feeding in the state of satiety (Koch et al., 2015). The cannabinoid induced activation of POMC was described to rely on presynaptic and mitochondrial mechanisms. Additionally, CB1's activation was found to mediate dose-dependent effects as lower doses lead to depolarization, whereas higher doses induce hyperpolarization of POMC neurons (Koch et al., 2015).

Next to POMC, CB1's contribution on SF1-positive neurons was investigated and found to regulate Leptin responses within the ventromedial hypothalamic nucleus. While a lack of CB1 led to Leptin resistance, SF1-CB1 may be a switch adapting to dietary changes (Cardinal et al., 2014).

1.3 Translational Research on Psychiatric Diseases

Patient care, clinical-, and preclinical- research stay in close interaction defining translational research in psychiatry. In one direction, diseases were back translated into preclinical research. Validity criteria such as face-, predictive-, construct- and etiological- validity were decisive: Mirroring human symptoms in the animal model is described by the face validity, reproducibility of (pharmacological) therapy (e.g., increased serotonin treats depressive symptoms; exposure-based therapy treats symptoms of phobias and anxiety disorders) by predictive validity, and the triggering factor as etiological validity (e.g., traumatic event leads to PTSD). With construct validity, there is a criterion between both directions of translation, describing the underlying biological processes (e.g., amyloid-ß in Alzheimer disease).

Knowledge gained from preclinical studies is ought to be translated into clinical research and, later, patient care. Even with increasing relevance of the so called third mission (Henke et al., 2016; Berghaeuser and Hoelscher, 2020), transfer of technology and innovation is difficult to plan. Next to the enormous social impact, its relevance on different levels of government increases. The foundation of the German Centers for Health Research (DZG) by the German ministry of research and education (BMBF) in 2009 were pioneering. Next to the centers for neurodegenerative diseases, centers for pediatric and adolescent health (Zentrum für Kinder und Jugendgesundheit) and mental health (Zentrum für Psychiatrische Gesundheit) were founded in 2021. One of the defined missions is the "Transfer of health relevant research findings into patient care" ("Überführung von gesundheitsrelevanten Forschungserkenntnissen in die Versorgungspraxis"), the back translation into clinic. The clinical development requires, next to time and recourses, strong financial (industry) partners.

One major component in the gain of knowledge are animal models in preclinical research. Next to a suitable model organism, an animal model comprises of a test situation and its defined readouts. Among vertebrates, fish (e.g., *danio rerio*, *oryzias latipes*) or mammals like rodents as mice or rats (e.g., *mus musculus*, *rattus norvegicus*) or non-human primates (e.g., rhesus macaque: *macaca mulatta*, ring-tailed lemur: *lemur catta*, common marmoset: *callithrix jacchus*) were frequently used. Due to their comparable simple and well-studied nervous system, invertebrates as *drosophila melanogaster* are suitable as a model organism for circuit studies and basic behavior. Mice were economically feasible (reasonable breeding and maintaining costs), due to the availability of genetic modifications and their homology of important physiological components of the central nervous system, the most commonly used model organism.

In the end, the experimental goal defines the proper strain and/or knockout and its test situation and readout. As an example, testing the efficiency of an anxiolytic substance requires a more anxious organism/strain in a situation without an acute threat.

In accordance with the RDoC (Research Domain Criteria, NIMH strategic plan 2008) system, psychiatric research such as behavioral investigations may be systematically classified. Human behavior and brain function were framed into different neuropsychological domains to synchronize clinical work with clinical and preclinical research. Among those domains are the positive- and negative valence systems, cognition, social processes, arousal and regulatory systems as well as the sensorimotor system. Each domain is sub-structured with so called constructs. Anxiety ("potential threat") and fear ("acute threat") were constructs of the negative valence system. Depression-like symptoms with constructs such as motivation, reward learning or reward habituation in the positive valence system. The cognitive system comprises constructs such as attention, perception and

memory (Ross and Margolis, 2019; Yücel et al., 2019). In order to align preclinical- and clinical- research, different, levels of descriptions were defined. Domains and subsequent constructs can be described at levels of genes, molecules, cells, circuits, physiological reactions, behavior or self-evaluation (Walter, 2017).

Within this study, the major focus is the positive- (working for food/reward, motivation, and hunger perception) and negative- (anxiety and fear) valence system, given the endocannabinoids implications in core symptoms of anxiety disorders and depression.

1.4 Aims of the Study

This study was interested in the effects of endocannabinoid signaling under different physiological and emotional conditions. Next to the motivational aspect of food intake, the negative valence system was investigated. By building on the panicolytic effects of AEA in a model organism of increased fear and anxiety responses (Heinz et al., 2017), a primary focus in this study were positive and negative effects of enhanced 2-AG signaling.
More specifically, the following objectives were investigated:

1) Given that pharmacological blockage of CB1 decreases appetite in human subjects (van Gaal et al., 2005), I aimed to evaluate exogenous and endogenous cannabinoids and related pharmacological substances on its effect on the willingness to work for food in mice, using the progressive ratio paradigm.
2) In line with this, I investigated the role of CB1 in different neuronal populations. With the use of local deletion of CB1, its retro- or anterograde projections as well as chemogenetic means, I aimed to dissect the underlying basis of the willingness to work for food.
3) As the key regulating enzyme of brain 2-AG levels, I aimed to investigate the mechanism of MAGL activity under food restriction.
4) Do pharmacologically enhanced levels of 2-AG enhance fear reactions? Since food restriction may elevate 2-AG levels *per se*, does the blockage of its major degrading enzyme mediate additive or synergistic emotional reactions?
5) A broad body of literature investigates underlying neurotransmitters and pathways in fear reactions. The importance of CB1 is omnipresent and the hypothalamus could be validated as an essential side of action. It remains to be shown, however, if the effects of 2-AG on the positive and negative valence system are mediated by the same hypothalamic circuits and/or neuronal populations.

2. MATERIALS AND METHODS

2.1 Animal Experiments – General

2.1.1. Animals

If not stated otherwise, animals used in this study were bred at the Max Planck Institute of Biochemistry, Martinsried-Planegg and housed at the facilities of the Max Planck Institute of Psychiatry, Munich under standard housing conditions (23 °C ±3, 40 ±10 %). Group housed adult (about 2-7 month), male mice had ad libitum access to food (Altromin Haltungsdiät 1328 or Zuchtdiät, Altromin Spezialfutter, Lage, Germany) and water. IVC cages (Greenline, Tecniplast) were equipped with bedding, nesting and enrichment material (wooden rodent tunnel; 4.5×4 cm, diameter: 30 mm; ABEDD, Vienna, Austria).

All experiential procedures were approved by the Government of Upper Bavaria (188-12, 142-12, Vet_03-16-08, Vet_02-16-134, Vet_02-17-171, Vet_02-17-206, Vet_02-17-213, Vet_02-17-223, Vet_02-17-224, Vet_02-18-55, Vet_02-18-159, Vet_02-20-60) and were in accordance with the recommendations of the Federation for Laboratory Animal Science Associations (FELASA) and the Society of Laboratory Animal Sciences (GV-SOLAS) recommendations.

Non modified mouse lines

C57Bl/6N (originated from Janvier) were bred at the Max Planck Institute of Biochemistry.

Transgenic mouse lines

Different transgenic mouse lines were maintained, generated, and used. Conditional CB1-deficient mice were generated by mating female

Cnr1tm1.2Ltz (CB1ff) with male Cre-recombinase driver mice differing in celltype specific promotor (Nex-Cre, Dlx-Cre, CamK-Cre, POMC-Cre, AgRP-Cre, SF1-Cre) resulting in Cre expression on one allele on a CB1ff background (Table 1).

Specific lines, having proteins as receptors or STOP-cassettes flanked by loxP sites (Ai9, CB1) were used for viral targeting expressing Cre-recombinase or were crossed with Cre-recombinase driver mice to obtain a selective *knock out* of the flanked protein.

Table 1: Overview about used mouse lines. Schematic overview of CB1 expressing populations is illustrated in Fig. 2. Genotyping was performed for CB1 and Cre as described before.

Strain	***Name***	***Description, Reference***
CB1ff	*Cnr1tm1.2Ltz*	CB1 flanked by lox-P-Sites (Marsicano et al., 2002, 2003).
CBN	*CB1-TgH*	Complete deletion of CB1 (Marsicano et al., 2002).
CaMK-CB1	*CB1f/f;CamKII-Cre*	Deletion of CB1 on cortical and subcortical projection neurons (Marsicano et al., 2003).
Nex-CB1	*CB1f/f;Nex-Cre*	Deletion of CB1 on cortical glutamatergic neurons (Monory et al., 2006).
Dlx-CB1	*CB1f/f;Dlx5/6-Cre*	Deletion of CB1 on forebrain GABAergic neurons (Monory et al., 2006).
AgRP-CB1	*Agrp$^{tm1(cre)Lowl}$*	Deletion of CB1 on AgRP-positive (Tong et al., 2008) neurons.
POMC-CB1	*Tg(Pomc-Cre)1Lowl*	Deletion of CB1 on POMC-positive (Balthasar et al., 2004) neurons.
POMC-Ai9	*Gt(ROSA)26Sor$^{tm9(CAG-tdTomato)\ Hze}$*	POMC-positive neurons co-expressing td-tomato as a fluorescent reporter (Madisen et al., 2010).
SF1-CB1	*Tg(Nr5a1-Cre)7Lowl*	Deletion of CB1 on SF1-positive (Dhillon et al., 2006) neurons (Cardinal et al., 2014).

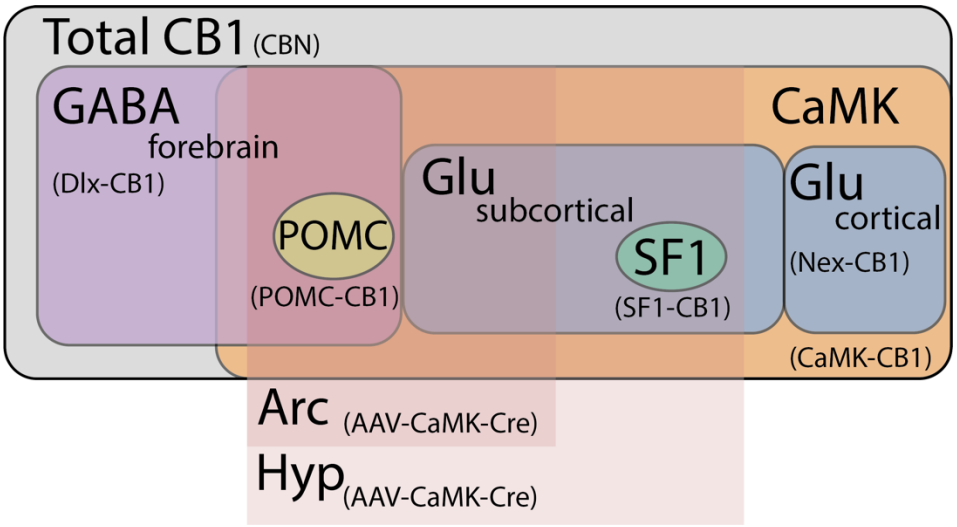

Figure 2: Schematic overview of used CB1-expressing neuronal populations targeted by conditional mutagenesis. Different colors represent different CB1-expressing neuronal populations. GABAergic knockouts partially overlap with, Glutamatergic knockouts as core of CaMK expressing projection neurons. Non overlapping GABAergic neurons represent interneurons. With the use of Cre expressing virus under a CaMK promotor, local knockout in the hypothalamus (Hyp) or, more specific, arcuate nucleus (Arc) was induced.

2.1.2 Food Restriction (FR+)

Some experiments required food restricted mice. Mice were single housed, and body weight was obtained on three consecutive days. Averaged weights were used as individual's baseline. Over the course of FR+, 80 – 85 % of the individual's baseline was approached. To achieve that, I fed defined, weighted food pellets reducing body weight by 1 – 2 g daily.

The time point of the daily routine was defined by the light phase. Mice housed in reverse rhythm were tested at the start of the dark phase. They were fed right after the experiment at defined times (± 2 h). Mice housed at the normal light-dark rhythm, tested in the light phase, were fed in the end of the light phase.

2.1.3 Pharmacological Interventions

I applied pharmacological substances as required during specific interventions (e.g., chirurgical procedures) or as pharmacological studies. The latter will be listed as follow, the doses applied were based on experiences and those reported in the literature:

Vehicle A: Working solution was prepared freshly and consisted of 15 % DMSO, 4.25 % PEG (Sigma; PubChem CID: 174), 4.25 % Tween80 (Sigma; PubChem CID: 5281955), and 76.50 % sterile saline (0.9 %, Fresenius Kabi, Bad-Homburg, Germany).

Vehicle B: NaCl (0.9 %, Fresenius)

Vehicle C: artificial ACSF (for detailed protocol see 2.3)

JZL184 (Tocris Biosciences, Bristol, UK), URB597 (Sigma), SR141716A (Sigma), CTEP (Sigma) were dissolved in 100 % DMSO, aliquoted and stored at -20 °C. Prior to use, working solution was prepared freshly (Vehicle A).

Speed Vac® (SC210, Savant, Thermo-Scientific; 30 min) was used to evaporate the ethanol from stock solution THC (in 100 % EtOH; Lipomed, Arlesheim, Suisse). Subsequently, THC was dissolved in 100 % DMSO, aliquoted and stored at 4 °C. Prior use, working solution was prepared freshly (Vehicle A).

Clozapine N-Oxide (Tocris Biosciences, Bristol, UK) was dissolved in DMSO 1 % (0.9 % NaCl solution) to a final concentration of 5-15 mg/ml.

For further details see table 2.

Table 2: Overview about pharmacological substances.

Drug, Supplier	**Target, Mechanism of action, Key Reference**	**Application**
Clozapine N-oxide (CNO), Tocris Biosciences	The synthetic drug CNO is an agonist of DREADDs. (Gerber et al., 2001; Manvich et al., 2018)	5, 15 mg/kg -45 min, i.p.
CTEP, Sigma-Aldrich	Negative allosteric modulator and inverse agonist of the metabotropic glutamate receptor 5 (mGluR5). (Lindemann et al., 2011)	2 mg/kg -24 h and -2 h, i.p.
Ghrelin (rat), Tocris Biosciences	Ghrelin is a peptide and agonize the ghrelin receptor. (Kojima et al., 1999)	0.08 mg/kg -90 min, s.c.
JZL184, Tocris Biosciences	Selective inhibitor of the main degrading enzyme, monoacylglycerol lipase (MAGL), of 2-AG. Inhibition results in enhanced 2-AG levels. (Long et al., 2009)	8, 16 mg/kg -1 h, i.p.
KT203, Sigma-Aldrich	KT203 inhibits ABHD6, a degrading enzyme of 2-AG. (Hsu et al., 2012)	1 mg/kg -1 h, i.p.
Mifepristone (RU486), abcam	The antiglucocorticoid Mifepristone antagonizes glucocorticoid and progesterone receptors. (Schreiber et al., 1983)	50 mg/kg -1 h, i.p.
MJN110, Sigma-Aldrich	Inhibitor of MAGL, the rate limiting degrading enzyme of 2-AG. (Niphakis et al., 2013)	5 mg/kg -1 h, i.p.
SR141716A, Sigma-Aldrich	Inverse agonist, antagonizing CB1 receptor. (Rinaldi-Carmona et al., 1994)	1, 3 mg/kg -1 h, i.p.
Testosterone, Jenapharm, Jena	The steroid testosterone is the primary male sex hormone. (Philibert et al., 2010)	5 mg/kg -1 h, i.p.
THC, Lipomed	Δ9-Tetrahydrocannabinol is the active constituent of hashish and described as CB1 agonist. (Gaoni and Mechoulam, 1964)	1, 3 mg/kg -1 h, i.p.
URB597, Sigma-Aldrich	Selective inhibitor of the main degrading enzyme, fatty acid amide hydrolase (FAAH), of AEA. Inhibition results in enhanced AEA levels. (Piomelli et al., 2006)	0.3, 1 mg/kg -1 h, i.p.
WWL113, Tocris Biosciences	Inhibitor of carboxylesterases 3 and 1f (Ces3, Ces1f) and ABHD6. (Dominguez et al., 2014)	50 mg/kg -1 h, i.p.
DH376, Generous gift by Prof. van der Stelt, Leiden, Netherlands	Selective inhibitor of the rate limiting synthesizing enzyme, diacylglycerol lipase alpha (DAGLα), of 2-AG. Inhibition results in reduced 2-AG levels. (Ogasawara et al., 2016)	50 mg/kg -1 h, i.p.

2.1.4 Surgical Procedures

Stereotactic virus injections

Mice were initially anesthetized, and anesthesia was maintained using Isoflurane (1.5 – 4 %). Head's fur was shaved and disinfected prior to skin opening. Prior surgery (10 min), analgesia was introduced using Metamizol (200 mg/kg s.c. in 0.9 % NaCl; Vetalgin, MSD Animal Health, Unterschleißheim, Germany) and Metacam (5 mg/kg s.c. in 0.9 % NaCl; Boehringer Ingelheim Vetmedica GmbH, Germany). Mice were placed onto a heating pad and eyes were covered with moisturizing ointment (Bepanthen, Bayer). For local analgesic treatment, lidocaine (Xylocain spray, AstraZeneca GmbH, Wedel, Germany) was applied before opening and removing periosteum. Cranial bones were cleaned with 3 % H_2O_2 and Bregma and Lamda were used to locate target coordinates. In preparation to target brain regions of interest holes were drilled into the skull. A Hamilton cannula, connected to a motorized frame, was placed accordingly and target volume was infused (see Table 3 for details). Cannula was left in place for 3-5 min before it was slowly removed. The skin was closed by surgical sutures and/or glue (Histoacryl, B.Braun, Rubin, Spain), and mice were allowed to recover for at least 5 days prior the next intervention. Post-surgery, mice were able to make use of a heating plate (>1h) before the cage was placed back to the IVC-rack. Analgesia was maintained by treatment of Metacam (s.c. or p.o.; 5 mg/kg) for at least three consecutive days, and on demand.

Table 3: Stereotactic coordinates of virus infusions (see Fig. 2 for schematics).

Target Region	**Coordinates**	**Infusion details**
Ventromedial Hypothalamus (vmH)	AP: -1.3 ML: 0.55 DV: 5.7	200 nL, 50 nL/min
Arcuate Nucleus (Arc)	AP: -1.5 ML: 0.25 DV: 5.8	100 nL, 25 nL/min

Viral Vectors

Viral vectors were produced in-house (2.5.1), gifted from Charité Berlin, or purchased from Addgene (Penn Vector Core).
Control groups were indicated in the corresponding figure legend, control mice and can be wildtype mice or mice infused with control-virus. In case of Cre-recombinase expressing viruses, control groups were injected with a similar, but non-Cre expressing construct, or non-floxed mice were used.

The Following viral constructs were used within this study:

- AAV1/2o-hSyn-HA-MAGL-140220; designed and produced in house (2.5.1) was used for making use of HA-tag (interactome, Western Blot, …) due to the lack of potent and reliable MAGL antibodies.
- AAV9-CamKII-Hi-GFP-Cre-WPRE-SV40 (1.64 x 10^9 gc/µL, used as: 1x10^7 gc/µL); Penn Vector Core; introducing Cre-expression in CaMK-positive cells.
- AAV1/2-hSyn-DIO-hM4D-mCherry (5x10^9 gc/µL); produced in house (2.5.1); introducing expression of the inhibitory DREADD construct.

2.1.5 Termination of Animals

For histological post-processing (staining; tracing experiments, fluorescent tags as for DREADDs) mice were terminally anesthetized (isoflurane anesthesia) and perfused with ice cold PBS followed by 4 % PFA. Subsequently, brains were collected and post-fixed in 4 % PFA overnight, followed by 20 % (w/v) sucrose solution at 4 °C until sectioning.

For RNA or protein work, mice were killed using isoflurane or cervical dislocation. Subsequently, brains were snap frozen using 2-methylbutane (on dry ice) following storing at -80 °C until post-processing.

If blood was needed, mice were slightly anesthetized using isoflurane followed by decapitation. Trunk blood was collected in EDTA tubes (Sarstedt) and stored on ice. Samples were centrifugated for 15 min at 20000 g at 4 °C. Plasma (supernatant) was aliquoted and stored on -80 °C for further analysis.

2.2 Post Processing

2.2.1 Radio-Immune Assay (RIA)

Plasma was thaw up on ice and diluted according to the manufacturer's instructions. Levels of Corticosterone and Ghrelin were determined using Corticosterone Double Antibody Kit (MP Biomedicals, Santa Ana, California, USA) and Ghrelin (Rat, Mouse) RIA Kit (Phoenix Pharmaceuticals Burlingame, California, USA).

Samples were pre-processed, diluted (Corticosterone: 1:50, 1:100, 1:200; Ghrelin: 1:20), and radioactivity labeled antibodies were detected using an automated gamma counter (WIZARD^2, Perkin Elmer, Waltham Massachusetts, USA).

2.2.2 *In Situ* Hybridization (ISH)

Freshly dissected and snap-frozen brains were sectioned at -20 °C using a cryostat microtome. Slices (20 µm) were thaw mounted on slides (Super Frost Plus), dried, and stored at -80 °C. ISH was used to validate mRNA expression of CB1 mouse lines and Cre-virus induced deletion/insertion of CB1. Ribonucleotide probes were synthetized as described previously (Marsicano and Lutz, 1999; Häusl et al., 2021), antisense cRNA probes were transcribed from a linearized plasmid and freshly labeled using ^{35}S UTP (approx. 1.5×10^6 cpm). Slides were defrosted at RT for 30 min, fixed

in cold 4 % paraformaldehyde (in PBS; 136 mM NaCl, 2.7 mM KCl, 10 mM Na_2HPO_4, 1.8 mM KH_2PO_4, pH 7.4) and rinsed in PBS. Subsequently, sections were acetylated in 0.25 % acetic anhydride in 0.1 M triethanolamine-HCl followed by dehydration in increasing concentrations of ethanol and delipidzitation in chloroform for 5 min. Hybridization buffer containing ^{35}S-labeled riboprobe was added to sections, covered with coverslips and incubated at 55 °C overnight. Thereafter, sections were rinsed in 2x SSC (standard saline citrate; 1x SSC: 150 mM NaCl, 15 mM $C_6H_5Na_3O_7$) supplemented with RNAse A (0.02 mg/mL) followed by washing in 0.1x SSC at 65 °C for 1 h. At last, slices were dehydrated by incubation in increasing concentrations of ethanol and air-dried. Slides were exposed to Kodak Biomax MR films (Eastman Kodak Co., Rochester, NY) for approx. 1 week and developed using a developing automate (Kodak).

2.2.3 Double *In Situ* Hybridization

Additionally, to the procedure of *in situ* hybridization, immunofluorescence probe of POMC was applied as described before (Refojo et al., 2011; Koch et al., 2015). Hybridized slides were dipped in autoradiographic emulsion (type NTB2), developed after 3-6 weeks and counterstained with cresyl violet. Pictures were taken using dark-field microscopy.

2.2.4 RNAScope

RNAScope was performed according to the manufacturers' instructions by Anna Bludau in the Laboratory of Prof. Neumann at Regensburg University. In short mice were perfused and incubated in sucrose solution (30 %) as described before. Brains were snap frozen using 2-Methylbutan and sectioned on a cryostate (16 µm slices). Slices were stored on -80 °C until

further processing. Following probes were used: Mm-Cnr1, Mm-Gad2-C2, Mm-Mgll, Mm-Slc17a6-C2 (ACD, BioTechne, Wiesbaden, Germany).

2.2.5 Histological Verification

Viral injections of Cre-expressing constructs were validated using *in situ* hybridization. Location of targeted Cre-expression was validated for each animal unaware of the behavioral outcome. Exclusion criteria were wrong target region, exorbitant spreading, e.g., along injection duct, weak expression. The absence of the floxed allele, e.g., CB1 (cnr1) was determined by corresponding *in situ* hybridization.

All generated mouse lines were validated on the knocked-out target gene (cnr1). Expression of new Cre-deleter lines was validated by breeding with Ai9 mice followed by fluorescence microscopy (Slide Scanner, Olympus). Experiments using DREADD constructs were validated using fluorescent microscopy (mCherry; Axioplan 2 microscope with AxioCam MRm greyscale ccd camera, Zeiss, Göttingen, Germany).

2.3 Electrophysiology

POMC-Ai9 mice were transferred to Münster, and electrophysiological properties were determined by Kay Jüngling and team as described previously (Jüngling et al., 2008). In short, transgenic POMC-Cre-Ai9 mice were decapitated and brains were dissected freshly. Coronal brain slices (350 µm thickness), containing the arcuate nucleus (cf. Fig. 13) were cut on a vibratome (VT1200S; Leica, Germany) in ice-cold cutting solution containing [in mM]: 2.5 KCl, 1.25 NaH_2PO_4, 10 $MgSO_4$, 20 PIPES, 10 glucose, 200 sucrose, 0.5 $CaCl_2$. The pH was set to 7.35 using NaOH.

Voltage-clamp recordings were performed at 30 °C in a submerged chamber perfused with artificial cerebrospinal fluid (ACSF) containing [in mM]: 120 NaCl, 2.5 KCl, 1.25 NaH_2PO_4, 2 $MgSO_4$, 2 $CaCl_2$, 22 $NaHCO_3$, and 20 glucose. The pH was set to 7.35 by gassing with carbogen. Perfusion speed was set to 3.5-4 ml/min. Patch pipettes (2.5–4 MΩ pipette resistance) were made of borosilicate glass (GC150T-10; Harvard Apparatus).

The intracellular solution contained (in mM): 10 NaCl, 88 potassium gluconate, 20 potassium citrate, 10 HEPES, 3 BAPTA, 0.5 $CaCl_2$, 1 $MgCl_2$, 3 MgATP, 0.5 NaGTP, and 15 phosphocreatin, pH adjusted to 7.25. To block inhibitory, GABAergic synaptic transmission, the ACSF contained gabazine ($GABA_A$ receptor antagonist, 10 µM; Tocris) and CGP55845 ($GABA_B$ receptor antagonist, 2.5 µM; Tocris). POMC neurons in the arcuate nucleus were identified by their expression of Ai9 using a 470 nm mic-LED (Prizmatix/Mountain Photonics GmbH, Germany) for excitation and a 525 nm GFP emission filter (Thorlabs, Germany). Identified POMC neurons were recorded in the voltage-clamp mode at a membrane potential of -65 mV. A tungsten bipolar stimulation electrode was placed in the ventromedial hypothalamus (vmH) to electrically evoke glutamatergic excitatory postsynaptic currents (eEPSC). Two stimuli (50 µs duration, 100-500 µA intensity) were applied with a paired-pulse interval of 100 ms every 10 s. The CB1 agonist arachidonyl-2'-chloroethylamide (ACEA; Tocris) was bath applied at a concentration of 1 µM for 3 minutes. Recorded eEPSCs and spontaneous excitatory postsynaptic currents (sEPSCs) were analyzed offline using Clampfit10 software (Molecular Devices, USA). Statistical analysis and data presentation were done using Origin9.1 (OriginLab Corporation, USA) and CorelDrawX4 (Corel Corporation, Canada) software, respectively.

2.4 Behavioral Investigations

Within this study, a variety of behavioral paradigms were used to assess different physiological, pathological and emotional states of mice.

Behavioral assessments took place during the dark phase of the circadian rhythm (except study 3.3). Between two different tests, animals recovered for a minimum of 2 days up to 1 week. On a test day, mice were transported from the holding to the dimly lit experimental room and individually placed into the setups that were separated from the rest of the experimental room by black walls and curtains. All apparatuses were cleaned with water containing detergent between the trials and carefully dried. In 2.4.1, holding chambers were in the same room and setup was cleaned at the end of the testing day. Experiments were performed and the behavior was scored by experimenters unaware of the experimental conditions.

2.4.1 Progressive Ratio Testing (PR)

Mice were food restricted as described before (see "Food Restriction"; (Heinz et al., 2021) and subsequently trained using a Bussey-Saksida Rodent Operant Touchscreen Testing System (Campden Instruments Ltd., Loghborough, UK). Purchased task schedules (ABETII Touch Mouse Task for Progressive Ratio, Campden Instruments) was operated by Whisker Server Version 4.6.2 (Cambridge University Technical Services Ltd., Cambridge, United Kingdom) and ABETII Touch Version 2.18 (Layafette Instrument Company, Lafayette, United States) as previously described (Heath et al., 2015, 2016; Heinz et al., 2021). As soon as mice reached a stable, restricted body weight, following habituation- and training protocols were run: During (1) reward habituation mice received approx. 2 mL of reward (10 % Nestlé Milchmädchen) in a scale pan in their home cage. To minimize potential neophobic reactions (Horner et al., 2013; Heath et al.,

2015), freshly prepared reward was delivered on two consecutive days overnight. During 20-min (2) chamber habituation mice were allowed to familiarize with the apparatus and the pre-filled reward magazine. Each mouse was assigned to a fix chamber over the course of experiments. On the following day, (3) initial touch training (ITT) introduced mice to the touch screen: 30 trials were required within 60 min, whereby reward was delivered (coupled to acoustic signal) upon nose poke to the screen (= one trial). A targeted nose poke to the illuminated central grid (out of five) resulted in the 3-fold amount of reward. When mice successfully completed ITT, they were trained in fixed ratio schedules on the subsequent day. (4) Fixed ratio is defined by a constant number of nose pokes required (1-, 3- or 5-times) for one reward delivery, equal one trial. 30 trials had to be completed within 60 min before proceeding to the next stage. After successful completion of the fixed ratio 5 protocol on two consecutive days, a target ratio of 3:1 (correct:blank touches) was required before advancing to the progressive ratio protocol (PR). During the (5) progressive ratio protocol (PR; more precisely known as PR4), the mice' willingness to work for food was evaluated. During PR animals could earn unlimited rewards within a 1-h session, whereby they had to spend increasing effort in order to trigger reward delivery. By each trial, the required number of nose pokes increased by 4, resulting in a series of 1, 5, 9, 13, 17, 21, … nose pokes. The sum of all correct touches within one session is defined as target touches, breaking point is defined as the trial in which mice stop to nose poke for more than 300 s (time out). Baseline PR was obtained on two blocks, each out of three consecutive days, flanked by tree days of fixed ratio 5. Pharmacological interventions took place acutely at defined times before PR (cf. Table 2). Pharmacological PRs were flanked by at least two days of fixed ratio 5 without treatment to maintain a stable performance

baseline. To avoid inhomogeneous motivational states, mice were tested daily over the course of experiments.

2.4.2 5-Choice Serial Reaction Time Task (5-CSRTT)

The 5-CSRTT was used to address potential side effects of the pharmacological treatment. Test naïve C57BL/6N mice were food restricted, habituated to reward and chamber as described before (see "Food Restriction"; (Heinz et al., 2021) and subsequently trained task specific. Different from the PR-scheme, 5-CSRTT uses not only one, but five different stimulus positions. During the must touch training mice were introduced to the touchscreen setup while 20 trials needed to be successfully absolved within 30 min. One trial consisted of a presented stimulus light that was required to touch. Similar to with the PR protocol, the presented stimulus disappeared after touch, reward was delivered, and food magazine illuminated. With entering the food magazine, a inter-trial interval of 5 s was initiated, before the next trial proceeded.

After successful completion of two must touch trainings on two consecutive days, baseline training with its different sessions started. During the different sessions, the stimulus duration (SD; time of stimulus presentation) and limited hold (LH; time to respond to the stimulus after its presentation) decreased (Session: SD, LH; 9: 32 s, 37 s; 10: 16 s, 21 s; 11: 8 s, 13 s; 12: 4 s, 9 s; 13: 2 s, 7 s; 14: 1.8 s, 6.8 s; 15: 1.6 s, 6.6 s) whereas inter-trial interval and time out remained stable (5 s). A session was counted successful when more than 40 trials were performed with an accuracy greater than 80 % while omissions were below 20 %. After two successful sessions on two consecutive days, next session was reached. Pharmacological intervention was performed in Session 15 (SD: 1.6 s, LH: 6.6 s). When touching incorrect, prematurely, or too late (no touch), a time out period with illuminated house light followed. All parameters were

recorded, accuracy (# correct responses / # executed responses, in %), omissions (# trials without response / # presented stimuli, in %) and premature responses (# responses made before stimulus presentation) were analyzed.

2.4.3 Open Field Test (OFT)

A white PVC box (L40 x W40 x H40 cm; illumination: <25 Lux) was split into two virtual zones (outer zone: 10 cm away from the walls, inner zone: remaining part of 20 x 20 cm). Mice were placed into the chamber, facing the wall, and were allowed to explore the arena for 15 minutes. ANY-maze (4.99, Stoelting CO., USA) automatically assess the following parameters: time in zones, distance in zones, latency until the first entry into the center zone. Total distance moved was analyzed in 5-min bins. I analyzed risk assessment (stretch attend posture, SAPs) and rearing by an experimenter blind to the experimental conditions from recorded videos.

2.4.4 Elevated Plus Maze (EPM)

The plus-shaped, elevated (30.5 cm) maze consisted of four arms (L27.5 x W6 cm), connected by a central area (L6 x W6 cm). Two opposing arms were defined as "open", only engulfed by a 0.5 cm high rim, whereas the two others, "closed" arms contained side and end walls (H14.5 cm). In the 15 minutes test phase, mice were placed in the closed arms facing the end wall. Time and Distance in the closed, open and center zone was automatically tracked by ANY-maze. Videos for subsequent manual scoring of latency to first open arm entry, total duration of SAPs, rearing and head dipping events were recorded.

2.4.5 Dark Light Box (DaLi)

The setup is known as the dark light transition task, or light-dark box. Two compartments, dark (black PVC; W21 x L16 x H25 cm; illumination: <25 Lux) and lit (white PVC; W21 x L30 x H25 cm; illumination: 300 Lux) were connected by a small opening (W6.5 x H10). For 10 minutes, mice were allowed to explore the maze after they were placed into the dark compartment facing the wall. We analyzed the latency entering the lit compartment (full step-out with 4 paws) from videos, recorded using ANY-maze.

2.4.6 Beetle Mania Task (BMT)

The Beetle Mania Task (BMT) was performed during the inactive (3.3) or active (3.4) phase of the circadian rhythm. For each trial, mice were transported from the holding to the dimly lit experimental room and individually placed into the setups. Experiments were performed and the behavior was scored by experimenters unaware of the experimental conditions as essentially described before (Heinz et al., 2017, 2021).

In brief, during habituation, mice were allowed to acclimatize to the empty arena (grey PVC, L150 × W15 × H37 cm, illuminated with <25 Lux) for 5 min. During this habituation period, vertical (number of rearings) and horizontal (latency until exploration of the other end of the arena) exploration was scored. Thereafter, an erratically moving robo-beetle (Hexbug Nano, Innovation First Labs Inc., Greenville, TX, USA; L4.5 × W1.5 × H1.8 cm, weight: 7.3 g, mean speed: 25 cm/s) was placed into the arena and the behavior was scored for another 10 min. Upon physical contact with the beetle, the following behavioral parameters were scored online and expressed as a percentage of total contacts: tolerance (ignorance of the approaching robo-beetle), avoidance behavior

(withdrawals from the beetle with accelerated speed), the number of approach (whereby the experimental subject was following the robo-beetle in close contact) and the number of jumps.

2.5 Molecular Assessment and Proteomics

2.5.1 Generation of a MAGL-HA Virus

Cloning and virus packing took place in house in collaboration with Claudia Kühne, Carola Eggert and the Viral Core Unit.

HA-tag (atg taccctatgacgtgcccgattacgct) was N-terminally fused to mgll (NM_011844.4; TGA removed) and gblock construct was cloned into a viral suitable vector (Fig. 3). pAAV-hSyn-Dio-mCherry-plasmid (#50459) was purchased from addgene (Watertown, USA). Digestion of plasmid was performed with KpnI-HF and EcoRV-HF, and cloning was performed according to the manufacturer's instructions (Gibson Assembly® Cloning Kit; New England Biolabs, Frankfurt, Germany).

Target construct was amplified in competent bacteria (DH5α *e. coli*), incubated with 100 ng DNA on ice for 30 min, followed by a 42 °C heat shock for 2 min. Bacteria were plated, colony was picked and incubated in lysogeny broth medium overnight (37 °C). Plasmid DNA was extracted by Midiprep (PureLink® HiPure Plasmid Midiprep Kit; Qiagen, Hilden, Germany) according to the manufacturer's instructions.

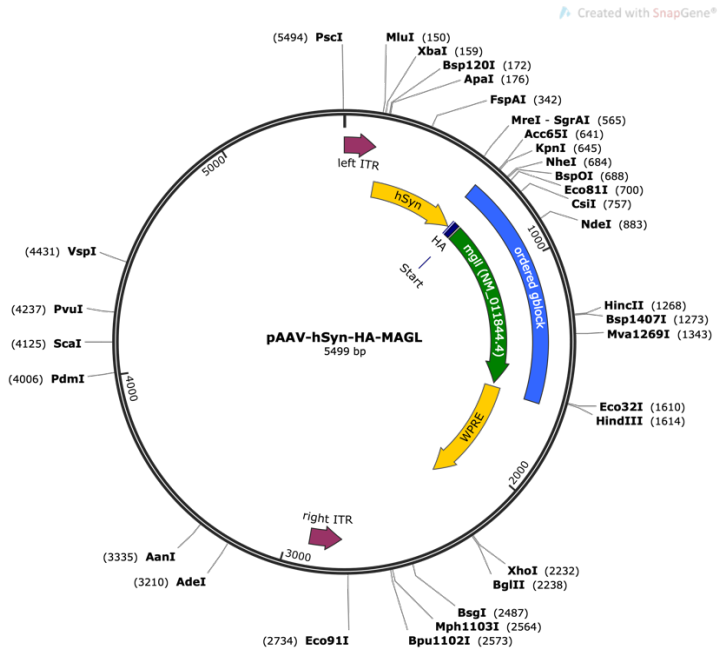

Figure 3: Cloning map of AAV1/2o-hSyn-HA-MAGL. MAGL-HA was fused to pAAV-hSyn-Dio-mCherry and packed as AAV.

Construct was packed into adeno associated virus (AAV; AAV1/2o-hSyn-HA-MAGL). Human embryonic kidney 293 cells (HEK293) were cultivated at 37 °C (5 % CO_2) in DMEM (Dulbecco's Modified Essential Medium; Life Technologies™) supplemented with heat inactivated fetal calf serum (10 %, hiFCS), non-essential amino acids, sodium pyruvate (1 mM) and penicillin-streptomycin.

HEK293 cells were plated onto 14.5 cm dishes and medium was changed to IMDM (Iscove's Modified Dulbecco's Medium; supplemented with 5 % hiFCS), 2-3 h prior transfection. Calcium Phosphate transfection (160 mM $CaCl_2$, 140 mM NaCl, 25 mM HEPES, 750 µM Na_2HPO_4) took place with 62.5 µg of target vectors mixed with helper plasmids (125 µg pFdelta6, 31.25 µg pRVI, 31.25 µg PH21).

Medium was changed to DMEM 20 h post transfection and cells were harvested after additional 48 h. Cells were transferred to falcon tubes in

PBS and resuspended in 150 mM NaCl, 20 mM Tris supplemented with 50 U/mL benzonase in 0.5 % sodium deoxycholate for 1 h at 37 °C and subsequently frozen at -20 °C.

For heparin affinity purification columns (HiTrap HeparinTM HP by GE Healthcare, Munich, Germany) were equilibrated (150 mM NaCl, 20 mM Tris). Supernatant (3000 g, 15 min, 4 °C) of defrosted (RT), samples was transferred onto column (flow rate: 1 mL/min). Before elution, columns were washed using increasing concentrations of NaCl (100mM NaCl, 20mM Tris; 200 mM NaCl, 20 mM Tris; 300 mM NaCl, 20 mM Tris). Further increasing concentrations (400, 450, 500 mM NaCl, 20 mM Tris) eluted virus using Amicon® Ultra-4-concentrators (Merck Millipore, Darmstadt, Germany).

2.5.1 Membrane Protein Biotinylation

In order to determine membrane composition, mouse hippocampal slices were prepared freshly from adult C57BL/6N mice using vibratome (Vibratom HM560, Thermo Fisher), and membrane proteins were biotynilated after vehicel or dexamethason stimulation as described before (Gabriel et al., 2014; Stepan et al., 2021). In brief, slices recovered in ACSF (artificial cerebrospinal fluid; 125 mM NaCl, 2.5 mM KCl, 1.2 mM NaH_2PO_4, 1.2 mM $MgCl_2$, 2.4 mM $CaCl_2$, 26 mM $NaHCO_3$, and 11 mM glucose) in self build chambers under constant supply of 95 % O_2 and 5 % CO_2 for 40 min (37 °C). Slices were washed (3 x with prewarmed ACSF) and incubated in oxygenated ACSF (95 % O_2 and 5 % CO_2) supplemented with vehicle or Dexamethason (Fortecortin® Inject; 100 mM) for 45 min. Subsequently, slices were cooled down by washing in ice cold ACSF (3 x). Biotinylation with sulfo-NHS-SS-biotin (1 mg/ml; #21331, Pierce) in ACSF took place in 12 well plates for 45 min on ice. Slices were washed (2 x ice

cold ACSF; 10 min) and free biotin was quenched by incubation in ice cold quench buffer (125 mM NaCl, 2.5 mM KCl, 1.2 mM NaH_2PO_4, 1.2 mM $MgCl_2$, 2.4 mM $CaCl_2$, 26 mM $NaHCO_3$, and 11 mM glucose, 100 mM glycine) for two times 25 min on ice. Repeated washing (3 x ice cold ACSF) was followed by transfer to LoBind (Eppendorf) tubes for lysis in ice cold RIPA buffer (10 mM Tris, pH 7.4, 150 mM NaCl, 1.0 mM EDTA, 1 % Triton-X-100, 0.1 % SDS, 1 % Na deoxycholate; Merck Millipore) supplemented with protease inhibitors (PI; Merck Millipore). Repeated pipetting using P100 pipette was followed by slightly rotating for 30 min at 4 °C. Cell debrits were pelleted by centrifugation (15 min, 4 °C, 18,000 x g) and protein concentration of supernatant was determined using BCA-assay (Pierce™ BCA Protein Assay Kit, Thermo Fisher).

Magnetic streptavidin beads (#11206D, Thermo) were equilibrated (3 x RIPA+PI on RT) and 20 µL were added to 400 µL of supernatant equalized in protein levels (diluted in RIPA+PI). Binding took place over night at 4 °C while rotating. Incubated beads were washed (3 x RIPA+PI) and air-dried. Pellet was sent to Mass Spectrometry for further analysis.

2.5.2 Interactome

Sample generation and preparation

C57BL/6N mice were stereotactically injected with AAV1/2o-hSyn-HA-MAGL or control virus in the hypothalamus (AP: -1.5; ML: 0.4; DV: 5.4; 300 nL) as described before (2.1.4). After more than 14 days, food restriction took place for at least one week (as described before 2.1.2). Brains were dissected and snap frozen on dry ice. Hypothalamus was collected using Sample Corers (Fine Science Tools, Heidelberg, Germany) in Protein LoBind (Eppendorf, Hamburg, Deutschland) tubes. Lysis took place using T-PER™ Protein Extraction Buffer (Thermo Fisher). Protein

concentration was determined using BCA (Pierce™, Thermo Fisher) and adjusted to 1.3 mg. 2.5 µg of anti-HA antibody (#C29F4 rabbit mAB; Cell Signaling) was added and incubated over night at 4 °C (on overhead shaker). Magnetic Protein G-Dynabeads (Invitrogen) were blocked with BSA, equilibrated and 20 µL were added to the lysate-antibody mix. Beads were incubated with lysate-antibody mix for 4 h at 4 °C and protein-beads mix was washed 3 times using DynaMag™ 2-magnet. Samples were air-dried and Mass Spectrometry performed at the Max Planck Institute of Biochemistry, Martinsried, Germany.

LS MS/MS

Mass Spectroscopy was performed in collaboration with the Core Facility Mass Spectrometry at the Max Planck Institute of Biochemistry (Nicole Krombholz, Barbara Steigenberger).

Data Analysis

Post-processing of the obtained data was performed in collaboration with the Gassen Lab, University Hospital Bonn, Bonn University, by Andreas Zellner.

2.5.3 Western Blot Candidate Proteins

Chosen proteins of interest were quantified in a second cohort of mice injected with AAV1/2o-hSyn-HA-MAGL into the ventral hypothalamus followed by ad libitum diet or FR+ as described above.

To investigate the location in the cellular compartments, membranous fraction was isolated using Calbiochem Proteo-Extract Kit (EMD Biosciences) as described before (Wagner et al., 2012, 2013). Equalized

protein content of both, cytosolic and membranous fractions were analyzed on following proteins: HA-tag (1:100; #C29F4, Cell Signaling) and HSP40 (1:100; #4868S, Cell Signaling). Images were analyzed and band intensities determined using ImageLab (BioRad).

2.5.4 Activity-Based Protein Profiling (ABPP)

Sample Preparation/ Lysis

Procedure was performed as collaboration with Mario van der Stelt, Leiden University, Netherlands. Samples were thawed on ice and a 15 µL/mg of ice-cold lysis buffer was added to each sample. Lysis buffer consists of 20 mM HEPES pH7.2, 2 mM DTT, 1 mM $MgCl_2$, 2.5 U/mL Benzonase in distilled water. Homogenization was performed using glass beads (1.0 mm, BioSpec, cat. No 11079110) in a FastPrep-24 homogenizer (MP biomedicals) for two times, 10 s.

Subsequently lysates were aliquoted, snap-frozen in liquid nitrogen and stored or used for gel analysis.

ABPP Measurements

Lysates (~1.5-2 µg/µL, 19 µL) were brought to room temperature (RT) and 0.5 µL of a 40x concentrated stock of probe in DMSO was supplemented.

FP-BODIPY and MB064 were combined by sequential addition beginning with MB064 (0.5 µL from a 10 µM stock), incubated for 15 min at RT, followed FP-BODIPY (0.5 µL from a 20 µM stock) incubated for 15 min at RT.

All samples were quenched by the adding 7.5 µL of 4*Laemmli buffer supplemented with β-Mercaptoethanol (1.25 v/v %). 15 µL of each sample was loaded on an acrylamide gel for SDS-PAGE (10 %) and resolved at

180 V for 75 min on RT. Gel was removed from glass plates and washed three times in distilled water.

Gels were analyzed on channels Cy5/near IR (120 s), Cy3/red (120 s) and Cy2/green (120 s) using ChemidocMP. Coomassie R250 staining and fixing solution was applied to gels for 30 min, followed by destaining in distilled water with a tissue paper overnight. One sample (nb. 1) was excluded due to strongly different protein pattern on the gel.

2.6 Statistical analysis

If not stated otherwise, data were post-processed using Microsoft Excel (v16.49; Microsoft, Redmond, USA). Statistic was calculated and plots were created using GraphPad Prism 9 (v9.1.1; GraphPad Software, La Jolla, CA, USA). If not stated otherwise data are presented as mean ± standard error of mean (SEM).

Behavioral studies: Statistical details about the used test and, if applicable, post-hoc test applied for each individual analysis are indicated in the results section. Two groups were compared using two-tailed (un-) paired t-test as (non-)repeated measures; 2-way ANOVA was used for multiple groups' comparison and repeated measures followed by Tukey's or Bonferroni post-hoc test. All Data are presented as mean ± standard error of mean (SEM). Significance was accepted as $p < 0.05$ (*/#), $p < 0.01$ (**/##), $p < 0.001$ (***/###) and $p < 0.0001$ (****/####).

Membranome/Interactome: Perseus software suite (v. 1.6.0.9) was used for filtering out containments, reverse hits, and protein groups, which were only identified by site. Membranome was analyzed by Frederik Dethloff (RG Turck, MPI Psychiatry), Interactome was analyzed by Andreas

Zellner (RG Gassen, UKB). Protein groups that were detected in at least 70 % of the replicates per condition were considered for the analysis, exclusively. The filtered data was log(2) transformed and missing values were imputed according to the normal distributed imputation algorithm implemented in the Perseus framework. Default values were used (width: 0.3; down shift: 1.8). To find the significantly regulated protein groups Students t-Test, analysis of variance (ANOVA), and volcano plot analysis, were performed with a false discovery rate (FDR) correction for multiple testing.

3. RESULTS

The following chapter contains four sections (3.1-3.4). I investigated the **Willingness to Work for Food** (3.1) in naïve wildtyp mice. With the use of targeted CB1 knockouts and chemogenetics, I evaluated CB1's role on a local, projections and network as well as biochemical perspective. The next section of this chapter (3.2) follows up on the main degrading enzyme of 2-AG. **Activity-dependent shuttling of MAGL** investigates the underlaying mechanism and tries to proof stated hypothesis in its regulation (Labar et al., 2010). **Measures of Anxiety and Fear** (3.3) investigates the impact of food restriction (FR+) and the pharmacological treatment with JZL184 as enzyme blocker of MAGL. Since CB1 is a key player in mediating the effects of enhanced 2-AG signaling – responsible for active fear reactions – I further evaluated its role. In section 3.4, **Effect of targeted deletion of the CB1 receptor on fear responses**, conditional and virally induced CB1 knockouts were tested on their behavior in the beetle mania task (BMT), as a measure of unconditioned, active fear responses (Heinz et al., 2017).

3.1 Working for Food

The willingness to work for food was assessed using the Bussey-Saksida touchscreen system (Horner et al., 2013; Heath et al., 2015). Within the Progressive Ratio (PR4) protocol, mice were allowed to unlimited work for food within a one-hour session while increasing effort (required Target Touches) from trial to trial. The session was completed after one hour or when the subject stopped to work for food (Breaking Point, BP). The number of total touches (Target Touches, TT) was assessed and illustrated in the following sections.

3.1.1 General Involvement of the ECS

Pharmacological blockade of CB1 using the inverse agonist SR (rimonabant, SR141716A; 3 mg/kg) did not affect the willingness of the animals to work for food (Fig. 4a) (RM one-way ANOVA: Treatment: $F(1.852, 20.38) = 0.773$, $p = 0.466$, followed by Tukey's post-hoc: Vhc-SR[3] $p = 0.921$). The failure to affect target touches by SR may indicate the general lack of involvement of the ECS under our experimental conditions. Treatment with exogenous agonists such as THC (Δ9-tetrahydrocannabinol; 1, 3 mg/kg), however, resulted in an increased willingness to work for food compared to vehicle (Vhc) treatment (Fig. 4b) in a CB1-dependent manner since the effect could be blocked by co-treatment with SR (Fig. 4b) (RM one-way ANOVA, Mixed-effect analysis: Treatment: $F(5, 49) = 15.40$, $p < 0.0001$, followed by Tukey's post-hoc: Vhc-THC[1] $p = 0.0001$, Vhc-THC[3] $p < 0.0001$, Vhc-THC[1]/SR[3] $p = 0.707$). Therewith, the ECS holds the general potential to increase appetite/ hunger via CB1. This, however, was only the case in food restricted mice but not after refeeding overnight (Fig. 4c) (Unpaired t-test, $t(28) = 1.162$, $p = 0.255$). Consequently, activation of CB1 receptors seems to enhance hunger rather than appetite for highly incentive food such as sweetened milk.

Since the ECS, in general, holds the capability to enhance the willingness to work for food, our failure to observe changes in operant behavior after treatment with the CB1 antagonist may reflect that either the ECS is not activated or endogenous tone of ECS is tightly controlled in food restricted animals, likely by the highly efficient degradation processes. Therefore, I blocked the degradation of 2-AG and AEA. Blockade of MAGL (monoacylglycerol lipase) as the main degrading enzyme of 2-AG using JZL184 (8, 16 mg/kg) caused the animals to work more for food (Fig. 4d) (RM one-way ANOVA, Mixed-effect analysis: Treatment: $F(4, 40) = 24.58$,

$p < 0.0001$, followed by Tukey's post-hoc: Vhc-JZL[8] $p = 0.0002$, Vhc-JZL[16] $p = 0.0021$). Co-treatment with SR blocked and reversed the effect (Fig. 4d) (Tukey's post-hoc: Vhc-JZL[16]/SR[3] $p = 0.0024$). The effects of JZL184 were transient and returned to baseline (PR) within 24 h (PR d+1; Fig. 4e) (RM one-way ANOVA, Mixed-effect analysis: Treatment: $F (2, 21) = 26.89$, $p < 0.0001$, followed by Tukey's post-hoc: PR-JZL[16] $p < 0.0001$, JZL[16]-PRd+1 $p < 0.0001$), and was absent in mice with free access to food the night before testing (Fig. 4f) (Unpaired t-test, $t(7) = 0.674$, $p = 0.523$). Blockage of FAAH using URB597 (0.3, 1 mg/kg) failed to modulate target touches (Fig. 4g) (RM one-way ANOVA, Mixed-effect analysis: Treatment: $F (3, 31) = 0.2815$, $p = 838$, followed by Tukey's post-hoc: Vhc-URB[.3] $p = 0.983$, Vhc-URB[1] $p = 0.836$).

I conclude from those data that activation of CB1 receptors increases the willingness of food-restricted animals to work for food. The bioavailability of 2-AG, however, which has similar consequences as exogenous THC, is tightly controlled by its degrading enzyme (MAGL). AEA, in contrast, is not implicated in the control of the willingness to work for food.

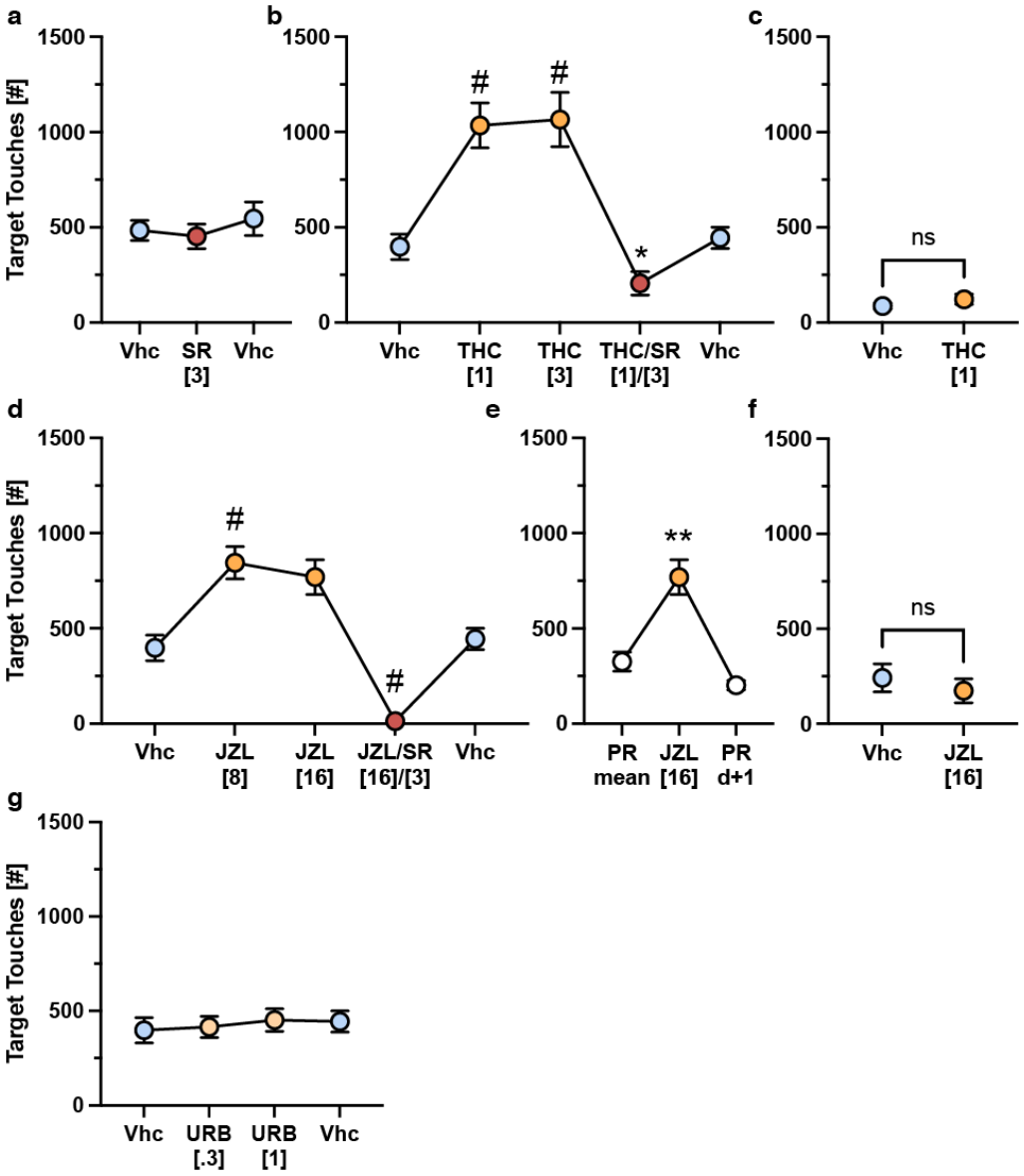

Figure 4: Pharmacological modulation of working for food. The number of Target Touches in the PR4 protocol are presented. The effect of **a** rimonabant (SR at 3 mg/kg, SR141716A), **b** THC (Δ9-tetrahydrocannabinol) at different dosages [1 and 3 mg/kg] and the co-treatment with THC and SR were shown under FR+. **C** Pharmacology of vehicle or THC in Devaluation (ad libitum fed overnight) mice. **D** Administration of JZL184 at 8 or 16 mg/kg was followed by a co-treatment with SR. **e** Untreated mice (white) were tested in PR4 (PR mean, twice three subsequent days) followed by at least two days FR5 and PR4 with pharmacological treatment and without treatment on the subsequent day (PR d+1). **F** Devaluated animals were treated with vehicle or JZL184 and tested in PR4. **G** Pharmacological injection of URB597 at 0.3 and 1 mg/kg. [#] Dose in mg/kg. # significantly different compared to Vhc, * significantly different to all other conditions. For further details see text.

To further explore consequences of pharmacologically enhanced 2-AG levels on motivational and consumption behavior, I performed the 5-choice serial reaction time task (5CSRTT) with a new cohort of mice. The effects of vehicle, JZL184 (16 mg/kg) and THC (1 and 3 mg/kg) were evaluated on accuracy, omissions, and the number of trials (Fig. 5a-c). None of the substances was able to interfere with the accuracy (RM one-way ANOVA: Treatment $F(4, 60) = 2.446$, $p = 0.0560$). Omissions, however, were influenced by THC at a dose of 3 mg/kg (RM one-way ANOVA: Treatment $F(4, 60) = 3.572$, $p = 0.0112$ followed by Tukey's post-hoc: Vhc-JZL[16] $p > 0.9999$, Vhc-THC[1] $p = 0.9931$, Vhc-THC[3] $p = 0.0376$). Number of trials could, similar to target touches in PR4, be enhanced (RM one-way ANOVA: Treatment $F(4, 60) = 5.030$, $p = 0.0015$ followed by Tukey's post-hoc: Vhc-JZL[16] $p = 0.1141$, Vhc-THC[1] $p = 0.0425$, Vhc-THC[3] $p = 0.8300$).

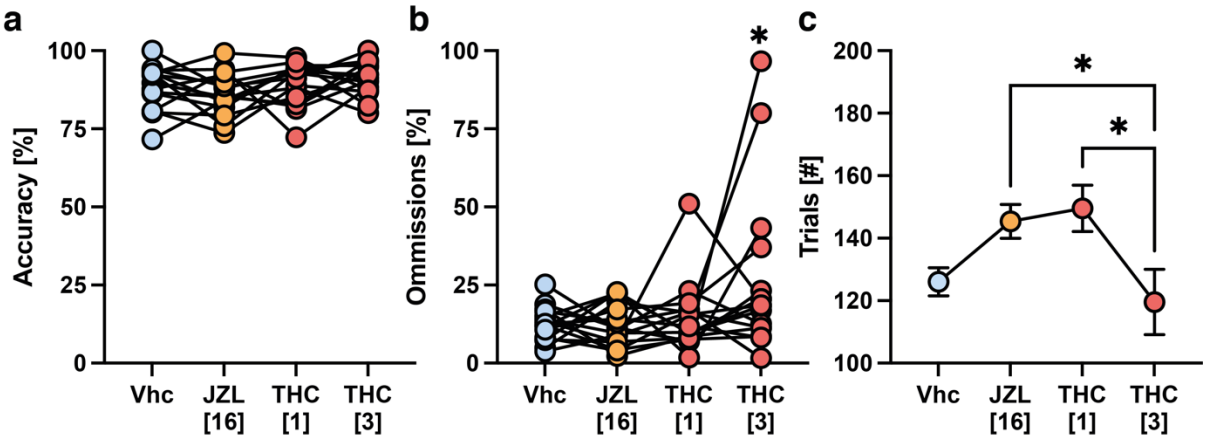

Figure 5: 5-Choice Serial Reaction Time Task (5CSRTT). The effect JZL184 and THC treatment assessed in **a** accuracy, **b** omissions and the **c** number of trials. For further details see text.

To conclude, JZL184 and THC (1, but no 3 mg/kg) were able to increase the willingness to work for food measured with the number of trials. Accuracy and omissions remained stable, increasing concentration of THC

(3 mg/kg), in contrast lead to increases in omissions. Thus, increased 2-AG levels seem to selectively increase the willingness to work for food.

3.1.2 Biochemical confirmation of 2-AG degradation

Many of the pharmacological compounds used to manipulate the ECS show promiscuous modes of action. To confirm the specificity of targeted MAGL inhibition by JZL184 (16 mg/kg), I evaluated the enzymatic profile (CES, FAAH, MAGL) of food restricted mice in specimens of the hypothalamus HYP) and nucleus accumbens (NAcc) of vehicle or JZL184 (16 mg/kg) treated, ad libitum fed and food restricted mice (FR-, FR+).

JZL184 caused a significant reduction in MAGL in both HYP (Fig. 6a; Treatment: $F(1, 16) = 14.39$, $p = 0.0016$, FR: $F(1, 16) = 1.229$, $p = 0.2841$, Interaction: $F(1, 16) = 0.2368$, $p = 0.6331$ followed by Tukey's post-hoc) and NAcc (Fig. 6d; ordinary two-way ANOVA Treatment: $F(1, 16) = 72.77$, $p < 0.0001$, FR: $F(1, 16) = 0.7061$, $p = 0.4131$, Interaction: $F(1, 16) = 1.459$, $p = 0.2447$ followed by Tukey's post-hoc) irrespective of the feeding state of the animals (Fig. 6). In addition, FAAH was significantly decreased in brain specimens of food restricted animals (Fig. 6b; Treatment: $F(1, 16) = 13.09$, $p = 0.0023$, FR: $F(1, 16) = 7.274$, $p = 0.0159$, Interaction: $F(1, 16) = 0.1695$, $p = 0.6860$ followed by Tukey's post-hoc; NAcc Fig. 6e; Treatment: $F(1, 16) = 6.001$, $p = 0.0262$, FR: $F(1, 16) = 1.821$, $p = 0.1960$, Interaction: $F(1, 16) = 0.955$, $p = 0.3430$ followed by Tukey's post-hoc), and CES1 almost completely blocked (Fig. 6c; Hyp: Treatment: $F(1, 16) = 20.57$, $p = 0.0003$, FR: $F(1, 16) = 1.793$, $p = 0.1993$, Interaction: $F(1, 16) = 1.649$, $p = 0.2173$ followed by Tukey's post-hoc; NAcc Fig. 6f; Treatment: $F(1, 16) = 8.127$, $p = 0.0116$, FR: $F(1, 16) = 0.0892$, $p = 0.7690$, Interaction: $F(1, 16) = 0.0356$, $p = 0.8529$ followed by Tukey's post-hoc).

To further demonstrate the selectivity of engagement of MAGL, I administered the MAGL inhibitor MJN110 (5 mg/kg) and observed a significant increase in the willingness to work for food, similar to JZL184 (Fig. 6i) (RM one-way ANOVA, Mixed-effect analysis: Treatment: $F(3, 41) = 31.04$, $p < 0.0001$, followed by Tukey's post-hoc: Vhc-JZL[16] $p < 0.0001$, Vhc-MJN110[5] $p = 0.0001$). In contrast, inhibition of ABHD6, another enzyme involved in the degradation of 2-AG, by KT203 (1 mg/kg) failed to affect the behavior (Fig. 6j). To reassure that the consequences of MAGL inhibition relate to the action of 2-AG, I inhibited DAGLα (by DH376, 50 mg/kg), the main synthesizing enzyme of 2-AG, and observed a significant decrease in the willingness to work for food, in particular in combination with the MAGL inhibitor JZL184 (Fig. 6k) (RM one-way ANOVA: Treatment: $F(3, 33) = 8.331$, $p = 0.0003$, followed by Tukey's post-hoc: Vhc-DH[50] $p = 0.127$, Vhc-DH[50]/JZL[16] $p = 0.0036$).

A contribution of the inhibition of FAAH to the behavioral consequences of JZL184 can be excluded since direct inhibition of the enzyme by URB597 has failed to alter the behavior (cf. Fig. 4g). To exclude a contribution of Ces1, I blocked the enzyme by WWL113 (50 mg/kg) but failed to observe any effect on the willingness to work for food in FR+ mice (Fig. 6l) (RM one-way ANOVA, Mixed-effect analysis: Treatment: $F(2, 26) = 1.408$, $p = 0.263$, followed by Tukey's post-hoc).

Finally, I measured endocannabinoid levels in brain punches from the nucleus accumbens and hypothalamus of ad libitum fed or food restricted mice 60 min after treatment with JZL184 (8 mg/kg) or vehicle. Treatment with JZL184 resulted in significantly enhanced 2-AG (Fig. 7a,d; Ordinary two-way ANOVA: Hyp: Treatment: $F(1, 18) = 28.27$, $p < 0.0001$, FR: $F(1, 18) = 3.009$, $p = 0.100$, Interaction: $F(1, 18) = 9.439$, $p = 0.0066$, followed by Tukey's post-hoc), but not AEA or AA (Fig. 7b,c,e,f; AEA: Treatment: $F(1, 18) = 0.5844$, $p = 0.455$, FR: $F(1, 18) = 0.2478$,

p = 0.625, Interaction: F (1, 18) = 1.720, p = 0.2062, AA: Treatment: F (1, 18) = 1.453, p = 0.244, FR: F (1, 18) = 0.351, p = 0.561, Interaction: F (1, 18) = 2.342, p = 0.143), levels in both brain structures and irrespective of the feeding status of the mice (NAcc: 2-AG: Treatment: F (1, 19) = 52.03, p < 0.0001, FR: F (1, 19) = 2.904, p = 0.105, Interaction: F (1, 19) = 2.766, p = 0.112 followed by Tukey's post-hoc; AEA: Treatment: F (1, 19) = 0.06, p = 0.810, FR: F (1, 19) = 0.620, p = 0.441, Interaction: F (1, 19) = 1.188, p = 0.2894; AA: Treatment: F (1, 19) = 6.555, p = 0.019, FR: F (1, 19) = 0.792, p = 0.385, Interaction: F (1, 19) = 2.476, p = 0.132). Interestingly, food restriction *per se* failed to affect 2-AG levels (FR-/VHC *vs.* FR+/VHC), thus confirming our initial assumption of highly efficient degradation by MAGL. Moreover, 2-AG levels were even more pronounced in the hypothalamus of food restricted vs. ad libitum fed mice after treatment with JZL184, pointing to a state-dependent increase in 2-AG metabolism in this brain area.

Taken together, I provide substantial evidence that the increased bioavailability of 2-AG after blockade of its degrading enzyme MAGL increases the willingness of the animals to work for food.

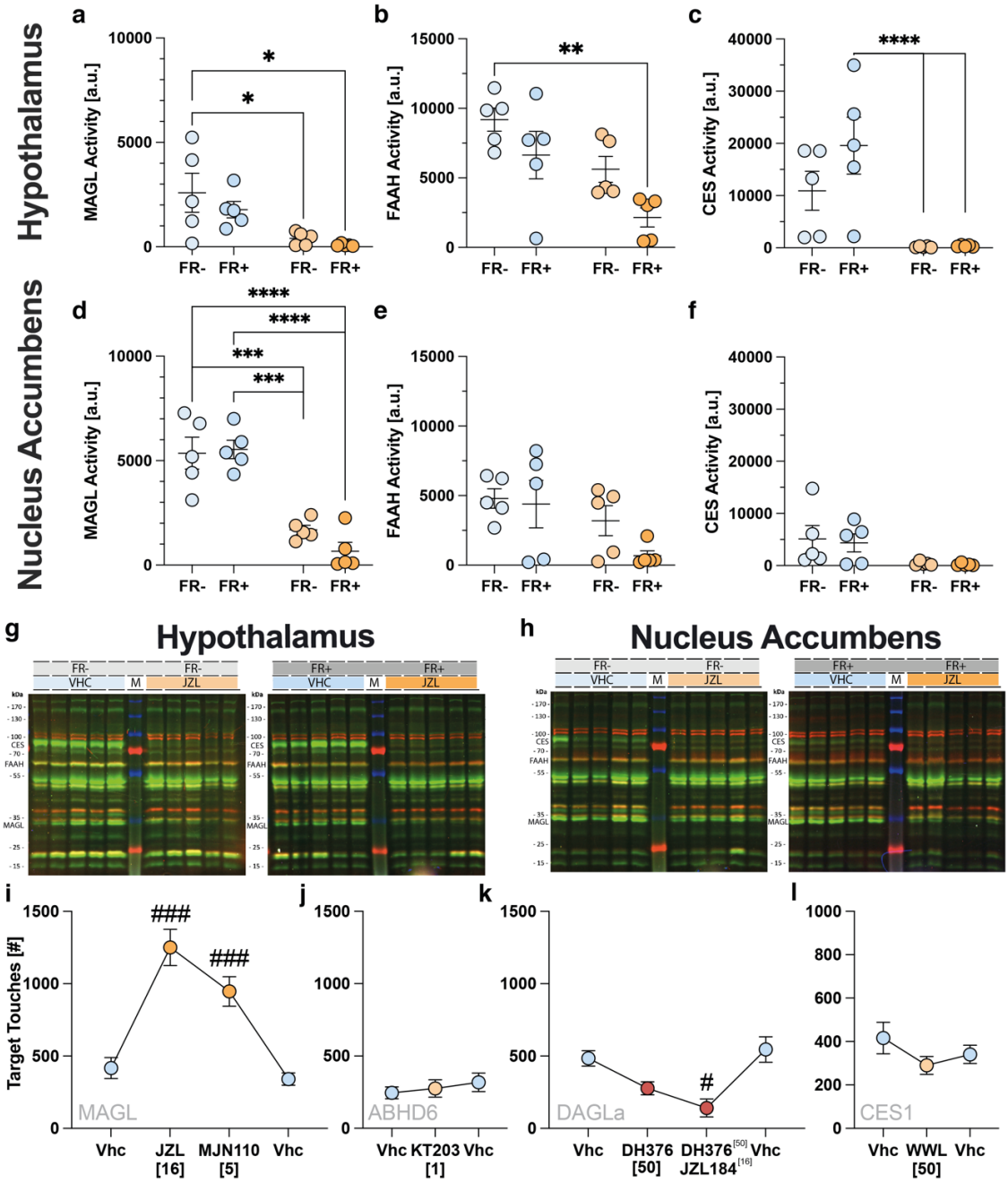

Figure 6: Biochemical profiling of FR+ and JZL184 by ABPP. Enzyme activity was determined of ad libitum fed (FR-) and food restricted (FR+) under vehicle (blue) or JZL184 (yellow) treatment in the hypothalamus (**a-c,g**) and the nucleus accumbens (**d-f,h**). Activity of monoacylglycerol lipase (MAGL; **a,d**), fatty acid amide hydrolase (FAAH; **b,e**) and carboxylesterase 1 (CES; **c,f**) were measured. Subsequent blockade of **i** MAGL by JZL184 (16 mg/kg) and MJN110 (5 mg/kg), **j** ABHD6 by KT203 (1 mg/kg), **k** DAGLa by DH376 (50 mg/kg) and the co-treatment with JZL184 (16 mg/kg), and **l** CES by WWL113 (50 mg/kg) in FR+ mice in the PR4 paradigm. #: data point different from vehicle. For further details see text.

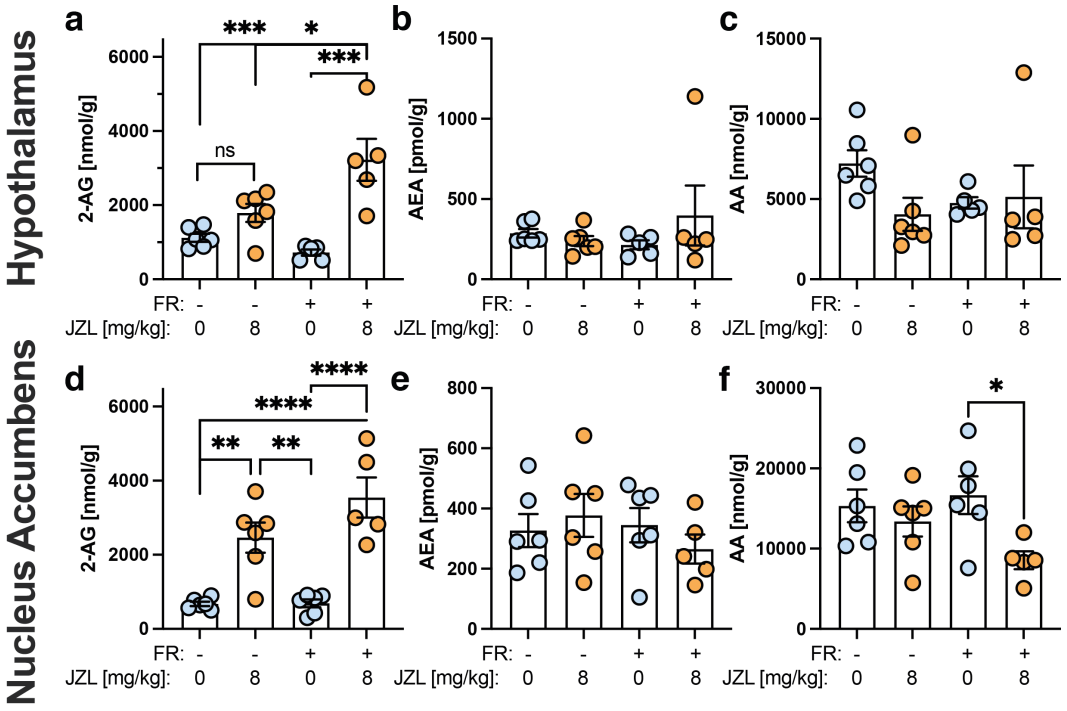

Figure 7: Endocannabinoid level under FR+ and JZL184 treatment. Endocannabinoid level determined of ad libitum fed (FR-) and food restricted (FR+) mice under vehicle (blue) or JZL184 (yellow) treatment in specimens from the hypothalamus (**a-c**) and the nucleus accumbens (**d-f**). Levels of **a,d** 2-AG, **b,e** anandamide and **c,f** arachidonic acid (AA). For further details see text.

3.1.3 Neuronal basis of 2-AG-mediated willingness to work for food

To identify the neuronal structures implicated in the JZL184-mediated effects on willingness to work for food, I studied its consequences in mice, which lack the expression of CB1 in distinct cell types or neuronal populations.

The effects of JZL184 were preserved in mice with selective deletion of CB1 from cortical glutamatergic neurons (Glu-CB1 (Nex-CB1); Fig. 8a; Two-way ANOVA: Treatment: $F(4, 76) = 47.75$, $p < 0.0001$, Genotype: $F(1, 20) = 0.07307$, $p = 0.790$, Interaction: $F(4, 76) = 2.065$, $p = 0.0937$, followed by Tukey's post-hoc: wt: Vhc-JZL[16] $p < 0.0001$; ko: Vhc-

JZL[16] p < 0.0001) and GABAergic forebrain neurons (GABA-CB1 (Dlx-CB1); Fig. 8b; Treatment: F (4, 56) = 10.30, p < 0.0001, Genotype: F (1, 14) = 3.730, p = 0.739, Interaction F (4, 56) = 0.3181, p = 0.8647, followed by Tukey's post-hoc: wt: Vhc-JZL[8] p = 0.0072; ko: Vhc-JZL[8] p = 0.0002).

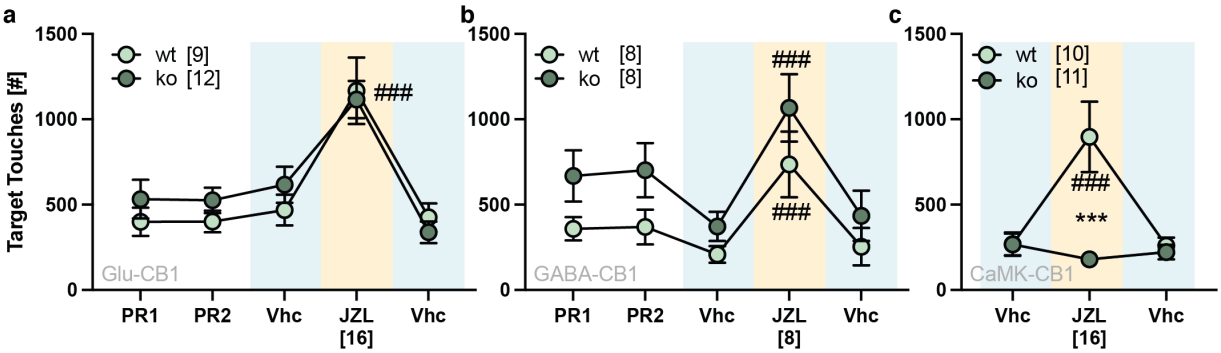

Figure 8: JZL184 effects upon cell type and brain region specific deletion of CB1 expression. Wildtype (wt) and knockout (ko) mice of **a** cortical glutamatergic CB1 (Nex-CB1), **b** forebrain GABAergic CB1 (Dlx-CB1) and **c** cortical and subcortical CaMK CB1. #: data point different from vehicle. *: difference between wt/B6 and ko/CB1ff. For further details see text.

Deletion from cortical and subcortical projection neurons of the forebrain, however, completely abolished the effects of JZL184 (CamK-CB1; Fig. 8c; Treatment: F (2, 37) = 6.456, p = 0.0039, Genotype: F (1, 20) = 10.44, p = 0.0042, Interaction F (2, 37) = 9.702, p = 0.0004, followed by Tukey's post-hoc: wt: Vhc-JZL[16] p < 0.0001, Vhc-JZL[16] p = 0.7775 or Bonferroni's post-hoc: JZL[16]: wt-ko p < 0.0001).

Given the overlap in recombination in the three mutant lines (Monory et al., 2007), Fig. 9, Fig. 2 as schematic overview) the exclusive absence of JZL184 effects in CamK-CB1 points towards an involvement of CB1 expression in subcortical glutamatergic neurons. Indeed, *in situ* hybridization revealed the almost complete absence of CB1 expression at

level of the posterior hypothalamus of CamK-CB1-KO, with no change in Glu-CB1-KO and a "slight" reduction in GABA-CB1-KO.

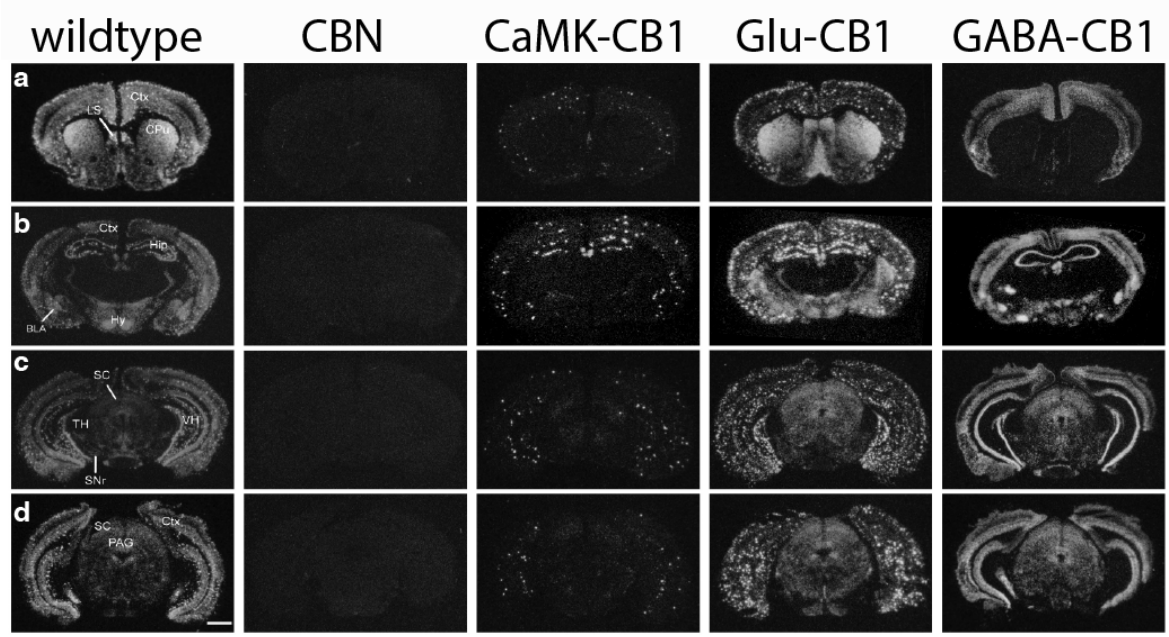

Figure 9: CB1 *in situ* hybridization of conditional CB1 knockouts. Different planes were shown: **a** Ctx: Cortex, CPu: Caudate Putamen, LS: Lateral Septum; **b** BLA: basolateral Amygdala, Hip: dorsal Hippocampus, Hy: Hypothalamus; **c** SC: Superior Colliculus SNr: Substantia Nigra, TH: Thalamus, VH: ventral Hippocampus. Adapted from Heinz, 2017.

With the help of our cooperation partners in Regensburg, I could confirm the selective expression of CB1 in subcortical glutamatergic hypothalamic neurons using RNAScope. There was an almost complete overlap in the expression of CB1 and VGlut2 (Fig. 10a), but not of CB1 and Gad2 as marker of GABAergic neurons (Fig. 10b).

Therefore, I can conclude that enhanced 2-AG level might mediate the increase in willingness to work for food via hypothalamic glutamatergic neurons.

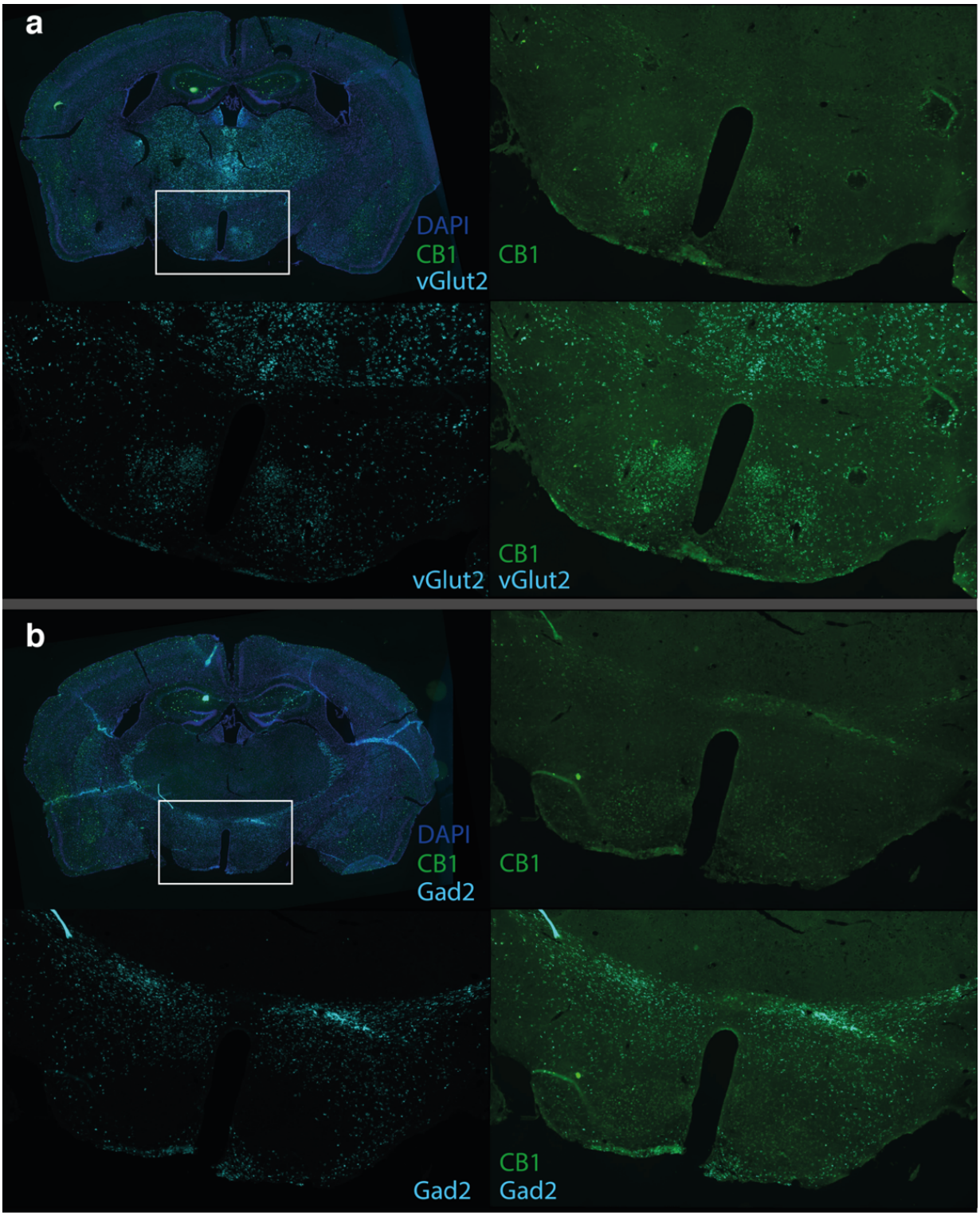

Figure 10: RNAScope *in situ* of wildtype B6N mice. Different markers as DAPI, CB1, **a** vGlut2 or **b** Gad2 were represented in different colors.

Enhanced 2-AG signaling is expected to restrict transmitter release from the projection neurons of the hypothalamus. To confirm the impact of this mode of action on the willingness to work for food, I expressed inhibitory DREADDs in projection neurons of the hypothalamus by injecting AAV-hSyn-DIO hM4Di into CamK-Cre mice. Treatment with CNO increased the willingness to work for food in a dose- and CB1-dependent manner (Fig. 11a) (One-way ANOVA: Treatment: $F(6, 61) = 8.357$ $p < 0.0001$. followed by Tukey's post-hoc: Vhc-CNO[5] $p = 0.9915$; Vhc-CNO[10] $p = 0.2665$; Vhc-CNO[15] $p < 0.0001$; CNO[15]-CNO/SR[15]/[3] $p = 0.0049$; SR[3]-Vhc $p = 0.9995$), which was not the case in control subjects (Fig. 11b; Paired t-test, $t(6) = 0.151$, $p = 0.885$).

To demonstrate the behavioral relevance of CB1 expression within this brain structure, I deleted CB1 from projection neurons of the hypothalamus using AAV-Cre under a CaMK promotor. Reconstruction of the recombination sites by *in situ* hybridization confirmed the deletion of CB1 expression in the entire posterior hypothalamus (Fig. 11d). Deletion of CB1 expression not only caused a general decrease in working for food but also completely abolished the JZL184-mediated effects on the willingness to work for food (Fig. 11c; Treatment: $F(4, 66) = 10.10$, $p < 0.0001$, Genotype: $F(1, 21) = 21.37$, $p = 0.0001$, Interaction $F(4, 66) = 5.696$, $p = 0.0005$, followed by Tukey's post-hoc: wt: Vhc-JZL[16] $p = 0.0004$; ko: Vhc-JZL[16] $p = 0.9991$; or Bonferroni's post-hoc: JZL[16]: wt-ko $p < 0.0001$).

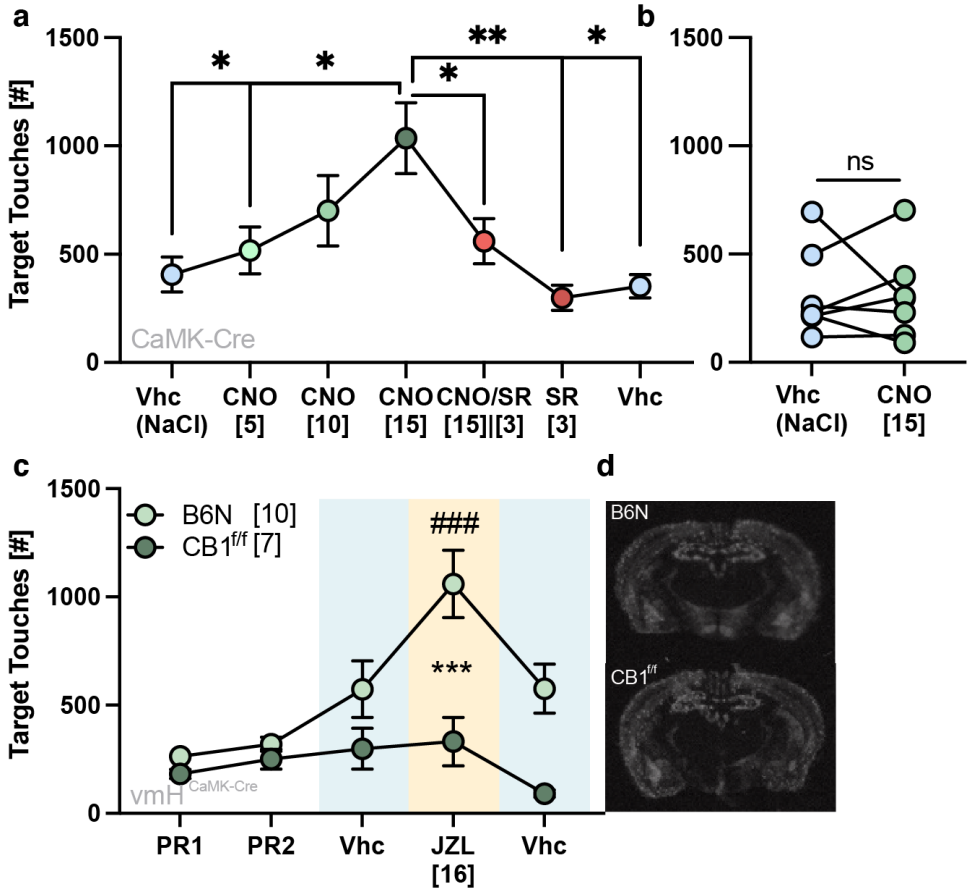

Figure 11: Selective manipulations of CaMK-positive hypothalamic neurons. a CaMK-Cre mice were targeted with an inhibitory DREADD construct (hM4Di) and pharmacologically exposed to CNO at 5, 10 or 15 mg/kg on different days (< two days of FR5 in between), followed by co-treatment with rimonabant and rimonabant alone followed. **b** A different cohort of mice injected with a control-virus was treated with vehicle an CNO and tested in the PR4 paradigm. **c** injection of AAV-CaMK-Cre into vmH of C57Bl6/N (B6N) or CB1ff mice with its **d** corresponding, representative CB1 *in situ* hybridization. #: data point different from vehicle. *: difference genotype. For further details see text.

To further dissect the neuronal population responsible for the JZL184 effects at level of the hypothalamus, I generated mice lacking CB1 on SF1-positive neurons. *In situ* hybridization confirmed the selective deletion of CB1 in the vmH of SF1 positive neurons (Fig. 12a). Other than its consequences on eating and hunger regulation by itself (Cardinal et al., 2014), selective deletion of CB1 from SF1-positive neurons failed to affect the willingness of the animals to work for food upon JZL184 treatment (Fig.

12b; Treatment: F (5, 80) = 32.74, p < 0.0001, Genotype: F (1, 21) = 1.327, p = 0.262, Interaction F (6, 80) = 1.955, p = 0.0944, followed by Tukey's post-hoc: wt: Vhc-JZL[8] p = 0.0076, Vhc-JZL[16] p < 0.0001; ko: Vhc-JZL[8] p = 0.0091, Vhc-JZL[16] p < 0.0001), with the exception of reduced target touches upon treatment with the highest dose (Bonferroni's post-hoc: JZL[16]: wt-ko p = 0.0109).

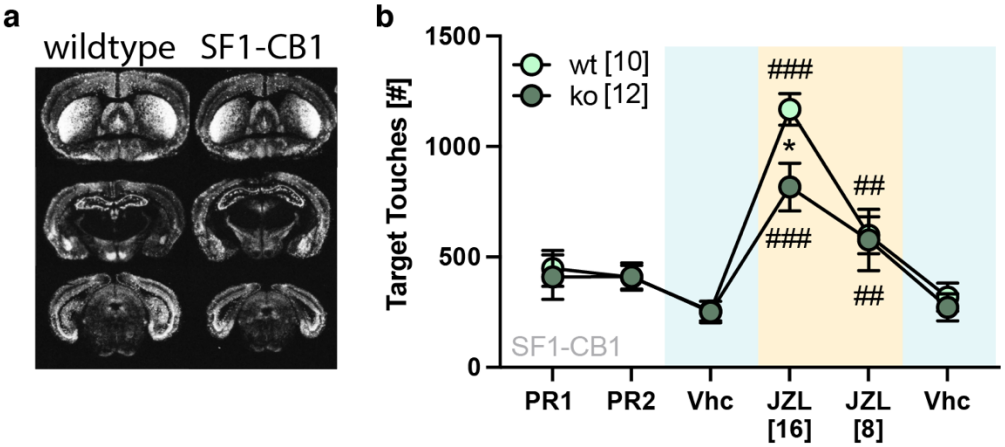

Figure 12: SF1-CB1 mice in the PR4 paradigm. a Expression pattern of Steroidogenic factor 1 (SF1)-CB1 wildtype and knockout mice. **b** SF1-CB1 wildtype (lit green) and knockout (dark green) mice were tested without (white) or with treatment (vehicle: blue, JZL184: yellow). #: data point different from vehicle. *: difference between wt and ko. For further details see text.

The effects of JZL184 were also preserved in mice with selective deletion of CB1 from POMC neurons (Fig. 13a) (Two-way ANOVA: Treatment: F (4, 76) = 17.79, p < 0.0001, Genotype: F (1, 19) = 0.0343, p = 0.8551, Interaction F (4, 76) = 0.586, p = 0.6740, followed by Tukey's post-hoc: wt: Vhc-JZL[16] p < 0.0001; ko: Vhc-JZL[16] p < 0.0001). In contrast to previous reports (Koch et al., 2015), I failed to demonstrate co-expression of POMC and CB1 in the Arc. This may explain the lack of effects seen in POMC-CB1 mice (Fig. 13b).

Still there is the opportunity that 2-AG mediated inhibition of excitatory projection from the hypothalamus to POMC neurons (i.e., the satiety neurons) (Conde et al., 2016) mediate the increase in food upon treatment with MAGL inhibitors. To explore this possibility, I studied afferents to POMC

neurons by patching tdTomato-positive POMC neurons while stimulating putative afferent sites within the hypothalamus. I failed to observe changes in electrophysiological properties by agonizing CB1 receptor on projections to POMC neurons by ACEA for any of the stimulation sites (Fig. 13c-e; Site S1, S2). This argues against the scenario suggested above. However, ACEA reduced spontaneous excitatory postsynaptic currents (sEPSCs; Fig. 13f,g; paired t-test, $t(20) = 4.989$, $p < 0.0001$). Therefore, this regulatory mechanism seem to exist for other glutamatergic afferences to POMC neurons than those originating from S1 or S2.

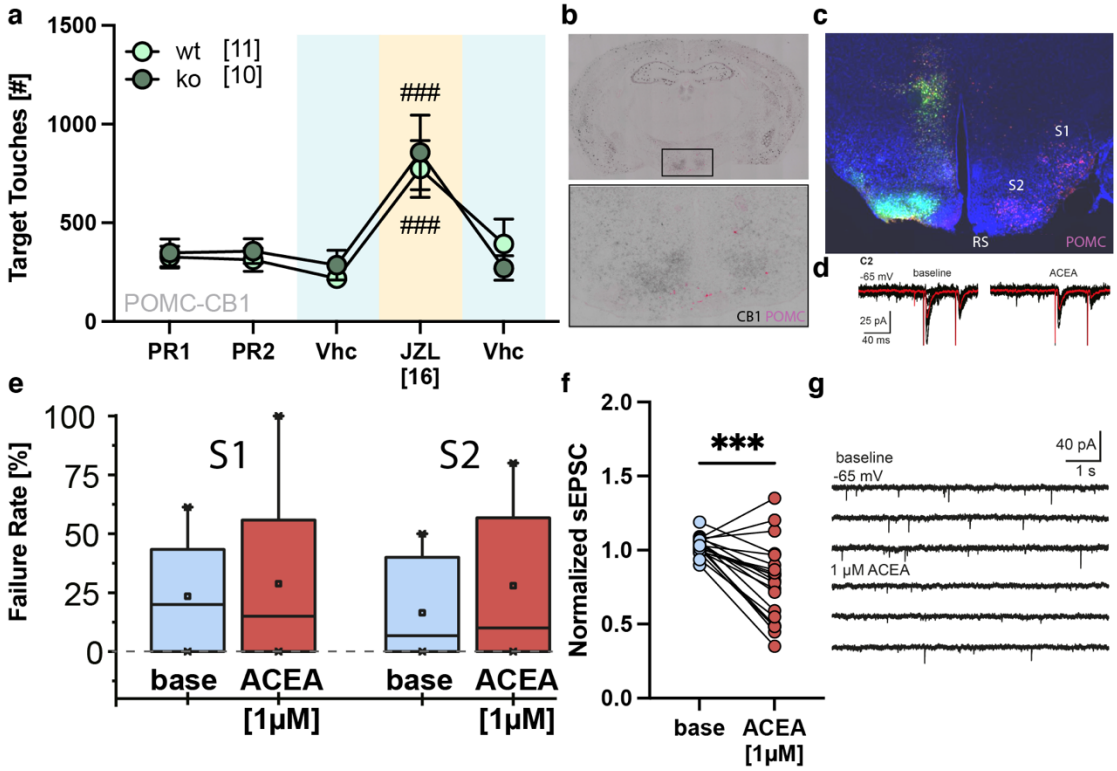

Figure 13: CB1's role in regulating the activity of pro-opio-melanocortin (POMC) positive neurons. a POMC wildtype (lit green) and knockout (dark green) mice were tested without (white) or with treatment (vehicle: blue, JZL184: yellow). **b** Virtually no co-expression of CB1 (black) and POMC (red) in the vmH and Arc of wildtype littermates (contrast and brightness adjusted) revealed by double ISH. **c** POMC-Cre-Ai9 mice were used to dissect electrophysiological properties of glutamatergic afferences from two different stimulus sites (S1, S2) to tdTomato-positive neurons of the Arc (recording site, RS). **d,e** Infusion with ACEA as a CB1 agonist did not result in changes in electrophysiological properties when stimulation in S1 or S2. **f,g** sEPCSs could be modulated by stimulation of CB1 with ACEA. #: data point different from vehicle. For further details see text.

In order to validate the arcuate nucleus as a potential key regulator of the CB1 mediated effect in working for food, I injected small volumes of AAV-CaMK-Cre into the Arc of CB1ff and B6N control mice. Targeted deletion of CB1 in the Arc and nearly hypothalamic areas (Fig. 14a) led to slight changes in baseline working for food (Fig. 14b). The effect of JZL184 was completely absent in CB1ff, but not in wildtype controls (Fig. 14b; Treatment: $F(4, 32) = 16.90$, $p < 0.0001$, Genotype: $F(1, 8) = 34.31$, $p = 0.0004$, Interaction $F(4, 32) = 12.43$, $p < 0.0001$, followed by Bonferroni's post-hoc: PR1: B6N-CB1ff $p = 0.8118$; Vhc: B6N-CB1ff $p = 0.0006$; JZL[16]: B6N-CB1ff $p < 0.0001$ and Tukey's post-hoc: B6N: Vhc-JZL[16] $p < 0.0001$; CB1ff: Vhc-JZL[16] $p = 0.9521$).

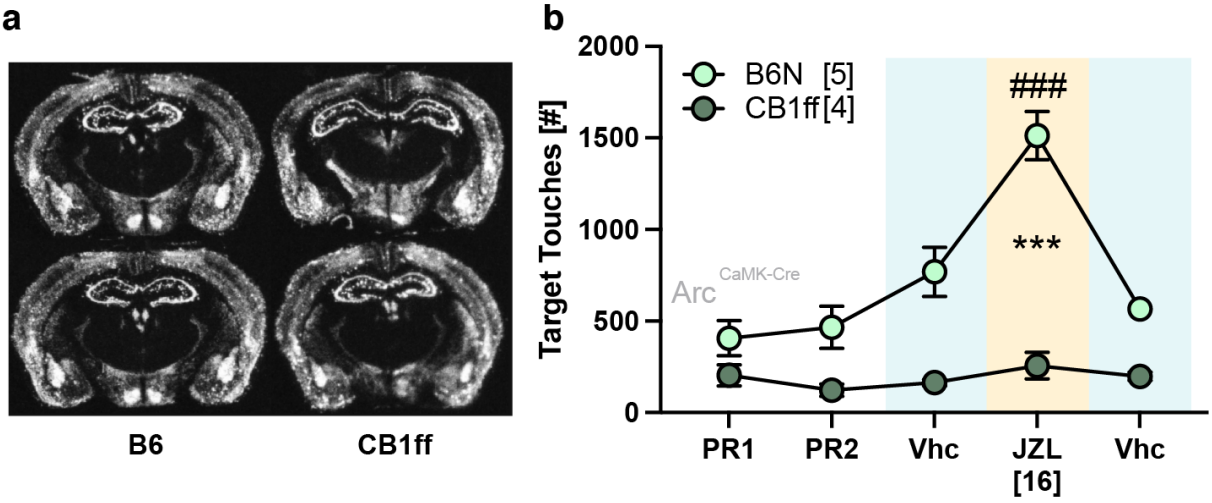

Figure 14: Targeted deletion of CB1 in the neurons of the Arcuate Nucleus (Arc). a Performance in the Progressive Ratio (PR) Task and **b** representative pictures of two CB1 situ hybridizations per condition. #: data point different from vehicle. *: difference between B6 and CB1ff. For further details see text.

With these data I could pin down the essential contribution of CB1 in the Arc as a sub-structure of the Hyp (Fig. 2, Fig. 28a). Further effort is needed to fully understand the underlying projections outgoing from CaMK-positive neurons in the Arc.

3.1.4 What drives the 2-AG system in food restricted mice?

After successful characterization of the neuroanatomical basis of the effects of MAGL inhibition, the question remains as to the mechanism underlying 2-AG release and MAGL activation upon food restriction. From the literature it is known, that the "on demand" synthesis and the subsequent release of 2-AG is controlled by a variety of factors such as the activation of mGluR5 (Ohno-Shosaku et al., 2002; Batista et al., 2016), Ghrelin (Kola et al., 2008; Lim et al., 2013), testosterone (Conde et al., 2017) or corticosterone (Hill et al., 2010b).

To assess the contribution of mGluR5 signaling to JZL184 effects on the willingness to work for food, I blocked mGluR5 by repeated injections of CTEP (24 and 2 hours before exposure to PR) before treatment with JZL184. Against our expectations (Batista et al., 2016), blockade of mGluR5 not only failed to attenuate the promoting effects of MAGL inhibition, but even further enhanced the willingness to work for food (Fig. 15a) (One-way ANOVA: Treatment: $F(4, 38) = 23.99$, $p < 0.0001$ followed by Tukey's post-hoc: Vhc-JZL[16] $p = 0.0387$, Vhc-JZL/CTEP[16]/[2] $p < 0.0001$, Vhc-CTEP[2] $p = 0.4832$).

Hormones from the general circulation may trigger 2-AG synthesis within the brain. Depending on the animal's feeding state, Ghrelin (i) holds the potential to activate 2-AG signaling (Kola et al., 2008), and (ii) plasma levels of Ghrelin are significantly elevated in food restricted vs. ad libitum fed mice independent of MAGL inhibition (Fig. 15b) (Treatment: $F(1, 44) = 0.7338$, $p = 0.3963$, FR: $F(1, 44) = 32.89$, $p < 0.0001$, Interaction: $F(1, 44) = 0.1196$, $p = 0.7322$ followed by Tukey's post-hoc: FR[-]Vhc-FR[+]Vhc $p = 0.0023$, FR[-]Vhc-FR[-]JZL $p = 0.9835$, FR[-]Vhc-FR[+]JZL $p = 0.0002$, FR[+]Vhc-FR[-]JZL $p = 0.0066$, FR[+]Vhc-FR[+]JZL $p = 0.8306$, FR[-]JZL-FR[+]JZL $p = 0.0005$). In turn, treatment with JZL184 failed to affect Ghrelin levels (Fig. 15b), thus precluding that its

effects on the willingness to work for food is mediated via changes in the "hunger" hormone Ghrelin. Systemic administration of Ghrelin to food restricted animals failed to further enhance the JZL184-mediated effects in food restricted or devaluated (ad libitum feeding overnight) mice (Fig. 15c; RM One-way ANOVA: Treatment: $F(3, 33) = 13.46$, $p < 0.0001$ followed by Tukey's post-hoc: Vhc-Ghrelin[.08] $p = 0.8749$, Vhc-G/JZL[.08]/[16] $p < 0.0001$; unpaired t-test: $t(10) = 0.2592$, $p = 0.8007$), which does not support a role as a trigger of 2-AG signaling.

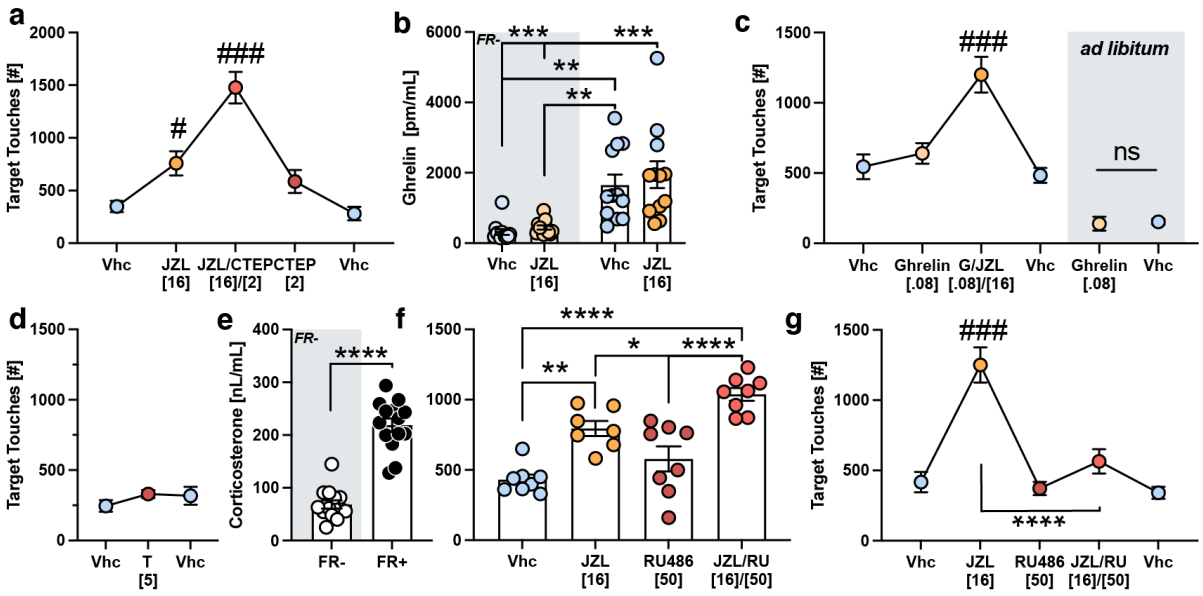

Figure 15: Role of mGluR5, Ghrelin (G), Testosterone (T) and the Glucocorticoid receptor (GR) in the willingness to work for food. a Receptor blockage of mGluR5 using CTEP (2 mg/kg; 24 and 2 h before PR) alone or co-treated with JZL184. **b** Plasma levels of Ghrelin of ad libitum (FR-, left, lit colors) and food restricted (FR+, right, dark colors) mice treated with vehicle (blue) or JZL184 (yellow) 1 h before blood collection. **c** Behavioral consequences of Ghrelin (G, 80 µg/kg) administration to food restricted (FR+) mice or after ad libitum feeding overnight. **d** Treatment with testosterone (5 mg/kg) in the PR4 paradigm. Corticosterone levels of **e** naïve FR- or FR+ mice or **f** FR+ mice pre-treated with vehicle, JZL184, the GR antagonist RU486 or co-treated with JZL184 and RU486. **g** behavioral evaluation of RU486 in a new cohort of FR+ mice. #: data point different from vehicle. For further details see text.

Exogenous testosterone may restrain the activity of the "satiety" (i.e., POMC) neurons of the arcuate nucleus by attenuating the excitatory drive in a CB1-mediated manner (Conde et al., 2016). Under very experimental conditions, however, treatment with testosterone failed to affect the willingness to work for food (Fig. 15d; One-way ANOVA: Treatment: $F(2, 18) = 2.840$, $p = 0.0847$).

Food restriction also led to increased plasma levels of corticosterone in untreated mice (Fig. 15e; unpaired t-test $t(26) = 10.20$, $p < 0.0001$), which holds the capability of activating endocannabinoid signaling (Hill et al., 2010b). Strikingly, treatment with JZL184 even further enhance corticosterone level (Fig. 15f, Vhc vs. JZL184). These effects were largely independent of potential feedback loops of corticosterone via glucocorticoid receptors, since treatment with RU486 failed to affect them. If at all, co-treatment of JZL184 and RU486 slightly enhanced plasma corticosterone compared to JZL184 alone (Fig. 15f; two-way ANOVA: RU486: $F(1, 27) = 10.57$, $p = 0.0031$, JZL184: $F(1, 27) = 47.14$, $p < 0.0001$, Interaction: $F(1, 27) = 0.6503$, $p = 0.4270$ followed by Tukey's post-hoc: Vhc-JZL[16] $p = 0.0014$, Vhc-RU486[50] $p = 0.3140$, Vhc-JZL/RU[16]/[50] $p < 0.0001$).

Co-treatment of JZL184 and RU486 completely abolished the increased willingness to work for food induced by JZL184 alone (Fig. 15g; one-way ANOVA: Treatment $F(4, 55) = 34.21$, $p < 0.0001$, followed by Tukey's post-hoc: Vhc-JZL[16] $p < 0.0001$, Vhc-RU486[50] $p = 0.9951$, Vhc-JZL/RU[16]/[50] $p = 0.4506$, JZL[16]-JZL/RU[16]/[50] $p < 0.0001$). Consequently, elevated plasma levels of corticosterone hold the capacity of increasing the willingness to work for food by activating 2-AG signaling in a GR-dependent manner. This effect, however, is constrained if not abolished by efficient MAGL-mediated degradation of 2-AG.

3.2 Activity-dependent shuttling of MAGL

If glucocorticoids (e.g., corticosterone) trigger 2-AG signaling which, however, only becomes evident if 2-AG degradation by MAGL is blocked, the question arose of whether or not they may also affect MAGL itself. To explore this supposition, I used unbiased membrane biotinylation to compare the membrane's composition of vehicle vs. dexamethasone treated mouse hippocampi. Freshly dissected hippocampi were allowed to recover and subsequently incubated in vehicle or dexamethasone (100 nM). Biotin was added and membranous proteins were labelled accordingly (Fig. 16a). Brain tissue was lysed, and biotin labeled proteins were precipitated using streptavidin magnetic beads. Purified beads with proteins were analyzed using mass spectrometry (Fig. 16b). The unbiased experiment resulted in various changes in membrane composition (parts of the data were published elsewhere: Stepan et al., 2021). Dexamethasone treatment led to less MAGL in the membranous fraction compared to vehicle treated slices (Fig. 16c) (unpaired t-test, $t(6) = 3.654$ $p = 0.0053$; processing details are given in the Methods section).

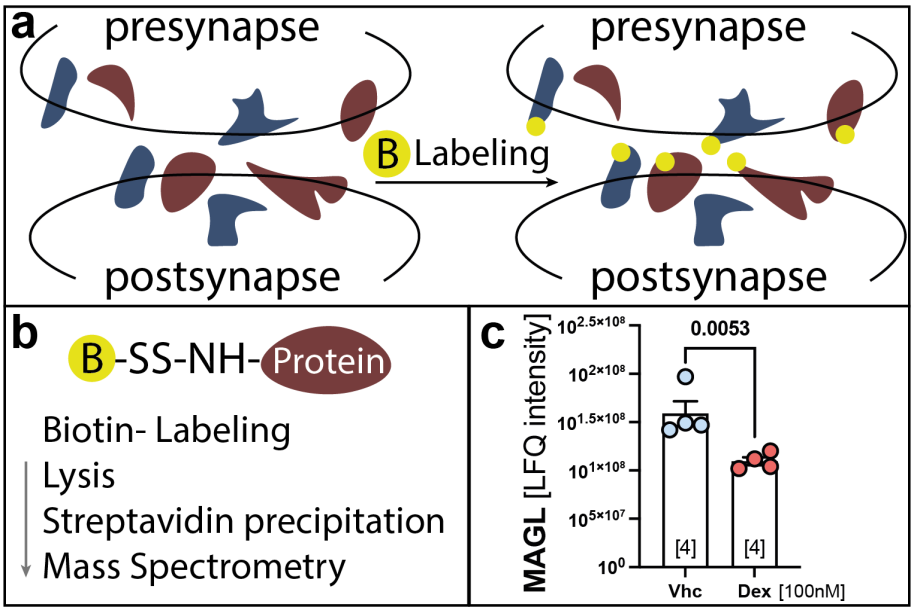

Figure 16: Biotin labeling of membranous N-termini. a pre- and postsynaptic proteins were labeled with Biotin (yellow, B). **b** After labeling, tissue was lysed, and target proteins were purified by streptavidin precipitation followed by mass spectrometry. **c** Membranous MAGL was reduced in Dexamethasone (Dex) treated compared to vehicle (Vhc) treated brain slices.

In order to control between cytosolic and membranous fractions, I generated a MAGL-construct expressing an artificial HA-tag (cf. Fig. 3). Comparing FR- and FR+ mice in their membrane composition, MAGL was detectable by Western blot in membranes of FR+, but not ad libitum fed mice, exclusively (Fig. 17).

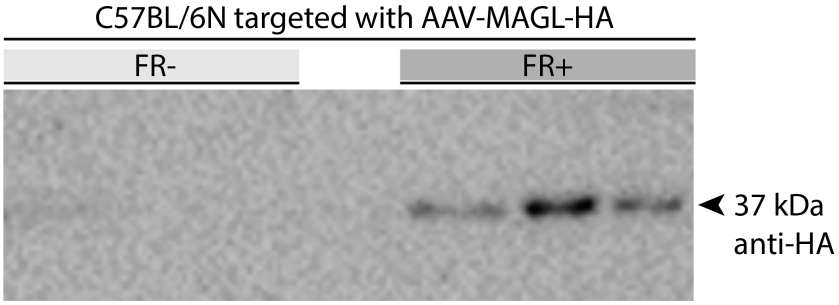

Figure 17: Membranous MAGL-HA in FR- and FR+ animals. C57BL/6N were virally targeted with MAGL-HA expressing construct. Mouse Hyp were dissected, and membranous fraction analyzed on HA (37 kDa)-expression.

By the use of MAGL-HA, I was able to identify interaction partners of MAGL in three groups: control (without HA-tag), MAGL-HA in FR+ and MAGL-HA in FR- mice. MAGL was shown to significantly interact with itself in FR+, compared to FR- mice (table 4; ANOVA, $p < 0.0001$). This supports a potential di- or mulit- merization of MAGL. Additional significant interaction partners of MAGL-HA in FR+ mice were: DnaJ homolog subfamily A member 1 (ANOVA, $p = 0.0007$), Protein FAM49B (ANOVA, $p = 0.0005$), 60s acidic ribosomal protein P2 (ANOVA, $p = 0.0043$), and Transmembrane emp24 domain-containing protein 2 (ANOVA, $p = 0.0034$).

Taken together, MAGL translocation seems to be influenced by physiological and pharmacological stressors. It remains to be shown if dexamethasone may influence protein synthesis as well. Further validation is needed to characterize MAGL's potential interaction partners including a potential dimerization.

Table 4: MAGL-Interactome. Table displays ANOVA-results of the MAGL-HA interactome analysis. Detected proteins of technical nature were *italic*. Proteins in **bold** were showed to be significant after t-test between groups.

Proteins interacting with MAGL-HA		
Protein names	**Gene names**	**p value**
Immunoglobulin kappa variable 9-123	*Igkv9-123*	*0.0000*
Monoglyceride lipase	Mgll	0.0000
Protein FAM49B	Fam49b	0.0005
DnaJ homolog subfamily A member 1	Dna ja 1	0.0007
Transmembrane emp24 domain-containing protein 2	Tmed2	0.0034
60S acidic ribosomal protein P2	Rplp2	0.0043
	Ighv7-1	*0.0090*
Hippocalcin-like protein 1	Hpcal1	0.0103
Prolactin	Prl	0.0119
	Ighv7-3	*0.0154*
1g lambda-2 chain C region	*Iglc2*	*0.0158*
Vesicle-associated membrane protein 1	Vamp1	0.0242
Amino acid transporter;Neutral amino acid transporter A	Slcla4	0.0267
	Ighv1-80	*0.0380*
Syntaxin-1B	Stx1b	0.0413
GTPase KRas;GTPase KRas, N-terminally processed	Kras;Hras	0.0428
Golgi-associated plant pathogenesis-related protein 1	Glipr2	0.0516
Myelin proteolipid protein	Plp1	0.0551
Histone H4	Histlh4a	0.0563
NADH dehydrogenase [ubiquinone] iron-sulfur protein 7, mitochondrial	Ndufs7	0.0581
Glial fibrillary acidic protein	Gfap	0.0606
Complement C1q subcomponent subunit B	C1qb	0.0630
Claudin-11	Cldn11	0.0392
Syntaxin-1B	Stx1b	0.0413
Ig kappa chain V-V region L6; 1g kappa chain V-V region T1		*0.0672*

3.3 Measures of Anxiety and Fear

Whereas the first chapters investigated the role of elevated 2-AG levels within the positive valence system, in this chapter I focus on its implications on the negative valence system. Previously, I could demonstrate the impact of food restriction on anxiety and fear behavior (Heinz et al., 2021). Here, I investigate potential interactions between FR+ and the inhibition of MAGL. To this end, mice were randomly assigned to four groups (n=12 each) before the start of experiments. Baseline body weight was assessed and optimum range (85 % ±5 %; dotted lines, Fig. 18a) was calculated. Two groups were food restricted (FR+, dark green), whereas the remaining mice were fed ad libitum (FR-, lit green) over the course of experiments. Treatment groups were assigned and remained throughout the different behavioral tasks as acutely treated with Vehicle (0, blue, Fig. 18-21) or JZL184 (16 mg/kg, yellow, Fig. 18-21). With one week in between, mice were exposed to open field task (OFT), elevated plus maze (EPM), dark light box (DaLi) and beetle mania task (BMT) behavioral paradigms (Fig. 18a).

3.3.1 Exploration-based tests

Mice were allowed to freely explore the OFT for 15 min. Locomotion was significantly reduced in FR+, JZL184-treated mice compared to the other groups for which locomotion was unchanged (Fig. 18b ordinary two-way ANOVA, Treatment: $F(1, 44) = 0.731$, $p = 0.3972$, FR: $F(1, 44) = 3.831$, $p = 0.0567$, Interaction: $F(1, 44) = 3.715$, $p = 0.0604$, followed by Tukey's post-hoc: FR-[16]-FR+[16] $p = 0.0416$). Most animals entered the center zone with short latency (Fig. 18c). FR+, vehicle treated mice, tended to show longer latencies (Treatment: $F(1, 44) = 1.480$, $p = 0.2303$, FR: $F(1, 44) = 3.210$, $p = 0.0801$, Interaction: $F(1, 44) = 2.990$, $p = 0.0908$,

followed by Tukey's post-hoc: FR-[0]-FR+[0] p = 0.0756). Measures within the center zone were reduced under FR+ (FR+<FR-) independent of the respective treatment group (Fig. 18d,e; Center Zone Time, Fig. 18d, Treatment: F (1, 44) = 0.0312, p = 0.8607, FR: F (1, 44) = 3.515, p = 0.0675, Interaction: F (1, 44) = 0.0651, p = 0.7998; Center Zone Distance, Fig. 18e, Treatment: F (1, 44) = 0.1491, p = 0.7013, FR: F (1, 44) = 7.096, p = 0.0108, Interaction: F (1, 44) = 0.0043, p = 0.9480.)

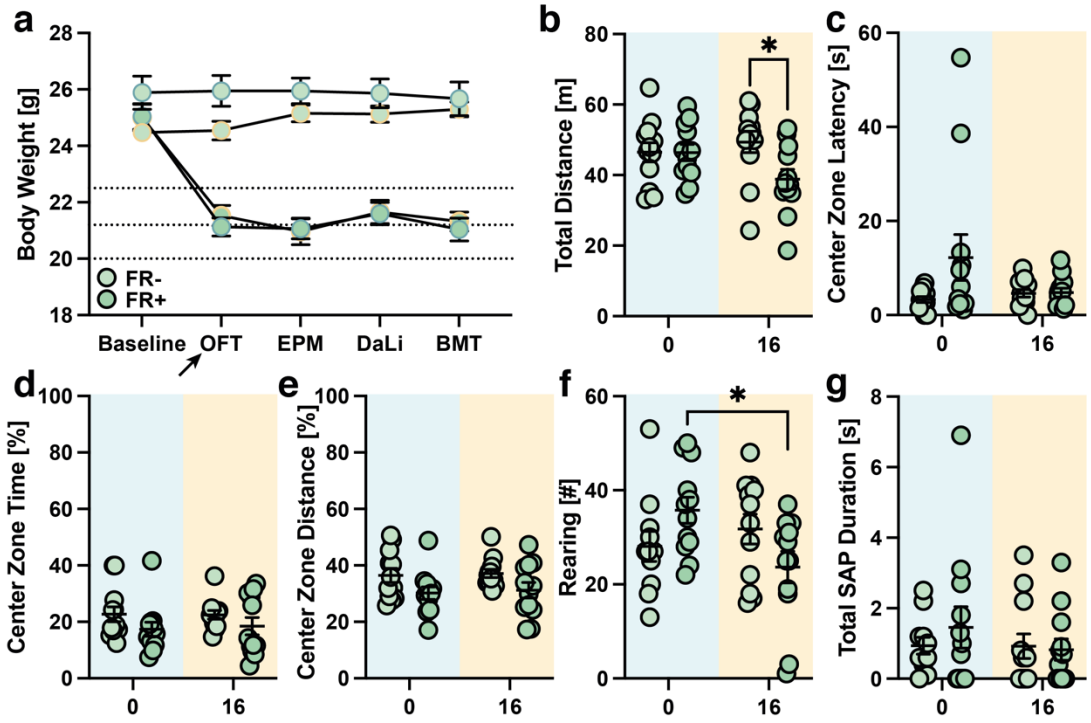

Figure 18: Experimental Overview and Open Field Task (OFT). a After a baseline measurement, mice were ad libitum fed (FR-, lit green, left) or food restricted (FR+, dark green; right) over the course of the experiment. Optimum body weight range is indicated (upper: 90 %, middle: 85 %, lower 80 % from the groups baseline body weight). Mice were intraperitoneally injected with 0 (blue) or 16 (yellow) mg/kg of JZL184 one hour before exposure to the behavioral test. **b-g**: OFT behavior with **b** total distance moved, **c** Latency to enter the center zone, **d** time and **e** distance in the center zone (normalized to total distance), **f** number of rearing and **g** duration of stretch attend postures (SAP) were assessed. For further details see text.

Rearing as active markers of vertical activity was significantly reduced after treatment of JZL184 in FR+ mice (Fig. 18f, ordinary 2-way ANOVA,

Treatment: F (1, 43) = 1.803, p = 0.1864, FR: F (1, 43) = 0.0046, p = 0.9464, Interaction: F (1, 43) = 6.297, p = 0.0159, followed by Tukey's post-hoc: FR+[0]-FR+[16] p = 0.0411). Risk assessment (stretch-attend-postures, SAP) was not influenced by food restriction or treatment (Fig. 18g, ordinary 2-way ANOVA, Treatment: F (1, 43) = 0.6548, p = 0.4228, FR: F (1, 43) = 0.2805, p = 0.5991, Interaction: F (1, 43) = 0.6095, p = 0.4393).

Mice were exposed to height and open spaces in the elevated plus maze (EPM). Total distance moved was not different between groups (Fig. 19a, Treatment: F (1, 44) = 0.7708, p = 0.3848, FR: F (1, 44) = 0.0739, p = 0.7870, Interaction: F (1, 44) = 1.973, p = 0.1671). Recorded open arm time was different between the physiological conditions towards more open arm time (Fig. 19b) among FR+ animals (Treatment: F (1, 44) = 0.0230, p = 0.8801, FR: F (1, 44) = 4.439, p = 0.0409, Interaction: F (1, 44) = 0.0140, p = 0.9063), whereas distance (Fig. 19c) was not significantly changed (Treatment: F (1, 44) = 1.400, p = 0.2431, FR: F (1, 44) = 4.026, p = 0.0510, Interaction: F (1, 44) = 0.2522, p = 0.6180). Vehicle-treated FR+ mice exhibit significantly more risk assessment than FR- mice, whereas the effect is abolished when treated with JZL184 (Fig. 19d, Treatment: F (1, 42) = 17.47, p = 0.0001, FR: F (1, 42) = 1.685, p = 0.2013, Interaction: F (1, 42) = 8.767, p = 0.005, followed by Tukey's post-hoc: FR-[0]-FR+[0] p = 0.0219, FR+[0]-FR-[16] p = 0.0016, FR+[0]-FR+[16] p < 0.0001). Rearing, however, was reduced in JZL184-treated FR+ mice, exclusively (Fig. 19e, Treatment: F (1, 42) = 19.38, p < 0.0001, FR: F (1, 42) = 2.353, p = 0.1325, Interaction: F (1, 42) = 4.147, p = 0.0481, followed by Tukey's post-hoc: FR-[0]-FR+[16] p = 0.0010, FR+[0]-FR+[16] p = 0.0003). Head dipping (Fig. 19f), in contrast, was unaffected (Treatment: F (1, 42) = 3.981, p = 0.0525, FR: F (1, 42) = 2.248, p = 0.1412, Interaction: F (1, 42) = 0.5582, p = 0.4592).

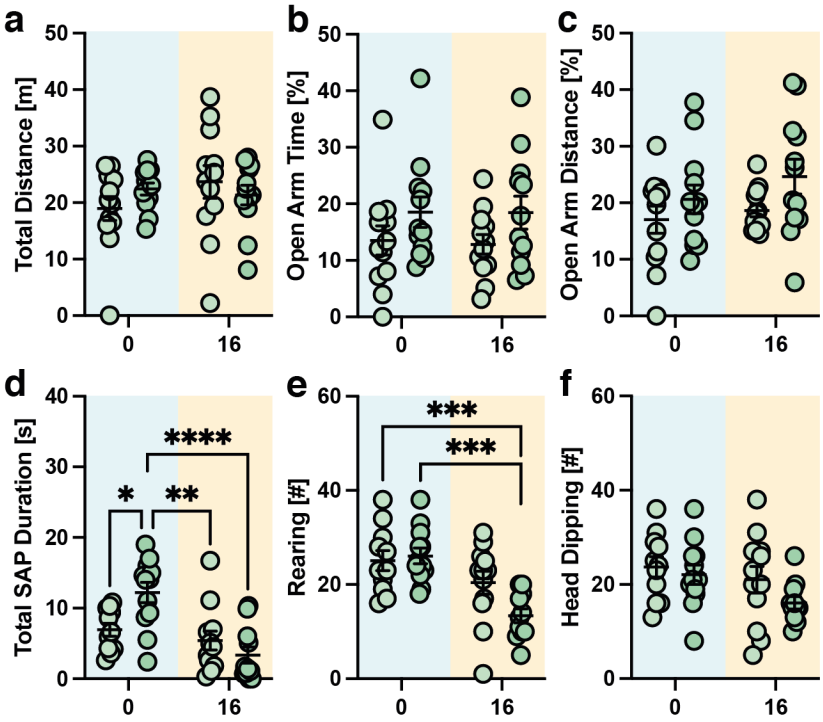

Figure 19: Elevated Plus Maze (EPM). Mice were ad libitum fed (FR-, lit green, left) or food restricted (FR+, dark green; right) over the course of the experiment. Mice were intraperitoneally injected with 0 (blue) or 16 (yellow) mg/kg of JZL184 one hour before exposure to the behavioral test. With the EPM, the second behavioral test was performed, and **a** total distance moved, **b** time and **c** distance on the open arms, **d** duration of stretch attend postures (SAP), number of **e** rearing and **f** head dipping were assessed. For further details see text.

In a series of anxiety-related behavioral tasks, mice were also exposed to the Dark Light box (DaLi; Fig. 20). Latency (Fig. 20a) and time in the lit compartment (Fig. 20b) were unaffected by treatment and physiological conditions, (Latency, Treatment: $F(1, 43) = 1.835$, $p = 0.1826$, FR: $F(1, 43) = 0.0186$, $p = 0.8921$, Interaction: $F(1, 43) = 0.3083$, $p = 0.5816$; Time: Treatment: $F(1, 43) = 0.1346$, $p = 0.7156$, FR: $F(1, 43) = 0.1577$, $p = 0.6933$, Interaction: $F(1, 43) = 3.759$, $p = 0.0591$).

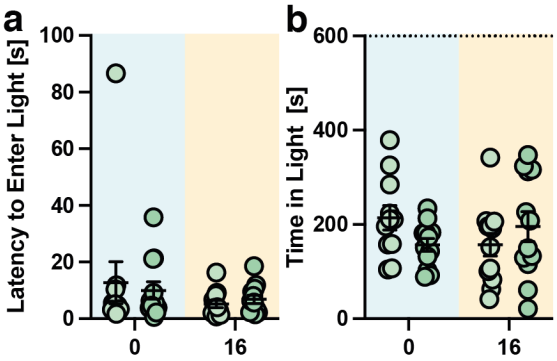

Figure 20: Dark Light Test (DaLi). Mice were ad libitum fed (FR-, lit green, left) or food restricted (FR+, dark green; right) over the course of the experiment. Mice were intraperitoneally injected with 0 (blue) or 16 (yellow) mg/kg of JZL184 one hour before exposure to the behavioral test. With the DaLi, the third behavioral test was performed, and **a** Latency to enter the lit zone and **b** time in the lit zone were assessed by experimenter blind to the experimental conditions. For further details see text.

3.3.2 Beetle Mania Task

Next to anxiety-related behavioral tests, I assessed active fear reactions. With the beetle mania task, mice were exposed to a potentially threatening, erratically moving robo-beetle. In order to habituate, mice were first allowed to freely explore the empty arena for 5 min. Within this time period, I assessed latency until full exploration of the arena (Fig. 21a) and rearing (Fig. 21b). Whereas vehicle-treated FR+ mice needed longer to explore the complete arena, this effect was abolished in JZL184-treated FR+ mice (Treatment: $F(1, 42) = 6.673$, $p = 0.0134$, FR: $F(1, 42) = 6.378$, $p = 0.0154$, Interaction: $F(1, 42) = 1.383$, $p = 0.2462$ followed by Tukey's post-hoc: FR+[0]-FR-[16] $p = 0.0033$, FR+[0]-FR+[16] $p = 0.0446$). The number of rearing events, however, remained stable between the groups (Treatment: FR: $F(1, 42) = 3.662$, $p = 0.0625$, $F(1, 42) = 1.734$, $p = 0.1951$, Interaction: $F(1, 42) = 0.0058$, $p = 0.9396$).

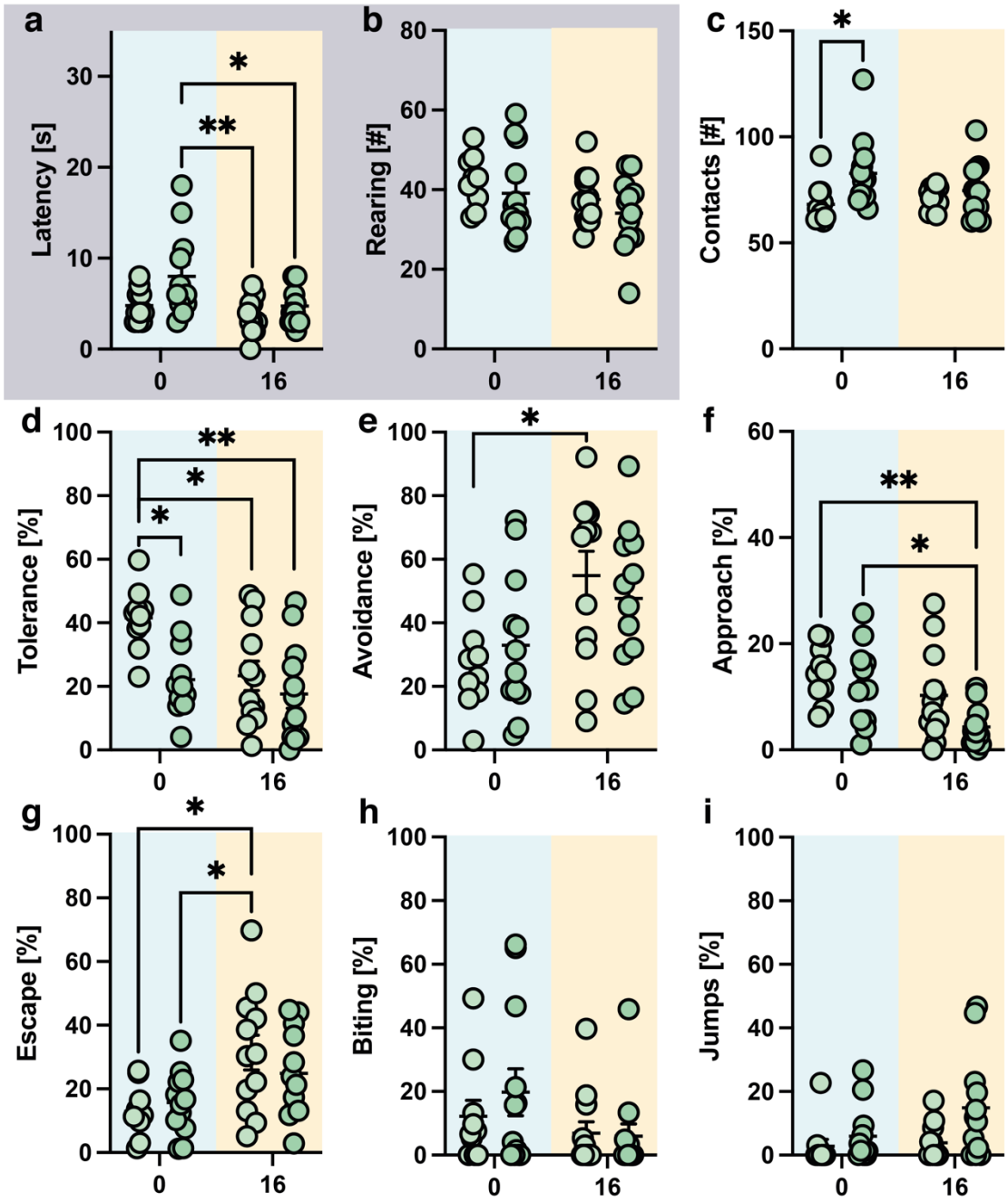

Figure 21: Beetle Mania Task (BMT). Mice were ad libitum fed (FR-, lit green, left) or food restricted (FR+, dark green; right) over the course of the experiment. Mice were intraperitoneally injected with 0 (blue) or 16 (yellow) mg/kg of JZL184 one hour before exposure to the behavioral test. With the BMT, the fourth behavioral test was performed. In a 5 min baseline period **a** Latency to explore the end of the arena and **b** number of rearings were assessed. In the following 10-min exposure to the robo-beetle **c** number of total contacts, and normalized to them **d** tolerance, **e** avoidance reactions (sum out of flight + **g** escape), **f** approach, **h** biting and **i** jumps were assessed. For further details see text.

During 10 min with exposure to the robo-beetle, number of encounters were assessed (Fig. 21c). Vehicle-treated FR+ showed significantly more encounters, exclusively (Treatment: $F(1, 42) = 0.5241$, $p = 0.4731$, FR: $F(1, 42) = 6.522$, $p = 0.0144$, Interaction: $F(1, 42) = 2.519$, $p = 0.1200$ followed by Tukey's post-hoc: FR-[0]-FR+[0] $p = 0.0320$). FR+ reduced tolerance in vehicle-treated mice, whereas JZL184-treated FR- mice show a lower tolerance by itself (Fig. 21d, Treatment: $F(1, 42) = 7.646$, $p = 0.0084$, FR: $F(1, 42) = 9.428$, $p = 0.0037$, Interaction: $F(1, 42) = 2.802$, $p = 0.1016$ followed by Tukey's post-hoc: FR-[0]-FR+[0] $p = 0.0109$, FR-[0]-FR-[16] $p = 0.0190$, FR-[0]-FR+[16] $p = 0.0013$). Avoidance (Fig. 21e) was calculated as the sum of flight and escape (Fig. 21g) reactions. JZL184 treatment significantly enhanced active reactions under FR- (Treatment: $F(1, 42) = 10.12$, $p = 0.0028$, FR: $F(1, 42) = 0.0180$, $p = 0.8938$, Interaction: $F(1, 42) = 0.8973$, $p = 0.3489$ followed by Tukey's post-hoc: FR-[0]-FR-[16] $p = 0.0327$). Food restriction and pharmacological means effected active approach behavior (Fig. 21f). FR+ seem to lower it with an add on effect by JZL184 treatment (Treatment: $F(1, 42) = 9.475$, $p = 0.0037$, FR: $F(1, 42) = 4.411$, $p = 0.0417$, Interaction: $F(1, 42) = 0.9172$, $p = 0.3437$ followed by Tukey's post-hoc: FR-[0]-FR+[16] $p = 0.0048$, FR+[0]-FR+[16] $p = 0.0273$). In line with general active avoidance reactions, escapes were enhanced in JZL184-treated FR- mice (Treatment: $F(1, 42) = 11.77$, $p = 0.0014$, FR: $F(1, 42) = 0.2287$, $p = 0.6350$, Interaction: $F(1, 42) = 1.330$, $p = 0.2553$ followed by Tukey's post-hoc: FR-[0]-FR-[16] $p = 0.0147$, FR+[0]-FR-[16] $p = 0.0343$). Some mice tended to attack the robo-beetle (Fig. 21h; Kolmogorov-Smirnov $p < 0.0001$, data not normally distributed; Kruskal-Wallis test with Dunn's correction, $p = 0.2084$) or showed jumping behavior (Fig. 21i; Kolmogorov-Smirnov $p < 0.0001$, data not normally

distributed; Kruskal-Wallis test with Dunn's correction, $p = 0.0549$) whereby groups do not differ.

Taken together, FR+ was able to enhance exploratory drive of mice as described previously (Heinz et al., 2021). Blockade of MAGL, however, decreased latency and abolished the effect on enhanced risk assessment, resulting in reduced exploration. In the BMT, blockade resulted in panicogenic behavior. In general, FR+ and JZL184-treament had only moderate behavioral consequences.

3.4 Targeted deletion of the CB1 Receptor in Fear

CB1's role in fear reaction was evaluated by the use of pharmacological means and different conditional CB1 knockouts in the beetle mania task (BMT, Heinz et al., 2017).

3.4.1 Inhibition of the CB1 Receptor prevents passive reactions

I investigated the global role of CB1 by its systemically blockade using rimonabant (SR141716A, Rim; Fig. 22a). In a dose dependent manner, 3 mg/kg was able to increase total contacts (ordinary one-way ANOVA followed by Tukey's post-hoc: Rim[0]-Rim[1] p = 0.2843, Rim[0]-Rim[3] p = 0.0074, Rim[1]-Rim[3] p = 0.1891) and to lower passive reactions upon encounter with the moving robo-beetle (Tukey's post-hoc: Rim[0]-Rim[1] p = 0.9910, Rim[0]-Rim[3] p = 0.0006, Rim[1]-Rim[3] p = 0.0009). Avoidance, on the other hand side was unchanged (Tukey's post-hoc: Rim[0]-Rim[1] p = 0.4572, Rim[0]-Rim[3] p = 0.0056, Rim[1]-Rim[3] p = 0.0964). Active approach was reduced in the 3 mg/kg group (Tukey's post-hoc: Rim[0]-Rim[1] p = 0.4572, Rim[0]-Rim[3] p = 0.0056, Rim[1]-Rim[3] p = 0.0964). A global genetic knockout, however, failed to result in any significant effect (Fig. 22b; unpaired t-test, contacts: p = 0.1182, passive: p = 0.0773, avoidance: p = 0.2935, approach: 0.0629).

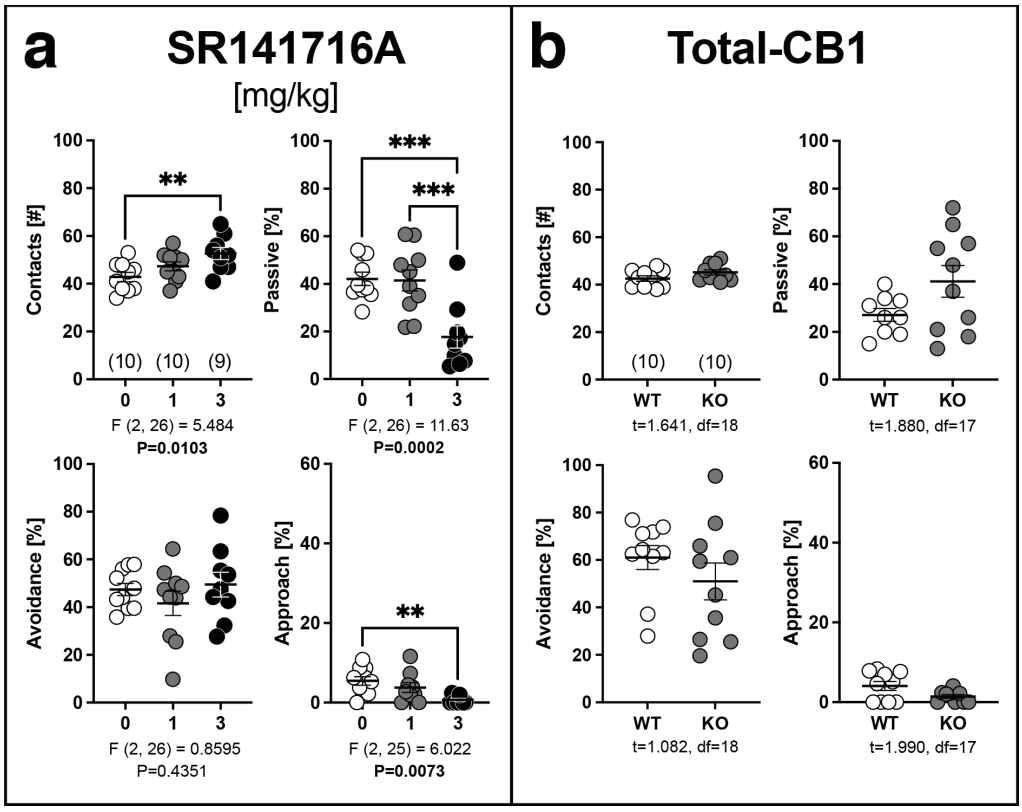

Figure 22: Global CB1 effect in the Beetle Mania Task (BMT). a Different dosages of rimonabant (SR141716A; 1 and 3 mg/kg) were used to systemically antagonize the CB1 receptor. **B** Complete genetic CB1 knockout (CBN, Total-CB1) mice were exposed to the erratically moving robo-beetle. *In situ* hybridization is presented in Fig. 8, schematic overview in Fig. 2. For further details see text.

3.4.2 Opposing effects of Dlx-, and CaMK-CB1 knockouts

In order to dissect different cell populations, I tested CB1's contribution on GABAergic (Dlx-CB1, Fig. 23a) or glutamatergic (Nex-CB1, Fig. 23b) forebrain neurons using conditional knockouts. The absence of CB1 on GABAergic forebrain neurons did not affect the number of total contacts (unpaired t-test; $p = 0.4664$) but decreased passive reactions ($p = 0.0039$) and, correspondingly, increased active fear responses ($p < 0.0001$). Knockouts exhibited less approach behavior towards the robo-beetle ($p = 0.0003$). Deletion of CB1 on glutamatergic cortical neurons, in contrast, was without effect on passive (unpaired t-test,

p = 0.0844) or active fear (p = 0.1931) responses. Contacts (p = 0.3253) and approach (p = 0.7373) behavior were also unaffected. As described before, CaMK-CB1 knockouts lack expression of CB1 on all projection neurons, which include cortical and subcortical glutamatergic as well as GABAergic projection neurons (cf. Fig. 2). These mice (Fig. 23c) showed increased passivity (unpaired t-test, p = 0.0124) with decreased active fear reactions (p = 0.0057) while contacts (p = 0.0702) and approach behavior (p = 0.3936) were stable.

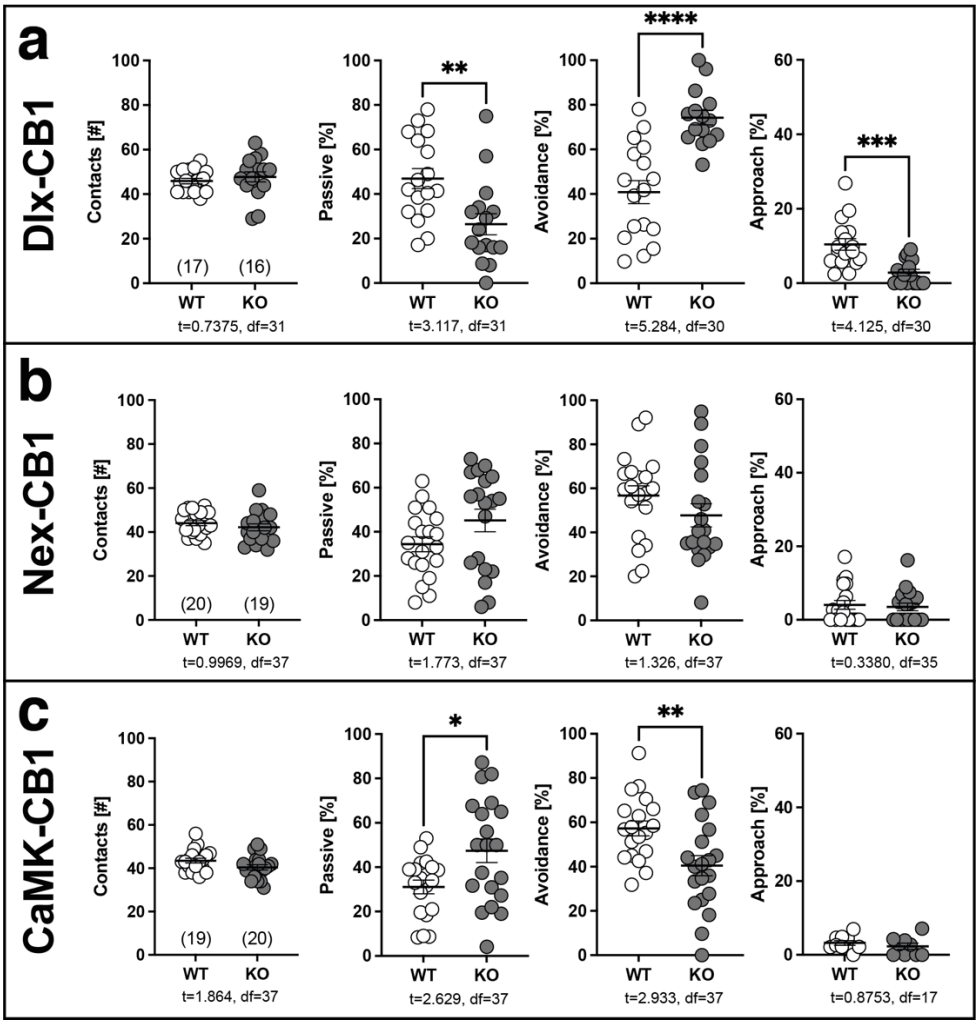

Figure 23: Conditional CB1 knockouts in the Beetle Mania Task (BMT). a GABAergic- (Dlx), **b** glutamatergic- (Nex), **c** and CaMK-CB1 knockouts were tested and compared on their reaction to the potentially threatening robo-beetle. *In situ* hybridization is shown in Fig. 8, schematic overview in Fig. 2. For further details see text.

3.4.3 Hypothalamic-, and SF1-CB1 knockouts show reduced active fear responses

C57Bl/6N (B6N) or CB1ff (floxed CB1) were targeted with a Cre-expressing virus driving the expression of the Cre-recombinase under the CaMK promotor within hypothalamus (Fig. 24a). With stable contacts between the groups (unpaired t-test, $p = 0.8162$), lack of CB1 in the hypothalamus resulted in a strong increase in tolerance behavior ($p = 0.0005$), while avoidance was significantly reduced ($p = 0.0008$). Local knockouts tent to approach the robo-beetle more frequently. However, this finding failed to reach significance ($p = 0.0858$).

To further dissect the cell population from the vmH, as a hotspot of CB1 expression within the hypothalamus, I generated SF1-CB1 specific knockout mice, since SF1 neurons have been shown to be implicated in fear regulation (Wang et al., 2015). SF1-CB1 mice (Fig. 24b) were not different in the numbers of encounters with the robo-beetle (unpaired t-test, $p = 0.5559$) and the percentage of tolerance behavior upon contacts ($p = 0.8162$).

Active fear responses, however, were significantly decreased ($p = 0.0092$) and SF1-CB1 knockouts approached the robo-beetle significantly more often compared to wildtyp littermates ($p = 0.0103$), thus resemble in part the phenotype of hypothalamic CB1 (cf. Fig. 24a) and CaMK-CB1 (cf. Fig. 23c) knockouts.

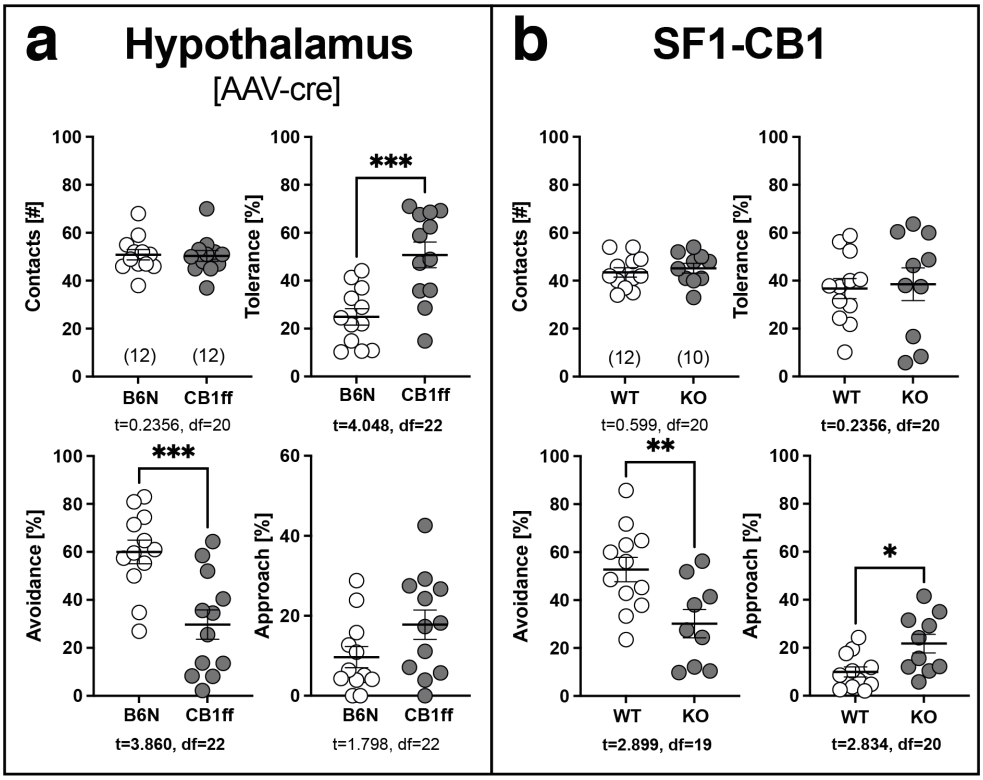

Figure 24: Beetle Mania Task (BMT). a C57Bl/6N (B6N) and CB1ff mice were locally injected with a Cre-expressing viral construct (AAV-CaMK-Cre) targeting the ventromedial Hypothalamus (vmH). **b** Conditional knockout of CB1 from steroid factor 1 (SF1)-positive neurons, which were largely located within the vmH (cf. Fig. 12a). For further details see text.

Taken together, I could identify SF1-expression of CB1 as a key element for the understanding of the switch between passive and active fear.

4. DISCUSSION

In this thesis I aimed to dissect the ambivalent roles of 2-AG in the positive and negative valence system. In doing so, it was challenging to dissect the yin and yang of both, 2-AG and AEA. Both seem to be within a highly regulated homeostatic principle. Varying physiological states such as high emotional load or hunger, however, cause long-term changes to the endocannabinoid signaling that may lead to imbalances.

High emotional load in posttraumatic stress disorders (PTSD) coincided with increased levels of endocannabinoids measured in human hair correlating with the severity of PTSD symptoms (Wilker et al., 2016). In line with that, enhancing levels of anandamide by blockade of FAAH was able to ameliorate PTSD-like symptoms in rodents (Fidelman et al., 2018; Sbarski and Akirav, 2020).

In 2017, I could demonstrate that pharmacological enhancement of AEA, through the blockade of its main degrading enzyme FAAH, led to reduced active fear in mice selectively bred for high anxiety behavior (Heinz et al., 2017). Later, I was able to demonstrate that the induction of a different physiological state by food restriction of the same high anxiety mice, led to an enhanced fear, but reduced anxiety-like phenotype (Heinz et al., 2021).

In the first part of my thesis, I focused on the positive valence system and the willingness of mice to work for food. Hunger, induced through food reduction, elevates not only Ghrelin (Tschöp et al., 2000, cf. Fig. 15), but also endogenous 2-AG levels (Kirkham et al., 2002). When elevated further by the blockade of its degrading enzyme MAGL, mice were shown to work more for food. As an exogenous ligand, THC mediated the same effect. Anandamide, in contrast, remained without any effect.

After demonstrating the systemic effect of 2-AG on the motivation to work for food, I aimed to systematically identify the side of action. Using

conditional mutagenesis, I could demonstrate that CB1 on CaMK-positive cells is essential: A lack of the CB1 receptor in cortical and subcortical projection neurons prevented the effect of enhanced 2-AG levels on the motivation to work for food. Further, the hypothalamus could be validated as a side of action.

I went on to further investigate the regulation of 2-AG and its hydrolyzing enzyme MAGL. Food restriction induced 2-AG synthesis within the hypothalamus and nucleus accumbens and elevated plasma levels of Ghrelin and corticosterone. Further I could demonstrate that food restriction led to the translocation of MAGL into the membrane.

In the second part of my thesis, I aimed to investigate the effect of CB1 signaling on the negative valence system. To do so, I linked pharmacological modulations of endocannabinoid levels with the modulation of the physiological state in healthy mice. Using conditional CB1 deletion, I subsequently focused on the neuronal interconnection of motivational behavior and active fear reactions. Thereby I took advantage of the use of the recently described confrontation with an erratically moving robotic beetle where anandamide was proven to be panicolytic, and pharmacological enhanced 2-AG levels were shown to promote fear responses (Heinz et al., 2017).

Lastly, I could identify unique neuronal populations differentially regulating endocannabinoid mediated motivational behavior and passive fear responses.

4.1 Working for Food and Appetite

Nothing comes closer to the evolutionary role as live and survive. Next to the role of reproduction for the total population, individuals need a balanced energy homeostasis by access to food.

To maintain energy homeostasis in periods of restricted food access, blood glucose and insulin are reduced, while the empty stomach releases Ghrelin. Next to them, reduction of leptin (the satiety hormone; Dhillon et al., 2006) further promotes the hunger signal. In a more mechanical fashion, the stomach elongation state is coupled via the vagus nerve to the brainstem and the nucleus tractus solitarii (NTS; Zittel et al., 2002; Valassi et al., 2008). All the primary responses of a negative energy homeostasis have the aim to mediate the search and intake of food.

The described state of hunger, defined as empty stomach and lack of energy is different from appetite, the urge to eat palatable food. Appetite can be described as feeding with a rewarding characteristic food (Giraudo et al., 1999). Intracerebral infusion with NPY (neuropeptide Y) or DAMGO (selective μ-opioid receptor agonist) led to increased food intake. Rats were allowed to eat corn flour or saccharose. AgRP/NPY led to primary intake of corn flour, whereas the opioid-antagonist DAMGO shifted the intake towards saccharose (Giraudo et al., 1999). Food intake without deficit in energy took place.

Different than hunger, appetite holds a psychological component (Nüsken and Jarz, 2010). Next to preference for sweet taste, cultural-, social- or ordinary- rituals and routine can mediate appetite that, again, can be conditioned with positive factors (e.g., family brunch as a ritual, ice cream in summer, Christmas treats with Christmas flavor; Mela, 2001; Lowe and Levine, 2005; Nüsken and Jarz, 2010).

Insulin, enhanced by the intake of sugar facilitates the uptake of tryptophane to the brain and, therewith, enhances serotonin signaling (Fernstrom and Fernstrom, 1995; Nüsken and Jarz, 2010). Serotonin correlates positively with mood and may correlate with so called comfort eating.

Another neurotransmitter responsible for positive mood is dopamine. Whereas "liking" (Fig. 25a) includes - among others - opioid signaling in the nucleus accumbens, motivation coupled "wanting" (Fig. 25b) includes the dopaminergic system (Berridge and Robinson, 2016).

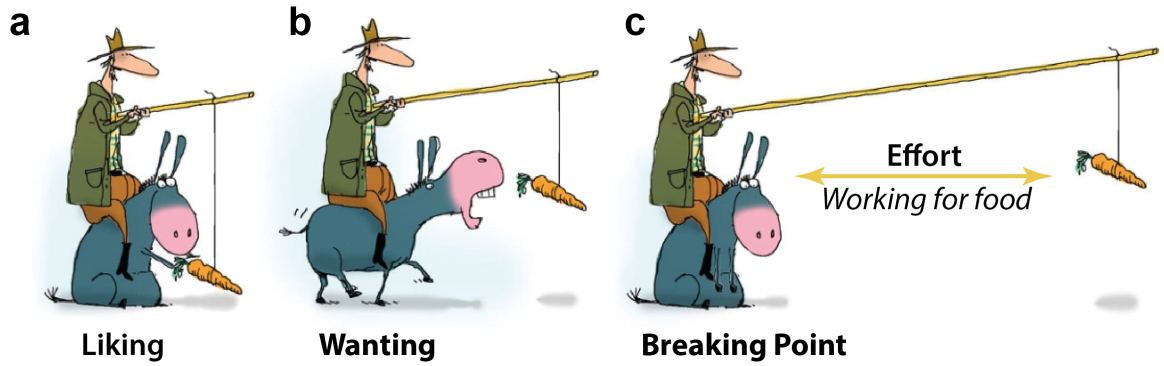

Figure 25: Different motivational states. Graphical definition of **a** liking and **b** wanting behavior. If the donkey wants to get the carrot, he invests a defined effort. If the effort is greater than the motivation, **c** breaking point is reached, and the donkey stops to work for food. Illustration modified from wordpress.com: pursuingawesomeness, June 2021.

In this part of my study, I aimed to modulate the motivation to work for food (Fig. 25b,c). Therefore, the effort until subjects stopped to work for food (breaking point) was assessed as the number of target touches within the Progressive Ratio (PR4) paradigm.

4.1.1 2-AG would if it could

Understanding the pathways of food-wanting behavior remains essential in the development of treatments against eating disorders such as obesity or anorexia nervosa. With Acomplia® (SR141716A, rimonabant), an anti-obesity drug was introduced to market that blocked the CB1 receptor (Rinaldi-Carmona et al., 1994; van Gaal et al., 2005; Tucci et al., 2006). Against our expectation, however, treatment with rimonabant alone was not able to decrease the willingness to work for food measured as the number of total target touches in the PR4 protocol. The reasons for that can be manifold as our study employed acute rather than chronic treatment. Importantly, Acomplia® was not applied to food restricted subjects, but to obese. In my experiments I could unmask an effect of rimonabant when simultaneously enhancing the levels of 2-AG. The same holds true when applying THC as an exogenous CB1 agonist. The cause that co-administration of rimonabant with JZL184 or THC not only abolished the effect on target touches (less evident from a return to vehicle levels), but even decreased them below baseline is puzzling and might be ascribed to inverse agonism. Future experiments may employ neutral antagonist such as AM4113 in order to resolve this problem (Sink et al., 2008; Janero and Makriyannis, 2009). A second factor to be considered is the difference between liking and wanting. Acomplia® was described to decrease eating by reducing appetite, rather than hunger (Després et al., 2005).

THC is known to positively modulate appetite and overall food intake (Sharma, 1972; Sofia and Barry, 1974). Medical marijuana is FDA approved and prescribed, among others, in patients with appetite loss as seen in chemotherapy (Joy et al., 1999).

In a dose dependent matter, however, THC can mediate psychoactive, "stoned"-like, up to tetrad effects (Monory et al., 2007; Metna-Laurent et

al., 2017; Kubilius et al., 2018). Interestingly, THC (1 and 3 mg/kg) mediated increased food intake in hungry mice, but not if the mice were fed ad libitum overnight. A potential overeating-effect ("I eat when I see food") in mice with free access to food after a period of food restriction cannot be excluded (Piazza et al., 2017). Naïve, untrained, ad libitum fed mice, however, were unable to proceed to the PR4 protocol (data not shown).

Similar to THC-treatment, pharmacologically enhancing 2-AG level caused by inhibition of the main degrading enzyme also enhanced the motivation to work for food. I could not observe a dose-dependent nor a U-shaped dose-response relationship as described for anandamide (Moreira et al., 2012; Heinz et al., 2017). Future studies will have to control for plasma exposure levels and proper pharmacokinetic-pharmacodynamic assessment. Remarkably, when co-treated with SR, mice treated with JZL184 completely stopped working for food. As suggested before, I tend to ascribe this to complex consequences of the inverse agonism of SR. JZL184-treatment affected the behavior only acutely with no carry-over effects to the next day. Again, pharmacokinetic-pharmacodynamic assessments are required which consider time course of irreversible blockade of MAGL vs. re-synthesis of new enzymes.

As observed for THC, JZL184 remained without any effect compared to vehicle upon devaluation. Blockage of MAGL can only result in enhanced levels of 2-AG if 2-AG is around. This, however, is not expected under ad libitum diet. Unexpectedly (Touriño et al., 2010), pharmacological enhancement of AEA by blocking FAAH failed to affect the willingness to work for food.

Taken together, I could demonstrate that 2-AG is highly controlled by MAGL in FR+ mice. Levels of 2-AG increase rapidly, and mice exert an increased motivation to work for food, when the degradation of 2-AG is blocked.

4.1.2 MAGL is the key enzyme in 2-AG's effect on the motivation to work for food

Once MAGL was validated as a key enzyme to restrict the actions of 2-AG on the motivation to work for food, I aimed to investigate potential off-target effects of JZL184 in more detail. Mice were chronically ad libitum fed or food restricted followed by an acute systemic vehicle- or JZL184-treatment followed by brain collection. In collaboration with the van der Stelt laboratory from Leiden University, Netherlands, I investigated the enzymatic activity in two hotspots for food intake regulation, the hypothalamus, and the nucleus accumbens. I treated FR- or FR+ mice with vehicle or JZL184 at 16 mg/kg. Even though a group size of n=4 mice is partially underpowered, the following picture emerged: JZL184 inhibited not only the activity of the MAGL (Long et al., 2009), but also of the Carboxylesterase CES1 and, interestingly, FAAH. In general, basal activity in the NAcc seems to be much lower after vehicle-treatment leading to non-significant blockage. Interestingly, FAAH activity is reduced under FR+, and further by an overall JZL184-effect. CES1 was suggested to indirectly interfere with levels of endocannabinoids (Carr et al., 2013) even if the involvement in the degradation of 2-AG could not be confirmed (Carr et al., 2014).

Considering the yin and yang of both endocannabinoids, a homeostatic counter-regulation may explain its activity. 2-AG levels were enhanced (cf. Fig. 7), and at the same time, the degradation of anandamide is reduced aiming at higher levels that may affect the negative valence system.

The fact that MAGL activity is unaffected of FR+ could be due to the localization within the cell. A methodological limitation prohibited a cell fractioning dissecting the different cell compartments. In case the later discussed hypothesis of MAGL's translocation after dimerization holds true, active MAGL would be in the membrane, whereas inactive would be in the

cytoplasm (Labar et al., 2010). Overall levels would not be expected to be changed. The effect of JZL184, however, was present as expected in both brain regions.

The observed off-target effects led me to investigate the involvement of other enzymes vs. MAGL as a key mediator of the enhanced working for food after JZL184-treatment. The specific blockage of CES1 failed to enhance working for food similar to the blockade of FAAH. In contrast a second, commonly used specific inhibitor of MAGL, MJN110 (Niphakis et al., 2013), was able to replicate the effect of JZL184. Next to MAGL as the major degrading enzyme of 2-AG, about 15 % of the total 2-AG-hydrolyzation comes to ABHD enzymes (Blankman et al., 2007). Pharmacological blockage of ABHD6 did not increase working for food. A specific role of ABHD6 can be excluded by the intraperitoneal injection of 1 mg/kg of KT203 (Hsu et al., 2013). Inhibition of ABHD6 may not be sufficient when MAGL and ABHD12 are still active and compensate the blockage. While more detailed dose-response studies are pending, MAGL, indeed, seems to be the key enzyme mediating increase in working for food. In line with this, the blockade of the main synthesizing enzyme of 2-AG, DAGLα (diacylglycerol lipase alpha; Stella et al., 1997; Deng et al., 2017) tended towards less working for food. This effect became even more pronounced if co-treated with JZL184 blocking MAGL next to DAGLα.

In a separate experiment I could validate that the inhibition of MAGL by JZL184 resulted in a selective decrease of 2-AG (Dinh et al., 2002; Saario et al., 2004), but not arachidonic acid (AA) or AEA, within the hypothalamus and nucleus accumbens.

4.1.3 The neuroanatomical basis of 2-AG mediated enhancement of working for food

After the dissection and validation of 2-AG's role, I further aimed to evaluate the neuroanatomical basis of this effect. Cortical glutamatergic-, or GABAergic- neurons of the forebrain failed to affect the stimulating effects of JZL184. This appears to be in contrast to previous studies that focused on liking behavior and appetite, by e.g., Bellocchio et al., where CB1-restrain of cortical glutamatergic transmission mediated orexigenic and of GABAergic signaling increased anorexigenic effects of THC (Bellocchio et al., 2010). In my study I focused on wanting behavior and, therewith, the motivation to work for food, which is apparently differently regulated than liking behavior involving CB1 expressed by glutamatergic neurons of the olfactory bulbus (Soria-Gómez et al., 2014).

Targeting CB1 by the infusion of AAV-CaMK-Cre into the hypothalamus of CB1ff mice completely abolished the motivational effect of JZL184. By the use of RNAscope I could demonstrate a co-expression of CB1 and glutamate, but not GABA, within the hypothalamus. SF1-positive neurons, however, exerted only a limited involvement, whereas POMC-positive neurons were without any effect on the motivation to work for food. Instead, I could further narrow down the localization of glutamatergic CB1-expressing neurons to the arcuate nucleus. It remains to be shown in future studies (e.g., by using OTR-CB1-KO), whether the population of anorexigenic oxytocin receptor-positive glutamatergic neurons (Ryan et al., 2017; Maejima et al., 2018) of the arcuate nucleus represent the primary target of 2-AG.

Activation of presynaptic CB1 by 2-AG is expected to decrease transmitter release. To simulate this mode of action, I explored chemogenetic inhibition of neuronal activity. Indeed, activation of inhibitory DREADDs restricted to CaMK-positive neurons of the hypothalamus caused an increase in the

motivation to work for food. This observation leads strong support to the assumption that 2-AG signaling inhibits neurotransmission, which increased the motivation to work for food. Strikingly, the DREADD-effect could be blocked by co-treatment of CNO and rimonabant. Again, I can only speculate about the underlying mechanism which needs to be explored in future studies.

The hypothalamus is described to hold a major role in the regulation of metabolic processes with an essential role of the arcuate nucleus which contains both, orexigenic agouti-related protein (AgRP) and anorexigenic pro-opiomelanocortin (POMC) neurons. The "hunger hormone" Ghrelin is produced in the periphery and secreted into the blood system. Due to its permeable blood brain barrier the arcuate nucleus is sensing blood Ghrelin levels (Guan et al., 1997). Ghrelin receptors are mainly found in AgRP and NPY expressing neurons (Zigman et al., 2006), whereby Ghrelin leads to a depolarization followed by orexigenic effects by e.g., reduced melanocyte stimulating hormone release (Cowley et al., 2003).

Previous studies showed, that the CB1 receptor is essential for Ghrelin's orexigenic effect and the subsequent elevation of endocannabinoid levels (Kola et al., 2008). It is suggested that CB1 and Ghrelin receptors may form di-/heteromers and influence each other in this way (Wellman and Abizaid, 2015).

Next to Ghrelin sensing orexigenic AgRP neurons, anorexigenic POMC-positive neurons represent the second important population expressed in the hypothalamus. With a opposite role, POMC neurons receive inhibitory inputs from AgRP neurons and are known to mediate the anorexigenic "satiety" response (Leptin-signaling; Dhillon et al., 2006; Balsevich et al., 2018; Perry et al., 2019).

Next to POMC and AgRP, SF1 is described in regulating food intake as well (Dhillon et al., 2006; Kim et al., 2011). SF1-positive neurons are mainly localized in the vmH. They send collaterals or projections to various brain structures, including the arcuate nucleus, hypothalamus, and the periaqueductal grey (Kunwar et al., 2015). As shown in guinea pigs, they seem to innervate POMC neurons, and activation of presynaptic CB1 seem to inhibit glutamatergic transmission (Fang et al., 1998; Fabelo et al., 2018). Selective activation of vmH^{SF1} positive cells, however, enhances food intake (Coutinho et al., 2017; Viskaitis et al., 2017; Jiang et al., 2020) which would argue against a significant involvement of this neuronal population in 2-AG's effect on working for food.

To shine light on those scenarios, I generated SF1-CB1 knockout mice. The effects of JZL184 were largely preserved in mutants, with only a slight decrease at higher but not intermediate doses (16 vs. 8 mg/kg). This finding indicates that the contribution of SF1 neurons to 2-AG controlled motivation to work for food is minor.

To explore the direct contribution of CB1-expressing neurons of the Arc, I locally recombinated CB1 in principal neurons by injecting small volumes of AAV-CamK-Cre into the Arc of CB1ff or control mice. This intervention not only led to a general decrease in working for food, but also completely abolished the potentiating effects of JZL184.

As confirmed by *in situ* hybridization, the recombination affected the Arc and nearly structures. Therefore, I cannot unequivocally conclude that neurons of the Arc mediate the JZL184 effects. Nevertheless, this scenario appears to be rather likely. Also, the lack of JZL184 effects observed upon AAV-CaMK-Cre injections in the posterior hypothalamus (which affected the Arc among others) and in CaMK-CB1-KO (which, again, deleted CB1 expression, among others, from the Arc) might be ascribed to this brain structure.

Given their role as "satiety" neurons (Sternson et al., 2005; Koch et al., 2015), CB1-controlled restriction of transmitter release from POMC neurons of the Arc may account for the 2-AG effects. Therefore, I generated POMC-CB1 mutants and tested their behavior in the operant task. Against the expectations (Koch et al., 2015), the effect of JZL184 was fully preserved in the mutants. This rules out a direct involvement of POMC neurons in the acute effects of increased 2-AG levels. Yet, acute vs. chronic hunger state may recruit different signaling patterns as similar to acute vs. tonic activations of synapses (Fenselau et al., 2017; Fabelo et al., 2018). POMC neurons may still serve as a putative indirect effector site for 2-AG controlled working for food, since excitatory afferences to these neurons are constraint by CB1 signaling.

Together with the slow dynamic and rather tonic involvement of POMC neurons in signaling satiety (Biglari et al., 2021), our data speak against a significant contribution of this cell type to the acute increase in working for food following pharmacological blockade of MAGL. Instead, it is tempting to assume that the recently discovered population of glutamatergic Arc neurons might play a key role. These neurons rather selectively express the oxytocin receptor (Ryan et al., 2017; Maejima et al., 2018). Therefore, it would be interesting to test mice with conditional deletion of CB1 expression from oxytocin receptor-positive neurons in the future (OTR-CB1-KO).

4.2 Mechanisms controlling MAGL activity

MAGL, ABHD6 and ABHD12 account for more than 98 % of 2-AG's degradation (Blankman et al., 2007). As both ABHD enzymes are membrane standing, the membrane's role in 2-AG degradation became evident (Blankman et al., 2007). 2-AG and AEA are highly lipophilic

molecules and were expected to stay in the membrane. It would not be surprising if 2-AG would be hydrolyzed almost exclusively at the membrane. Our obtained data support this hypothesis. Stress, in form of food restriction, or indirectly by elevated levels of corticosterone (cf. Fig. 15; Mlekusch et al., 1975; Perry et al., 2019) triggers the synthesis of 2-AG (Evanson et al., 2010; Hill et al., 2010a). Subsequently, 2-AG is enriched in the membrane fraction and – according to the homeostatic principle – needs to be hydrolyzed. Treatment with dexamethasone, however, resulted in lower membrane levels of MAGL compared to vehicle-treated brain slices from the dorsal hippocampus. Food restriction, in contrast, resulted in accumulation of MAGL in membrane fractions. Given that FR+ results in tonic increase in plasma corticosterone levels, it remains to be shown whether chronic activation of GR by Dexamethason would cause comparable effects as FR+. Prolonged activation would give the chance for gene regulation and subsequent protein synthesis.

My data support the theory of a potential shuttling mechanism. In what way MAGL starts to translocate is not yet understood. Labar and colleagues, however, proposed the theory of dimerization and translocation to the membrane (Labar et al., 2010). They stated that "it is also possible for a post-translational event […] to be involved in this translocation between the membrane and the cytosolic compartment" (Labar et al., 2010). Later it was demonstrated that sulfenylation regulates the activity state of MAGL (Dotsey et al., 2015). A translocation, however, was not further investigated. With two different sized protein bands of MAGL (cf. Fig. 6; Dinh et al., 2002; Long et al., 2009), the dimerization-hypothesis is supported as it is with the crystal structure of human MAGL (Labar et al., 2010; Schalk-Hihi et al., 2011). Additional support was gained by our data that revealed an increased interaction of MAGL-HA with MAGL under FR+.

In my hypothesis (Fig. 26) FR+ leads to a dimerization (=activation) of MAGL, followed by its translocation to the membrane. This increases the efficiency of 2-AG elimination before 2-AG would exert its effects via CB1. In the membrane, 2-AG is hydrolyzed.

Noteworthy, a published article reports a stress mediated phosphorylation of MAGL (Ziegler et al., 2021). The mechanism and the role of the phosphorylation, however, needs to be investigated further. The same is true for the translocation.

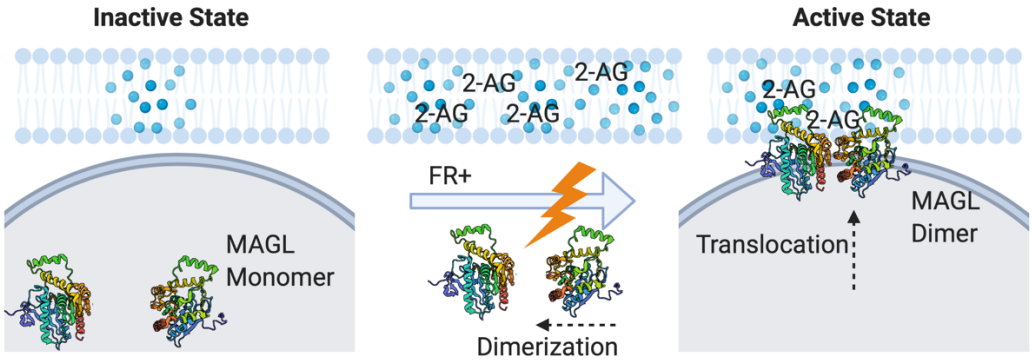

Figure 26: Proposed activity regulation of Monoacylglycerol lipase (MAGL). Figure created using BioRender.com under a Max Planck license.

It remains to be shown to what extent the activation of the GR-system (e.g., by corticosterone), the availability of membranous 2-AG and the activity state of MAGL influence each other. The fact that plasma concentrations of corticosterone were further enhanced by co-treatment of JZL184 and RU486, but less by RU486 alone highlight a close relation of both signaling systems. Together with the behavioral data, whereby co-treatment of JZL184 and RU486 completely abolished the effect of JZL184 on the motivation to work for food, two scenarios are possible:

First, corticosterone directly influences the activity of MAGL, or, second, corticosterone triggers 2-AG synthesis. Given the evidence from the literature (Hill et al., 2010a), it appears rather likely that the sustained elevation of plasma corticosterone upon food restriction constantly

activates 2-AG synthesis in a GR-dependent manner (Evanson et al., 2010). This would explain why the acute blockade of GR receptors completely abolished the motivational consequences of JZL184 treatment.

Still, the question remains why 2-AG levels are that tightly controlled by MAGL in food restricted mice. One reason for this homeostatic principle might be the close interactions between the positive and the negative valence system (Heinz et al., 2021) with the potential of detrimental panicogenic consequences of unrestrained 2-AG signaling (Heinz et al., 2017). Therefore, I performed a series of additional experiments in order to study (i) consequences of enhanced 2-AG signaling on fear- and anxiety-related behavior in food restricted vs. ad libitum fed mice, and (ii) to dissect the neuronal circuitry responsible for CB1-control of active vs. passive fear.

4.3 Reinforcement Sensitivity Theory and enhanced 2-AG Signaling

Different external and internal factors are responsible for different emotions and decisions taken. Factors such as sunlight, or open spaces trigger a cautious or anxious state in mice (Fig. 27).

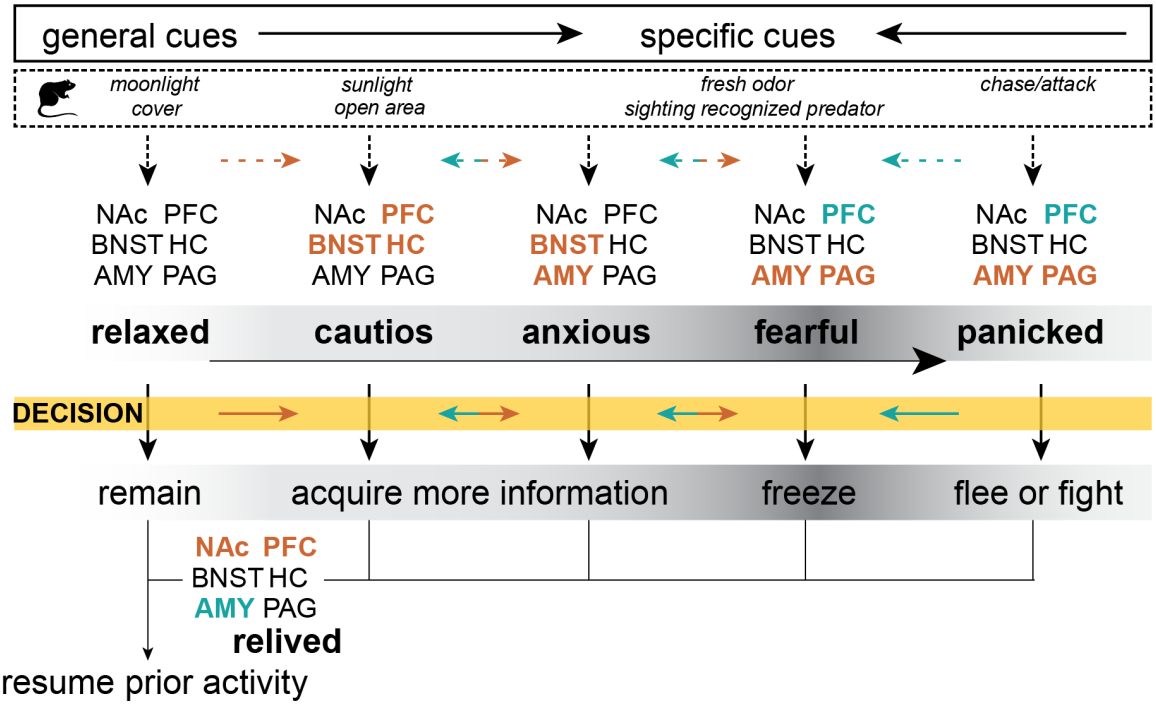

Figure 27: Anxiety-Fear Decision Matrix. Different external factors as general and specific cues lead to the activation of specific brain regions, a defined behavioral state and a decision followed by behavioral outcome.
AMY: Amygdala, BNST: bed nucleus of the stria terminalis, HC: Hippocampus, NAc: Nucleus accumbens, PAG: periaqueductal grey, PFC: prefrontal cortex. Illustration adapted from Fendt et al., 2020.

Risk assessment behavior (also known as stretch attend postures, SAP) enables the animals to carefully acquire more information about the situation. In laboratory conditions, exposure to open spaces (OFT), elevated and open spaces (EPM) or light (DaLi) simulate triggers of anxiety. With more specific, defined triggers, anxiety state can convert to a fearful or panicking state, whereby brain regions as the periaqueductal grey (PAG)

are activated (Fendt et al., 2020). Freezing, fleeing, or attacking behavior are caused. I used an erratically moving, vibrating robo-beetle, as an ambiguous threatening stimulus (Heinz et al., 2017). Anxiety-like behavior and the lack of motivation, especially induced by re-testing, were hard to discriminate. Gray's Reinforcement Sensitivity Theory provides a theoretical framework for three different dimensions: The Behavioral Inhibition System (BIS, conflict solving), Behavioral Activation System (BAS, approach, and exploratory drive) and the Fight Flight Freeze System (FFFS, avoidance). Whereas the BIS can be described with anxiety mediating behavior, BAS includes exploratory drive and motivation. With the use of behavioral data of normal-, and high anxiety behavior mice, I was able to perform a principal component analysis (Heinz et al., 2021). While doing so, I could assign different mouse behavior to the corresponding domains BIS, BAS and FFFS. Food restriction was able to increase fear responses (FFFS) and exploratory behavior (BAS), while the anxiety-like phenotype (BIS) of high anxious mice was abolished (Heinz et al., 2021).

In my thesis, I used a similar design which compares food restricted (FR+) vs. ad libitum fed (FR-) mice. As a second factor, I investigated the consequences of pharmacological inhibition of 2-AG degradation vs. control treatment. As described previously (Heinz et al., 2021), FR+ resulted in more rearing behavior, when treated with vehicle, but not JZL184. Total distance was decreased in JZL184-treated mice under FR+ mice compared to FR-. In line with our expectation, FR+ was able to enhance exploratory drive of mice.

Against our expectations, however, latencies (anxiety-like behavior) were enhanced in FR+ mice. Together with increased risk assessment, the latencies may be explained by longer exploration times before entering the "next zone". Enhanced levels of 2-AG, however, decrease latency and

abolished effect of enhanced risk assessment. Even if this may be unexpected at first, foraging behavior may be enhanced and animals work more for food as discussed in 4.1.

When exposed to the potentially threatening robo-beetle, more contacts shown by FR+ mice could reflect pro-active behavior while searching for food. However, approach behavior was even lower in JZL184-treated mice. Separately assessed "biting" as a hunting-phenotype tended towards increased biting in vehicle-treated FR+ mice (2 mice >60 %). JZL184 treatment seems to abolish the effect. At the same time, avoidance tended to be increased in FR+ mice, while the effect was significant for JZL184-treated FR- mice. Lastly, enhanced levels of 2-AG due to FR+ and the inhibited degradation had panicogenic consequences as measured by increased jumping behavior. 2-AG levels were tightly controlled by MAGL activity limiting enhanced 2-AG signaling. FR+ itself increased exploratory and foraging by reducing anxiety-like behavior. When blocking MAGL by the treatment of JZL184, FR+ resulted in increased anxiety-like behavior.

Taken together the fact that unrestrained 2-AG signaling in FR+ mice would cause an increase in anxiety suggests that MAGL activity tightly controls 2-AG upon food restriction in order to permit foraging behavior while maintaining precaution and adequate fear responses to "real" threatening stimuli. Anxiety-like behavior may underly different mechanisms as an unbalance of AEA and 2-AG. Whereas 2-AG was described to enhance fear behavior (Llorente-Berzal et al., 2015; Heinz et al., 2017), AEA holds beneficial effects on anxiety-like behavior (Heinz et al., 2017). Given the bimodal role of CB1 signaling in active vs. passive strategies (Metna-Laurent et al., 2012), the identification of different behavioral clusters may be favorable. As performed recently (Heinz et al., 2021), a principal component analysis (PCA) could cluster the effect of MAGL's blockage under ad libitum or FR+ state. Enhanced 2-AG levels may positively

correlate with the FFFS system, while the BIS is reduced by food restriction *per se*. The reinforcement sensitivity theory may provide further insights in the bimodal effect of enhanced 2-AG signaling.

In the final set of experiments, I went on to dissect the neuronal basis of CB1-mediated effects on defensive responses in the BMT with particular focus on the contribution of the hypothalamic neurons.

4.4 Hypothalamic SF1-CB1 mediates Relief of Active Fear

Marsicano and colleagues established and described various conditional CB1 mouse mutants (Marsicano et al., 2003; Monory et al., 2006, 2007); among them, a complete knockout of CB1 (CBN). Different than conditioned fear, I aimed to evaluate a more ethobehavioral role of the receptor. Administration of the inverse agonist of CB1 resulted in more contacts while less passive behavior occurred, coupled with fewer approaches. CB1-activation seems to balance and between active and passive fear reactions. Surprisingly, total CB1 deletion resulted in no effect, but tended towards the opposite direction. Taken CB1's multifaceted role into account, compensatory mechanisms may interfere and result in the lack of effect in full knockout mice.

As described previously (Heinz, 2017), lack of CB1 on GABAergic neurons leads to enhanced active fear behavior. Given the fact that CB1 negatively regulates GABA release (Katona et al., 1999), GABA seems to be responsible for active reactions (Llorente-Berzal et al., 2015). However, basket cells which highly abundantly express CB1 (Marsicano and Lutz, 1999) co-express GABA and CCK. CCK itself is panicogenic (Javanmard et al., 1999) which suggests a possible role of unrestrained CCK-release in the observed effects similar to previous observations in conditioned fear (Chhatwal et al., 2009).

The lack of CB1 on CaMK-positive, but not cortical glutamatergic neurons led to less active fear responses by enhanced tolerating responses. Thus, endocannabinoid signaling via CB1 on principal subcortical neurons seem to promote active, but not passive fear. To further evaluate their role, I virally targeted CaMK-CB1 within the vmH. The targeted knockout led to increased tolerance by reduced avoidance as in the conditional knockouts.

The hypothalamus is not only a key region mediating food intake and mating, but also controlling fear responses. For instance, SF1 neurons of the vmH project to the PAG, anterior hypothalamus, amygdala, and the Arc (Kunwar et al., 2015; Wang et al., 2015). Therefore, I tested mice lacking the CB1 receptor on SF1-postive neurons in the BMT. I observed a phenotype similar like to that shown by CaMK-CB1 mice and mice with local recombination of CB1 expression within the hypothalamus. Therewith I could narrow down the role of CB1 to hypothalamic SF1-positive neurons. Its activation triggers fear responses, as the projection to the PAG could be activated (Kunwar et al., 2015). With opposing roles of AEA and 2-AG, I propose a homeostatic principle within the different projections outgoing from the vmH – influenced directly by endocannabinoids or, indirectly by physiological factors. Hunger, induced by food restriction, enhanced fear reaction while reducing anxiety-like phenotypes (Heinz et al., 2021). It remains to demonstrated, that this shift, indeed is mediated by endocannabinoids and further, by influencing the CB1-dependent projections of SF1-positve neurons.

4.5 Limitations & Outlook

My study holds a number of limitations that require additional analyses and experiments to strengthen the conclusions drawn:

1) Δ9-THC and 2-AG enhanced the motivation to work for food at Arc^{CaMK}. CB1 on POMC or SF1-positive neurons, in contrast, failed to be essential for the effect. Even if AgRP-CB1 expression is not expected to be essential for more working for food (AgRP as "hunger" population), its role should be further evaluated, e.g., by generating AgRP-CB1-KO.
   With respect to the proposed involvement of $Arc^{OTR/glutamatergic}$ neurons, I would suggest investigating basal and JZL184-challenged PR performance of oxytocin receptor-CB1 wildtype and knockout mice.
2) The simultaneous blockade of CB1 and MAGL unexpectedly led to the complete stop in working for food. This phenomenon must be explored further.
3) The still speculative hypothesis of MAGL shuttling needs to be proven. With the use of different techniques such as a MAGL-Halo tag or MAGL-SEP (super ecliptic GFP; Kopec et al., 2006) construct, the translocation theory may be validated *in vitro* or *in-* and *ex- vivo*. Dimerization may be studied by its inhibition using side-directed mutagenesis. The use of immune-electron microscopy would help to localize MAGL in the cells of FR-, and FR+ mice at an ultra-structural level.
4) Homeostatic principle of 2-AG signaling has been studied in "normal", healthy subjects (mice). Studies should be extended to animal models of obesity or anorexia nervosa. The involvement of other species or even human subjects may be useful.
5) In line with my previous publication on FR+ NAB and HAB mice, I suggest a principal component analysis to further classify the obtained results.
6) Even though Hyp^{CaMK} and SF1-positive neurons were identified as a key population for mediating passive fear responses and likely the switch between passive and active fear, the dissection of the exact pathways remains elusive.

4.6 Conclusions

Everything created, in turn deserves to be annihilated
– JW Goethe, Faust I –

In my thesis I could demonstrate a multifaceted role of 2-AG mediated CB1 signaling on the positive (motivation) and negative (anxiety and fear) valence system. Using enzymatic assays and endocannabinoid measurements, I could validate a tight control of 2-AG signaling by its degrading enzyme MAGL within the hypothalamus and nucleus accumbens in healthy mice. Using conditional mutagenesis of CB1, hypothalamic neurons were shown to be important in both, the positive and negative valence system. In search of the neuronal population, however, the neuronal populations responsible for motivation and fear do not overlap (Fig. 28).

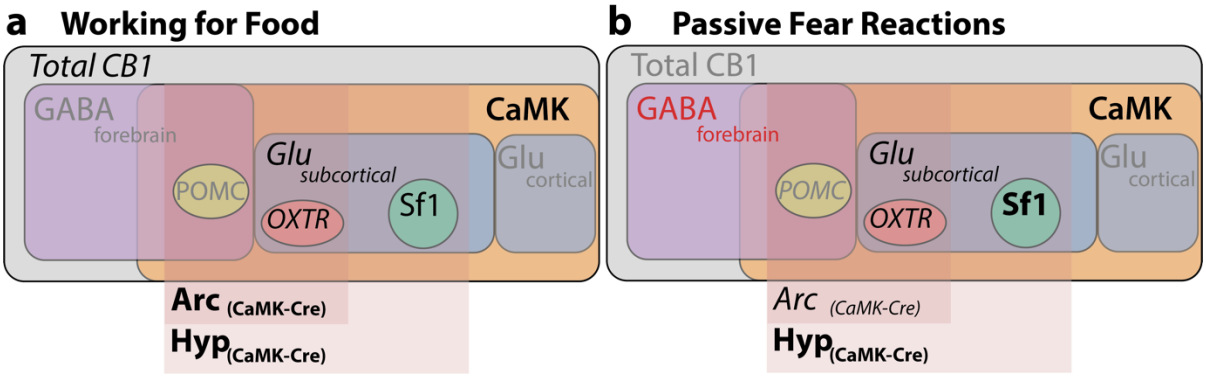

Figure 28: Summarized involvement of hypothalamic CB1 in the positive (a) and negative (b) valence system. a CaMK-positive neurons of the Arc mediate the working for food effect of increased 2-AG levels, whereas **b** SF1- (and CaMK-positive) neurons of the hypothalamus are responsible for passive fear reactions. **bold**: significant phenotype, grey: no phenotype, *italic*: not studied, red: opposite phenotype.

Whereby healthy mice show a finetuned homeostasis of 2-AG degradation, imbalances may cause pathologic states such as metabolic- or anxiety-disorders. With the proposed mechanism of MAGL dimerization and translocation and the involvement of the stress hormone corticosterone, I can propose novel targets, which are indeed worthwhile of being investigated in patient populations.

Curiosity is the driving force, liberty the indispensable basis of science

– O. Wiestler; HG –

Contributions

DEH was supervised by PD Dr. Carsten Wotjak and designed all the studies, supervised students, performed the experiments, analyzed, and interpreted the data and wrote this thesis.

Parts of experiments were supported or performed by internal, or external collaborators, or with the help of colleagues, technical staff or with the expertise of scientific core units. Parts of the BMT KO-Study were already presented in my master's thesis (Heinz, 2017). All contributions were highly appreciated and listed below:

PD Dr. Carsten T. Wotjak designed the studies with DEH and supervised him in all the studies. All obtained data were interpreted together.

Dr. Nils C. Gassen, TAC member, and group leader (RG Neurohomeostasis) at the University Hospital Bonn, supervised molecular and proteomic approaches including the generation, analysis, and interpretation of membranome and interactome data. DEH holds a contract as guest scientist at the Clinic of Psychiatry and Psychotherapy, University Hospital Bonn (Prof. Dr. Alexandra Philipsen) and performed parts of experiments in Bonn.

Prof. Dr. Elisabeth Binder and Monika Rex-Haffner supported me, especially in the end phase of the project with administrative support and provided me with sufficient lab space.

<u>Members of the (former) Wotjak-lab</u> contributed to projects of my doctoral thesis: DEH (partially) supervised projects of internship (2), Master's (1) and medical doctoral students (3), HiWis (4) and technicians (2) that contributed to projects. Mojan Parvaz, Maria Bartmann, Christin Weiß, Tibor Stark, Alice Hartmann, Paulina Nemcova, Vivian Schöttle, Nadine Brückner and Lea Bartmann.

Tim Ebert contributed with behavioral scoring of mice.

Paul Kaplick started and established the PR-Protocol in house.

Internal collaborative partners contributed to the PhD-Project:

Dr. Jan Deussing, as head of the Core Unit GEMM (Sabrina Bauer, Andrea Ressle Stefanie Unkmeir) essentially supported the project with expertise, genotyping of most and maintaining of some genetically modified mouse lines.

Dr. Rosa-Eva Hüttl performed and supported stereotactic virus injections of a variety of mice. Dr. Hüttl is affiliated with the Core Unit Viral Vectors (Maria Holzapfel), that organized all and produced some of the used viral vectors.

The department Stress Neurobiology and Neurogenetics of Prof. Dr. Alon Chen contributed with consumables, expertise, and hands on support by lab technicians: Andrea Parl, Carola Eggert and Dr. Claudia Kühne conceptually contributed to parts of the project and performed cloning, and (double) *in situ* hybridizations. Rainer Stoffel essentially contributed to touchscreen testing and food deprivation (days distributed between DEH and RS). RS performed the majority of radio immune assays (RIA). *In situ* hybridization, vibratome and cryostat slicing as well as the generation of basic lab solutions were (in parts) performed by the infrastructure of the Department Chen: Bianca Schmidt, Daniela Harbich, Emanuel Roos, Andrea Ressle, Andrea Parl, Dr. Claudia Kühne, Carola Eggert.

The animal facility (Albin Varga + Team) contributed with maintaining and breeding (especially Angelina Rusin and Anja Amann) of all laboratory mice and partially contributed to animal experiments with scoring of mice or transferring mice to external collaboration partners.

This PhD-project was supported by external collaborators:

The laboratory of Prof. Dr. Mario van der Stelt processed ABPP analysis of punched mouse brain samples and provided DH376.

Dr. Laura Bindila and Prof. Dr. Beat Lutz (University Clinic Mainz, Mainz University) measured hypothalamic endocannabinoid levels of food deprived vs. ad libitum fed mice.

Dr. Anna Bludau, a member of Prof. Dr. Inga Neumann's laboratory (Regensburg University), performed antero-, and retrograde tracing in the vmH, Arc and PAG. Pictures were taken, and RNAScope was performed.

Dr. Kay Jüngling and Dr. Maren Lange in the laboratory of Prof. Dr. Hans-Christian Pape (University Münster) performed electrophysiological measurements of POMC-Cre mice.

Financial support

Daniel Heinz was funded by the ministry of research and education (BMBF) and the Max Planck Society as a member of the Max Planck School of Cognition (2019-2020). Some of the projects were partly supported by the GIF (2017; 2019-2020; Grant Number: I-1442-421.13/2017).

Own publications

All studies were aimed to be published in peer review journals. At the time point of submission, not all manuscripts were submitted/accepted.

Next to the primary doctoral project, I contributed to the following publications as a (co-)author:

Ruat, J., **Heinz, D. E.**, Binder, F. P., Stark, T., Neuner, R., Hartmann, A., … Wotjak, C. T. (2021). Structural correlates of trauma-induced hyperarousal in mice. Progress in Neuro-Psychopharmacology and Biological Psychiatry, 111, 110404.

Martinelli, S., Anderzhanova, E. A., Bajaj, T., Wiechmann, S., Dethloff, F., Weckmann, K., **Heinz, D. E.**, … Gassen, N. C. (2021). Stress-primed secretory autophagy promotes extracellular BDNF maturation by enhancing MMP9 secretion. Nature Communications, 12(1), 4643.

Gassen, N. C., Papies, J., Bajaj, T., Emanuel, J., Dethloff, F., Chua, R. L., … **Heinz, D. E.**, … Müller, M. A. (2021). SARS-CoV-2-mediated dysregulation of metabolism and autophagy uncovers host-targeting antivirals. Nature Communications 2021 12:1, 12(1), 1–15.

Stepan, J., **Heinz, D. E.**, Dethloff, F., Bajaj, T., Hafner, K., Wiechmann, S., … Gassen, N. C. (2021). Hippo-Released WWC1 Primes Ampa Receptor Regulatory Complexes for Hippocampal Learning. SSRN Electronic Journal.

Heinz, D. E., Schöttle, V. A., Nemcova, P., Binder, F. P., Ebert, T., Domschke, K., & Wotjak, C. T. (2021). Exploratory drive, fear, and anxiety are dissociable and independent components in foraging mice. Translational Psychiatry, 11(1), 318.

Fendt, M., Parsons, M. H., Apfelbach, R., Carthey, A. J. R., Dickman, C. R., Endres, T., Frank, A. S. K., **Heinz, D. E.**, Jones, M. E., Kiyokawa, Y., Kreutzmann, J. C., Roelofs, K., Schneider, M., Sulger, J., Wotjak, C. T., & Blumstein, D. T. (2020). Context and trade-offs characterize real-world threat detection systems: A review and comprehensive framework to improve research practice and resolve the translational crisis. Neuroscience & Biobehavioral Reviews, 115, 25–33.

Hahn, C., Becker, K., Saghafi, S., Pende, M., Avdibašić, A., Foroughipour, M., **Heinz, D. E.**, Wotjak, C. T., & Dodt, H.-U. (2019). High-resolution imaging of fluorescent whole mouse brains using stabilised organic media (sDISCO). In Journal of biophotonics (Vol. 12, Issue 8, p. e201800368).

Genewsky, A. J., Albrecht, N., Bura, S. A., Kaplick, P. M., **Heinz, D. E.**, Nußbaumer, M., … Wotjak, C. T. (2018). How much fear is in anxiety? BioRxiv.

Almada, R. C., Genewsky, A. J., **Heinz, D. E.**, Kaplick, P. M., Coimbra, N. C., & Wotjak, C. T. (2018). Stimulation of the Nigrotectal Pathway at the Level of the Superior Colliculus Reduces Threat Recognition and Causes a Shift From Avoidance to Approach Behavior. Frontiers in Neural Circuits, 12, 36.

Genewsky, A., **Heinz, D. E.**, Kaplick, P. M., Kilonzo, K., & Wotjak, C. T. (2017). A simplified microwave-based motion detector for home cage activity monitoring in mice. Journal of Biological Engineering, 11, 36.

Heinz, D. E., Genewsky, A., & Wotjak, C. T. (2017). Enhanced anandamide signaling reduces flight behavior elicited by an approaching robo-beetle. Neuropharmacology, 126, 233–241.

BIBLIOGRAPHY

Ahn K, McKinney MK, Cravatt BF (2008) Enzymatic Pathways That Regulate Endocannabinoid Signaling in the Nervous System. Chemical Reviews 108:1687–1707 Available at: https://pubs.acs.org/doi/10.1021/cr0782067.

Alger BE, Kim J (2011) Supply and demand for endocannabinoids. Trends in Neurosciences 34:304–315 Available at: https://www.sciencedirect.com/science/article/pii/S0166223611000403?via%3Dihub [Accessed June 14, 2021].

Azad SC, Marsicano G, Eberlein I, Putzke J, Zieglgänsberger W, Spanagel R, Lutz B (2001) Differential role of the nitric oxide pathway on Δ ^{9} -THC-induced central nervous system effects in the mouse. European Journal of Neuroscience 13:561–568 Available at: http://doi.wiley.com/10.1046/j.1460-9568.2001.01431.x [Accessed January 17, 2021].

Balsevich G, Sticht M, Bowles NP, Singh A, Lee TTY, Li Z, Chelikani PK, Lee FS, Borgland SL, Hillard CJ, McEwen BS, Hill MN (2018) Role for fatty acid amide hydrolase (FAAH) in the leptin-mediated effects on feeding and energy balance. Proceedings of the National Academy of Sciences of the United States of America 115:7605–7610.

Balthasar N, Coppari R, McMinn J, Liu SM, Lee CE, Tang V, Kenny CD, McGovern RA, Chua SC, Elmquist JK, Lowell BB (2004) Leptin Receptor Signaling in POMC Neurons Is Required for Normal Body Weight Homeostasis. Neuron 42:983–991 Available at: https://www.sciencedirect.com/science/article/pii/S089662730400354X [Accessed June 23, 2021].

Batista EML, Doria JG, Ferreira-Vieira TH, Alves-Silva J, Ferguson SSG, Moreira FA, Ribeiro FM (2016) Orchestrated activation of mGluR5 and CB 1 promotes neuroprotection. Available at: http://creativecommons.org/publicdomain/zero/1.0/ [Accessed June 10, 2021].

Bellocchio L, Lafenêtre P, Cannich A, Cota D, Puente N, Grandes P, Chaouloff F, Piazza PV, Marsicano G (2010) Bimodal control of stimulated food intake by the endocannabinoid system. Nature neuroscience 13:281–283.

Bénard G et al. (2012) Mitochondrial CB1 receptors regulate neuronal energy metabolism. Nature Neuroscience 15:558–564 Available at: http://www.nature.com/articles/nn.3053 [Accessed June 14, 2021].

Berghaeuser H, Hoelscher M (2020) Reinventing the third mission of higher education in Germany: political frameworks and universities' reactions. Tertiary Education and Management 26:57–76 Available at: http://link.springer.com/10.1007/s11233-019-09030-3 [Accessed July 9, 2021].

Bernstein IL, Lotter EC, Kulkosky PJ, Porte D, Woods SC (1975) Effect of Force-Feeding Upon Basal Insulin Levels of Rats. Experimental Biology and Medicine 150:546–548 Available at: http://ebm.sagepub.com/lookup/doi/10.3181/00379727-150-39075 [Accessed May 23, 2021].

Berridge KC, Robinson TE (2016) Liking, wanting, and the incentive-sensitization theory of addiction. The American psychologist 71:670–679 Available at: http://www.ncbi.nlm.nih.gov/pubmed/27977239 [Accessed June 20, 2021].

Biglari N et al. (2021) Functionally distinct POMC-expressing neuron subpopulations in hypothalamus revealed by intersectional targeting. Nature Neuroscience:1–17 Available at: http://www.nature.com/articles/s41593-021-00854-0 [Accessed June 23, 2021].

Blankman JL, Simon GM, Cravatt BF (2007) A Comprehensive Profile of Brain Enzymes that Hydrolyze the Endocannabinoid 2-Arachidonoylglycerol. Chemistry & Biology

14:1347–1356 Available at: https://www.sciencedirect.com/science/article/pii/S1074552107003997?via%3Dihub [Accessed June 16, 2021].

Bosier B, Bellocchio L, Metna-Laurent M, Soria-Gomez E, Matias I, Hebert-Chatelain E, Cannich A, Maitre M, Leste-Lasserre T, Cardinal P, Mendizabal-Zubiaga J, Canduela MJ, Reguero L, Hermans E, Grandes P, Cota D, Marsicano G (2013) Astroglial CB1 cannabinoid receptors regulate leptin signaling in mouse brain astrocytes. Molecular Metabolism 2:393–404 Available at: https://www.sciencedirect.com/science/article/pii/S2212877813000707?via%3Dihub [Accessed June 14, 2021].

Bouaboula M, Rinaldi M, Carayon P, Carillon C, Delpech B, Shire D, Fur G, Casellas P (1993) Cannabinoid-receptor expression in human leukocytes. European Journal of Biochemistry 214:173–180 Available at: http://doi.wiley.com/10.1111/j.1432-1033.1993.tb17910.x [Accessed January 17, 2021].

Brown JE, Kassouny M, Cross JK (1977) Kinetic studies of food intake and sucrose solution preference by rats treated with low doses of Δ9-tetrahydrocannabinol. Behavioral Biology 20:104–110.

Buczynski MW, Parsons LH (2010) Quantification of brain endocannabinoid levels: methods, interpretations and pitfalls. British journal of pharmacology 160:423–442 Available at: http://www.ncbi.nlm.nih.gov/pubmed/20590555 [Accessed July 8, 2021].

Burstein S, Hunter SA, Latham V, Mechoulam R, Melchior DL, Renzulli L, Tefft RE (1986) Prostaglandins and cannabis XV. Comparison of enantiomeric cannabinoids in stimulating prostaglandin synthesis in fibroblasts. Life Sciences 39:1813–1823 Available at: https://www.sciencedirect.com/science/article/pii/0024320586901013?via%3Dihub [Accessed February 27, 2021].

Busquets-Garcia A, Puighermanal E, Pastor A, de la Torre R, Maldonado R, Ozaita A (2011) Differential Role of Anandamide and 2-Arachidonoylglycerol in Memory and Anxiety-like Responses. Biological Psychiatry 70:479–486 Available at: https://www.sciencedirect.com/science/article/pii/S0006322311004409?via%3Dihub [Accessed July 9, 2021].

Cabral GA, Toney DM, Fischer-Stenger K, Harrison MP, Marciano-Cabral F (1995) Anandamide inhibits macrophage-mediated killing of tumor necrosis factor-sensitive cells. Life Sciences 56:2065–2072 Available at: https://www.sciencedirect.com/science/article/pii/002432059500190H?via%3Dihub [Accessed February 27, 2021].

Cadas H, Gaillet S, Beltramo M, Venance L, Piomelli D (1996) Biosynthesis of an endogenous cannabinoid precursor in neurons and its control by calcium and cAMP. The Journal of neuroscience : the official journal of the Society for Neuroscience 16:3934–3942 Available at: http://www.ncbi.nlm.nih.gov/pubmed/8656287 [Accessed February 28, 2021].

Calignano A, Rana G la, Giuffrida A, Piomelli D (1998) Control of pain initiation by endogenous cannabinoids. Nature 394:277–281 Available at: http://www.nature.com/articles/28393 [Accessed February 27, 2021].

Cardinal P, André C, Quarta C, Bellocchio L, Clark S, Elie M, Leste-Lasserre T, Maitre M, Gonzales D, Cannich A, Pagotto U, Marsicano G, Cota D (2014) CB1 cannabinoid receptor in SF1-expressing neurons of the ventromedial hypothalamus determines metabolic responses to diet and leptin. Molecular Metabolism 3:705–716.

Carr RL, Adams AL, Kepler DR, Ward AB, Ross MK (2013) Induction of Endocannabinoid Levels in Juvenile Rat Brain Following Developmental Chlorpyrifos Exposure.

Toxicological Sciences 135:193–201 Available at: https://academic.oup.com/toxsci/article-lookup/doi/10.1093/toxsci/kft126 [Accessed June 18, 2021].

Carr RL, Graves CA, Mangum LC, Nail CA, Ross MK (2014) Low level chlorpyrifos exposure increases anandamide accumulation in juvenile rat brain in the absence of brain cholinesterase inhibition. NeuroToxicology 43:82–89 Available at: https://www.sciencedirect.com/science/article/pii/S0161813X13001903?via%3Dihub#bib0065 [Accessed June 18, 2021].

Chadwick VL, Rohleder C, Koethe D, Leweke FM (2020) Cannabinoids and the endocannabinoid system in anxiety, depression, and dysregulation of emotion in humans. Current Opinion in Psychiatry 33:20–42 Available at: https://journals.lww.com/10.1097/YCO.0000000000000562 [Accessed March 6, 2021].

Chávez AE, Chiu CQ, Castillo PE (2010) TRPV1 activation by endogenous anandamide triggers postsynaptic long-term depression in dentate gyrus. Nature Neuroscience 13:1511–1518 Available at: http://www.nature.com/articles/nn.2684 [Accessed February 28, 2021].

Chhatwal JP, Gutman AR, Maguschak KA, Bowser ME, Yang Y, Davis M, Ressler KJ (2009) Functional Interactions between Endocannabinoid and CCK Neurotransmitter Systems May Be Critical for Extinction Learning. Neuropsychopharmacology 34:509–521 Available at: http://www.nature.com/articles/npp200897 [Accessed July 27, 2021].

Childers SR, Deadwyler SA (1996) Role of cyclic AMP in the actions of cannabinoid receptors. Biochemical Pharmacology 52:819–827 Available at: https://www.sciencedirect.com/science/article/pii/0006295296004194?via%3Dihub [Accessed February 27, 2021].

Conde K, Fabelo C, Krause WC, Propst R, Goethel J, Fischer D, Hur J, Meza C, Ingraham HA, Wagner EJ (2017) Testosterone Rapidly Augments Retrograde Endocannabinoid Signaling in Proopiomelanocortin Neurons to Suppress Glutamatergic Input from Steroidogenic Factor 1 Neurons via Upregulation of Diacylglycerol Lipase-α. Neuroendocrinology 105:341–356 Available at: http://www.ncbi.nlm.nih.gov/pubmed/27871072 [Accessed June 10, 2021].

Conde K, Meza C, Kelly MJ, Sinchak K, Wagner EJ (2016) Estradiol Rapidly Attenuates ORL-1 Receptor-Mediated Inhibition of Proopiomelanocortin Neurons via Gq-Coupled, Membrane-Initiated Signaling. Neuroendocrinology 103:787–805 Available at: http://www.ncbi.nlm.nih.gov/pubmed/26765570 [Accessed June 10, 2021].

Correia-Sá IB, Carvalho CM, Serrão P v., Loureiro AI, Fernandes-Lopes C, Marques M, Vieira-Coelho MA (2020) A new role for anandamide: defective link between the systemic and skin endocannabinoid systems in hypertrophic human wound healing. Scientific Reports 10:11134 Available at: http://www.nature.com/articles/s41598-020-68058-3 [Accessed February 27, 2021].

Coutinho EA, Okamoto S, Ishikawa AW, Yokota S, Wada N, Hirabayashi T, Saito K, Sato T, Takagi K, Wang C-C, Kobayashi K, Ogawa Y, Shioda S, Yoshimura Y, Minokoshi Y (2017) Activation of SF1 Neurons in the Ventromedial Hypothalamus by DREADD Technology Increases Insulin Sensitivity in Peripheral Tissues. Diabetes 66:2372–2386 Available at: http://www.ncbi.nlm.nih.gov/pubmed/28673934 [Accessed June 22, 2021].

Cowley MA et al. (2003) The Distribution and Mechanism of Action of Ghrelin in the CNS Demonstrates a Novel Hypothalamic Circuit Regulating Energy Homeostasis. Available at: https://www.cell.com/neuron/pdf/S0896-6273(03)00063-1.pdf [Accessed June 19, 2021].

Deadwyler SA, Hampson RE, Mu J, Whyte A, Childers S (1995) Cannabinoids modulate voltage sensitive potassium A-current in hippocampal neurons via a cAMP-dependent process. Journal of Pharmacology and Experimental Therapeutics 273.

Delgado-Peraza F, Ahn KH, Nogueras-Ortiz C, Mungrue IN, Mackie K, Kendall DA, Yudowski GA (2016) Mechanisms of Biased β-Arrestin-Mediated Signaling Downstream from the Cannabinoid 1 Receptor. Molecular pharmacology 89:618–629 Available at: http://www.ncbi.nlm.nih.gov/pubmed/27009233 [Accessed February 27, 2021].

Deng H, Kooijman S, van den Nieuwendijk AMCH, Ogasawara D, van der Wel T, van Dalen F, Baggelaar MP, Janssen FJ, van den Berg RJBHN, den Dulk H, Cravatt BF, Overkleeft HS, Rensen PCN, van der Stelt M (2017) Triazole Ureas Act as Diacylglycerol Lipase Inhibitors and Prevent Fasting-Induced Refeeding. Journal of Medicinal Chemistry 60:428–440 Available at: https://pubs.acs.org/doi/10.1021/acs.jmedchem.6b01482 [Accessed June 18, 2021].

Després J-P, Golay A, Sjöström L (2005) Effects of Rimonabant on Metabolic Risk Factors in Overweight Patients with Dyslipidemia. New England Journal of Medicine 353:2121–2134 Available at: http://www.nejm.org/doi/abs/10.1056/NEJMoa044537 [Accessed June 20, 2021].

Devane WA, Hanus L, Breuer A, Pertwee RG, Stevenson LA, Griffin G, Gibson D, Mandelbaum A, Etinger A, Mechoulam R (1992) Isolation and structure of a brain constituent that binds to the cannabinoid receptor. Science (New York, NY) 258:1946–1949 Available at: http://www.ncbi.nlm.nih.gov/pubmed/1470919 [Accessed January 17, 2021].

Dhillon H, Zigman JM, Ye C, Lee CE, McGovern RA, Tang V, Kenny CD, Christiansen LM, White RD, Edelstein EA, Coppari R, Balthasar N, Cowley MA, Chua S, Elmquist JK, Lowell BB (2006) Leptin Directly Activates SF1 Neurons in the VMH, and This Action by Leptin Is Required for Normal Body-Weight Homeostasis. Neuron 49:191–203 Available at: https://www.sciencedirect.com/science/article/pii/S0896627305011347?via%3Dihub [Accessed June 14, 2021].

Dincheva I, Drysdale AT, Hartley CA, Johnson DC, Jing D, King EC, Ra S, Gray JM, Yang R, DeGruccio AM, Huang C, Cravatt BF, Glatt CE, Hill MN, Casey BJ, Lee FS (2015) FAAH genetic variation enhances fronto-amygdala function in mouse and human. Nature Communications 6:6395 Available at: http://www.nature.com/articles/ncomms7395 [Accessed March 6, 2021].

Dinh TP, Carpenter D, Leslie FM, Freund TF, Katona I, Sensi SL, Kathuria S, Piomelli D (2002) Brain monoglyceride lipase participating in endocannabinoid inactivation. Proceedings of the National Academy of Sciences of the United States of America 99:10819–10824 Available at: http://www.ncbi.nlm.nih.gov/pubmed/12136125 [Accessed June 16, 2021].

Dominguez E, Galmozzi A, Chang JW, Hsu K-L, Pawlak J, Li W, Godio C, Thomas J, Partida D, Niessen S, O'Brien PE, Russell AP, Watt MJ, Nomura DK, Cravatt BF, Saez E (2014) Integrated phenotypic and activity-based profiling links Ces3 to obesity and diabetes. Nature Chemical Biology 10:113–121 Available at: http://www.nature.com/articles/nchembio.1429 [Accessed July 10, 2021].

Dotsey EY, Jung K-M, Basit A, Wei D, Daglian J, Vacondio F, Armirotti A, Mor M, Piomelli D (2015) Peroxide-Dependent MGL Sulfenylation Regulates 2-AG-Mediated Endocannabinoid Signaling in Brain Neurons. Chemistry & Biology 22:619–628 Available at: https://www.sciencedirect.com/science/article/pii/S107455211500157X?via%3Dihub [Accessed June 16, 2021].

Eldeeb K, Leone-Kabler S, Howlett AC (2016) CB1 cannabinoid receptor-mediated increases in cyclic AMP accumulation are correlated with reduced Gi/o function. Journal of Basic and Clinical Physiology and Pharmacology 27:311–322.

EMEA (2008) The European Medicines Agency recommends suspension of the marketing authorisation of Acomplia. Available at: https://www.ema.europa.eu/en/documents/press-release/european-medicines-agency-recommends-suspension-marketing-authorisation-acomplia_en.pdf [Accessed May 23, 2021].

Evanson NK, Tasker JG, Hill MN, Hillard CJ, Herman JP (2010) Fast Feedback Inhibition of the HPA Axis by Glucocorticoids Is Mediated by Endocannabinoid Signaling. Endocrinology 151:4811–4819 Available at: https://academic.oup.com/endo/article/151/10/4811/2456329 [Accessed June 23, 2021].

Fabelo C, Hernandez J, Chang R, Seng S, Alicea N, Tian S, Conde K, Wagner EJ (2018) Endocannabinoid Signaling at Hypothalamic Steroidogenic Factor-1/Proopiomelanocortin Synapses Is Sex- and Diet-Sensitive. Frontiers in Molecular Neuroscience 11:214 Available at: https://www.frontiersin.org/article/10.3389/fnmol.2018.00214/full [Accessed July 27, 2021].

Fang Y, Kelly MJ, Rønnekleiv OK (1998) Proopiomelanocortin (POMC) mRNA expression: distribution and region-specific down-regulation by chronic morphine in female guinea pig hypothalamus. Molecular Brain Research 55:1–8 Available at: https://www.sciencedirect.com/science/article/pii/S0169328X97003483?via%3Dihub [Accessed July 27, 2021].

Felder CC, Joyce KE, Briley EM, Mansouri J, Mackie K, Blond O, Lai Y, Ma AL, Mitchell RL (1995) Comparison of the pharmacology and signal transduction of the human cannabinoid CB1 and CB2 receptors. Molecular pharmacology 48:443–450 Available at: http://www.ncbi.nlm.nih.gov/pubmed/7565624 [Accessed February 27, 2021].

Fendt M, Parsons MH, Apfelbach R, Carthey AJR, Dickman CR, Endres T, Frank ASK, Heinz DE, Jones ME, Kiyokawa Y, Kreutzmann JC, Roelofs K, Schneider M, Sulger J, Wotjak CT, Blumstein DT (2020) Context and trade-offs characterize real-world threat detection systems: A review and comprehensive framework to improve research practice and resolve the translational crisis. Neuroscience & Biobehavioral Reviews 115:25–33 Available at: https://www.sciencedirect.com/science/article/abs/pii/S0149763420303973?via%3Dihub [Accessed January 31, 2021].

Fenselau H, Campbell JN, Verstegen AMJ, Madara JC, Xu J, Shah BP, Resch JM, Yang Z, Mandelblat-Cerf Y, Livneh Y, Lowell BB (2017) A rapidly acting glutamatergic ARC→PVH satiety circuit postsynaptically regulated by α-MSH. Nature Neuroscience 20:42–51 Available at: http://www.nature.com/articles/nn.4442 [Accessed July 27, 2021].

Fernstrom MH, Fernstrom JD (1995) Brain tryptophan concentrations and serotonin synthesis remain responsive to food consumption after the ingestion of sequential meals. The American Journal of Clinical Nutrition 61:312–319 Available at: https://academic.oup.com/ajcn/article/61/2/312/4651280 [Accessed June 20, 2021].

Fidelman S, Mizrachi Zer-Aviv T, Lange R, Hillard CJ, Akirav I (2018) Chronic treatment with URB597 ameliorates post-stress symptoms in a rat model of PTSD. European Neuropsychopharmacology 28:630–642 Available at: https://www.sciencedirect.com/science/article/pii/S0924977X18300452?via%3Dihub [Accessed June 17, 2021].

Gabriel LR, Wu S, Melikian HE (2014) Brain slice biotinylation: an ex vivo approach to measure region-specific plasma membrane protein trafficking in adult neurons. Journal of visualized experiments : JoVE Available at: http://www.ncbi.nlm.nih.gov/pubmed/24747337 [Accessed June 6, 2021].

Gaoni Y, Mechoulam R (1964) Isolation, Structure, and Partial Synthesis of an Active Constituent of Hashish. Journal of the American Chemical Society 86:1646–1647 Available at: https://pubs.acs.org/doi/abs/10.1021/ja01062a046 [Accessed July 10, 2021].

Genewsky AJ, Wotjak CT (2017) The Endocannabinoid System Differentially Regulates Escape Behavior in Mice. Frontiers in Behavioral Neuroscience 11:201 Available at: http://journal.frontiersin.org/article/10.3389/fnbeh.2017.00201/full [Accessed March 6, 2021].

Gerber DJ, Sotnikova TD, Gainetdinov RR, Huang SY, Caron MG, Tonegawa S, Conklin BR (2001) Hyperactivity, elevated dopaminergic transmission, and response to amphetamine in M1 muscarinic acetylcholine receptor-deficient mice. Proceedings of the National Academy of Sciences 98:15312–15317 Available at: http://www.pnas.org/cgi/doi/10.1073/pnas.261583798 [Accessed July 10, 2021].

Giraudo SQ, Grace MK, Billington CJ, Levine AS (1999) Differential effects of neuropeptide Y and the μ-agonist DAMGO on `palatability' vs. `energy'. Brain Research 834:160–163 Available at: https://www.sciencedirect.com/science/article/pii/S0006899399015127?via%3Dihub [Accessed June 20, 2021].

Glass M, Felder CC (1997) Concurrent stimulation of cannabinoid CB1 and dopamine D2 receptors augments cAMP accumulation in striatal neurons: evidence for a Gs linkage to the CB1 receptor. The Journal of neuroscience: the official journal of the Society for Neuroscience 17:5327–5333 Available at: http://www.ncbi.nlm.nih.gov/pubmed/9204917 [Accessed January 17, 2021].

Gorzalka BB, Hill MN, Hillard CJ (2008) Regulation of endocannabinoid signaling by stress: Implications for stress-related affective disorders. Neuroscience & Biobehavioral Reviews 32:1152–1160 Available at: https://www.sciencedirect.com/science/article/pii/S0149763408000365 [Accessed March 1, 2021].

Grotenhermen F 1957-, Brenneisen R (n.d.) Cannabis und Cannabinoide Pharmakologie, Toxikologie und therapeutisches Potenzial. Available at: https://books.google.de/books/about/Cannabis_und_Cannabinoide.html?id=9KkWAQAACAAJ&source=kp_cover&redir_esc=y [Accessed January 17, 2021].

Guan X-M, Yu H, Palyha OC, McKee KK, Feighner SD, Sirinathsinghji DJS, Smith RG, van der Ploeg LHT, Howard AD (1997) Distribution of mRNA encoding the growth hormone secretagogue receptor in brain and peripheral tissues. Molecular Brain Research 48:23–29 Available at: https://www.sciencedirect.com/science/article/pii/S0169328X97000715 [Accessed June 17, 2021].

Guy GW (Geoffrey W, Whittle BA (Brian A, Robson Philip (2004) The medicinal use of cannabis and cannabinoids. Pharmaceutical Press. Available at: https://books.google.de/books/about/The_Medicinal_Uses_of_Cannabis_and_Canna.html?id=AznCzOxvrtwC&redir_esc=y [Accessed January 17, 2021].

Hampson RE, Evans GJO, Mu J, Zhuang S, King VC, Childers SR, Deadwyler SA (1995) Role of cyclic amp dependent protein kinase in cannabinoid receptor modulation of potassium "A-current" in cultured rat hippocampal neurons. Life Sciences 56:2081–2088 Available at:

https://www.sciencedirect.com/science/article/pii/0024320595001929?via%3Dihub [Accessed February 27, 2021].

Harkany T, Holmgren C, Härtig W, Qureshi T, Chaudhry FA, Storm-Mathisen J, Dobszay MB, Berghuis P, Schulte G, Sousa KM, Fremeau RT, Edwards RH, Mackie K, Ernfors P, Zilberter Y (2004) Endocannabinoid-Independent Retrograde Signaling at Inhibitory Synapses in Layer 2/3 of Neocortex: Involvement of Vesicular Glutamate Transporter 3. Available at: https://www.jneurosci.org/content/jneuro/24/21/4978.full.pdf [Accessed July 8, 2021].

Häusl AS et al. (2021) The co-chaperone Fkbp5 shapes the acute stress response in the paraventricular nucleus of the hypothalamus of male mice. Molecular Psychiatry:1–17 Available at: http://www.nature.com/articles/s41380-021-01044-x [Accessed May 24, 2021].

Heath CJ, Bussey TJ, Saksida LM (2015) Motivational assessment of mice using the touchscreen operant testing system: effects of dopaminergic drugs. Psychopharmacology 232:4043–4057 Available at: https://pubmed.ncbi.nlm.nih.gov/26156636.

Heath CJ, Phillips BU, Bussey TJ, Saksida LM (2016) Measuring Motivation and Reward-Related Decision Making in the Rodent Operant Touchscreen System. Current protocols in neuroscience 74:8.34.1-8.34.20.

Hebert-Chatelain E et al. (2016) A cannabinoid link between mitochondria and memory. Nature 539:555–559 Available at: http://www.nature.com/articles/nature20127 [Accessed June 14, 2021].

Heinz DE (2017) Role of endocannabinoid signaling in two new animal models of passive and active unconditioned fear.

Heinz DE, Genewsky A, Wotjak CT (2017) Enhanced anandamide signaling reduces flight behavior elicited by an approaching robo-beetle. Neuropharmacology 126:233–241 Available at: https://doi.org/10.1016/j.neuropharm.2017.09.010.

Heinz DE, Schöttle VA, Nemcova P, Binder FP, Ebert T, Domschke K, Wotjak CT (2021) Exploratory drive, fear, and anxiety are dissociable and independent components in foraging mice. Translational Psychiatry 11:318 Available at: http://www.nature.com/articles/s41398-021-01458-9 [Accessed May 26, 2021].

Henke J, Pasternack P, Schmid S (2016) Third Mission von Hochschulen. Eine Definition. Das Hochschulwesen 64:16–22.

Herkenham M, Lynn AB, Johnson MR, Melvin LS, de Costa BR, Rice KC (1991) Characterization and localization of cannabinoid receptors in rat brain: a quantitative in vitro autoradiographic study. The Journal of neuroscience: the official journal of the Society for Neuroscience 11:563–583 Available at: http://www.ncbi.nlm.nih.gov/pubmed/1992016 [Accessed February 27, 2021].

Herkenham M, Lynn AB, Litrle MD, Johnsont MR, Melvin LS, de Costa BR, Riceo KC (1990) Cannabinoid receptor localization in brain (tetrahydrocannabinol/autoradiography/basal ganglla/hippocampus/cerebeilum). Proc Nati Acad Sci USA 87:1932–1936 Available at: https://www.pnas.org/content/pnas/87/5/1932.full.pdf [Accessed January 17, 2021].

Hill MN, Karatsoreos IN, Hillard CJ, McEwen BS (2010a) Rapid elevations in limbic endocannabinoid content by glucocorticoid hormones in vivo. Psychoneuroendocrinology 35:1333–1338 Available at: https://www.sciencedirect.com/science/article/pii/S0306453010000831 [Accessed June 23, 2021].

Hill MN, McLaughlin RJ, Bingham B, Shrestha L, Lee TTY, Gray JM, Hillard CJ, Gorzalka BB, Viau V (2010b) Endogenous cannabinoid signaling is essential for stress adaptation. Proceedings of the National Academy of Sciences of the United States of America 107:9406–9411 Available at: http://www.ncbi.nlm.nih.gov/pubmed/20439721 [Accessed March 1, 2021].

Hillard CJ, Bloom AS (1983) Possible role of prostaglandins in the effects of the cannabinoids on adenylate cyclase activity. European Journal of Pharmacology 91:21–27 Available at: https://www.sciencedirect.com/science/article/pii/0014299983903576?via%3Dihub [Accessed February 27, 2021].

Horner AE, Heath CJ, Hvoslef-Eide M, Kent BA, Kim CH, Nilsson SRO, Alsiö J, Oomen CA, Holmes A, Saksida LM, Bussey TJ (2013) The touchscreen operant platform for testing learning and memory in rats and mice. Nature Protocols 8:1961–1984 Available at: http://www.nature.com/articles/nprot.2013.122 [Accessed March 14, 2021].

Howlett AC (2004) Efficacy in CB $_1$ receptor-mediated signal transduction. British Journal of Pharmacology 142:1209–1218 Available at: http://doi.wiley.com/10.1038/sj.bjp.0705881 [Accessed February 27, 2021].

Hsieh C, Brown S, Derleth C, Mackie K (2002) Internalization and Recycling of the CB1 Cannabinoid Receptor. Journal of Neurochemistry 73:493–501 Available at: http://doi.wiley.com/10.1046/j.1471-4159.1999.0730493.x [Accessed March 1, 2021].

Hsu K-L, Tsuboi K, Adibekian A, Pugh H, Masuda K, Cravatt BF (2012) DAGLβ inhibition perturbs a lipid network involved in macrophage inflammatory responses. Nature Chemical Biology 8:999–1007 Available at: http://www.nature.com/articles/nchembio.1105 [Accessed June 27, 2021].

Hsu K-L, Tsuboi K, Chang JW, Whitby LR, Speers AE, Pugh H, Cravatt BF (2013) Discovery and Optimization of Piperidyl-1,2,3-Triazole Ureas as Potent, Selective, and in Vivo-Active Inhibitors of α/β-Hydrolase Domain Containing 6 (ABHD6). Journal of Medicinal Chemistry 56:8270–8279 Available at: https://pubs.acs.org/doi/10.1021/jm400899c [Accessed June 18, 2021].

Hwang YS, Kim Y-J, Kim MO, Kang M, Oh SW, Nho YH, Park S-H, Lee J (2017) Cannabidiol upregulates melanogenesis through CB1 dependent pathway by activating p38 MAPK and p42/44 MAPK. Chemico-Biological Interactions 273:107–114 Available at: https://www.sciencedirect.com/science/article/pii/S0009279716304343 [Accessed February 27, 2021].

Janero DR, Makriyannis A (2009) Cannabinoid receptor antagonists: pharmacological opportunities, clinical experience, and translational prognosis. Expert Opinion on Emerging Drugs 14:43–65 Available at: https://www.tandfonline.com/doi/full/10.1517/14728210902736568 [Accessed July 27, 2021].

Javanmard M, Shlik J, Kennedy SH, Vaccarino FJ, Houle S, Bradwejn J (1999) Neuroanatomic Correlates of CCK-4-Induced Panic Attacks in Healthy Humans: A Comparison of Two Time Points. Available at: https://d1wqtxts1xzle7.cloudfront.net/46258267/s0006-3223_2898_2900348-520160605-24486-1filj1i.pdf?1465159831=&response-content-disposition=inline%3B+filename%3DNeuroanatomic_correlates_of_CCK_4_induce.pdf&Expires=1624456150&Signature=bKOwQwRRwltx9R6dGmls [Accessed June 23, 2021].

Jesudason D, Wittert G (2008) Endocannabinoid system in food intake and metabolic regulation. Current Opinion in Lipidology 19:344–348 Available at:

http://journals.lww.com/00041433-200808000-00004 [Accessed February 27, 2021].

Jiang J, Morgan DA, Cui H, Rahmouni K (2020) Regulation of food intake, insulin sensitivity and sympathetic nerve traffic by hypothalamic steroidogenic factor 1 neurons. The FASEB Journal 34:1–1 Available at: https://onlinelibrary.wiley.com/doi/abs/10.1096/fasebj.2020.34.s1.05580 [Accessed June 22, 2021].

Joy JE, Watson SJ, Benson JA (1999) Marijuana and Medicine: Assessing the Science Base. Available at: www.nap.edu. [Accessed June 20, 2021].

Jüngling K, Seidenbecher T, Sosulina L, Lesting J, Sangha S, Clark SD, Okamura N, Duangdao DM, Xu Y-L, Reinscheid RK, Pape H-C (2008) Neuropeptide S-Mediated Control of Fear Expression and Extinction: Role of Intercalated GABAergic Neurons in the Amygdala. Neuron 59:298–310 Available at: https://www.sciencedirect.com/science/article/pii/S0896627308005710?via%3Dihub [Accessed June 19, 2021].

Kannan H, Hayashida Y, Yamashita H (1989) Increase in sympathetic outflow by paraventricular nucleus stimulation in awake rats. American Journal of Physiology - Regulatory Integrative and Comparative Physiology 256 Available at: https://journals.physiology.org/doi/abs/10.1152/ajpregu.1989.256.6.R1325 [Accessed June 13, 2021].

Kano M, Ohno-Shosaku T, Hashimotodani Y, Uchigashima M, Watanabe M (2009) Endocannabinoid-Mediated Control of Synaptic Transmission. Available at: www.prv.org [Accessed February 28, 2021].

Katona I, Sperlágh B, Sík A, Käfalvi A, Vizi ES, Mackie K, Freund TF (1999) Presynaptically located CB1 cannabinoid receptors regulate GABA release from axon terminals of specific hippocampal interneurons. The Journal of neuroscience : the official journal of the Society for Neuroscience 19:4544–4558 Available at: http://www.ncbi.nlm.nih.gov/pubmed/10341254 [Accessed July 27, 2021].

Kim KW, Sohn J-W, Kohno D, Xu Y, Williams K, Elmquist JK (2011) SF-1 in the ventral medial hypothalamic nucleus: a key regulator of homeostasis. Molecular and cellular endocrinology 336:219–223 Available at: http://www.ncbi.nlm.nih.gov/pubmed/21111025 [Accessed June 22, 2021].

Kirkham TC, Williams CM (2001) Endogenous cannabinoids and appetite. Nutrition Research Reviews 14:65–86 Available at: https://www.cambridge.org/core/journals/nutrition-research-reviews/article/endogenous-cannabinoids-and-appetite/CDCB6D55C3661441AE1BD3533EECAFC4 [Accessed May 23, 2021].

Kirkham TC, Williams CM, Fezza F, Marzo V di (2002) Endocannabinoid levels in rat limbic forebrain and hypothalamus in relation to fasting, feeding and satiation: stimulation of eating by 2-arachidonoyl glycerol. British Journal of Pharmacology 136:550–557 Available at: http://doi.wiley.com/10.1038/sj.bjp.0704767 [Accessed June 17, 2021].

Kleinridders A, Könner AC, Brüning JC (2009) CNS-targets in control of energy and glucose homeostasis. Current Opinion in Pharmacology 9:794–804 Available at: https://pubmed.ncbi.nlm.nih.gov/19884043/ [Accessed June 13, 2021].

Koch JE, Matthews SM (2001) Δ9-tetrahydrocannabinol stimulates palatable food intake in lewis rats: Effects of peripheral and central administration. Nutritional Neuroscience 4:179–187 Available at: https://www.tandfonline.com/doi/abs/10.1080/1028415X.2001.11747361 [Accessed June 13, 2021].

Koch M, Varela L, Kim JG, Kim JD, Hernández-Nuño F, Simonds SE, Castorena CM, Vianna CR, Elmquist JK, Morozov YM, Rakic P, Bechmann I, Cowley MA, Szigeti-Buck K, Dietrich MO, Gao XB, Diano S, Horvath TL (2015) Hypothalamic POMC neurons promote cannabinoid-induced feeding. Nature 519:45–50 Available at: https://www.nature.com/articles/nature14260 [Accessed June 13, 2021].

Kojima M, Hosoda H, Date Y, Nakazato M, Matsuo H, Kangawa K (1999) Ghrelin is a growth-hormone-releasing acylated peptide from stomach. Nature 402:656–660 Available at: http://www.nature.com/articles/45230 [Accessed July 10, 2021].

Kola B, Farkas I, Christ-Crain M, Wittmann G, Lolli F, Amin F, Harvey-White J, Liposits Z, Kunos G, Grossman AB, Fekete C, Korbonits M (2008) The Orexigenic Effect of Ghrelin Is Mediated through Central Activation of the Endogenous Cannabinoid System Bartolomucci A, ed. PLoS ONE 3:e1797 Available at: https://dx.plos.org/10.1371/journal.pone.0001797 [Accessed June 10, 2021].

Kopec CD, Li B, Wei W, Boehm J, Malinow R (2006) Cellular/Molecular Glutamate Receptor Exocytosis and Spine Enlargement during Chemically Induced Long-Term Potentiation. Available at: www.jneurosci.org [Accessed July 27, 2021].

Kubilius RA, Kaplick PM, Wotjak CT (2018) Highway to hell or magic smoke? The dose-dependence of Δ9-THC in place conditioning paradigms. Learning & memory (Cold Spring Harbor, NY) 25:446–454 Available at: http://www.ncbi.nlm.nih.gov/pubmed/30115766 [Accessed June 20, 2021].

Kunwar PS, Zelikowsky M, Remedios R, Cai H, Yilmaz M, Meister M, Anderson DJ (2015) Ventromedial hypothalamic neurons control a defensive emotion state. eLife 4 Available at: https://elifesciences.org/articles/06633 [Accessed June 23, 2021].

Labar G, Bauvois C, Borel F, Ferrer J-L, Wouters J, Lambert DM (2010) Crystal Structure of the Human Monoacylglycerol Lipase, a Key Actor in Endocannabinoid Signaling. ChemBioChem 11:218–227 Available at: http://doi.wiley.com/10.1002/cbic.200900621 [Accessed June 16, 2021].

Lange MD, Daldrup T, Remmers F, Szkudlarek HJ, Lesting J, Guggenhuber S, Ruehle S, Jüngling K, Seidenbecher T, Lutz B, Pape HC (2017) Cannabinoid CB1 receptors in distinct circuits of the extended amygdala determine fear responsiveness to unpredictable threat. Molecular Psychiatry 22:1422–1430 Available at: http://www.ncbi.nlm.nih.gov/pubmed/27698427 [Accessed March 6, 2021].

Lastres-Becker I, Miguel R, Fernandez-Ruiz J (2003) The Endocannabinoid System and Huntingtons Disease. Current Drug Target -CNS & Neurological Disorders 2:335–347 Available at: http://www.eurekaselect.com/openurl/content.php?genre=article&issn=1568-007X&volume=2&issue=5&spage=335 [Accessed February 27, 2021].

Laviolette SR, Grace AA (2006) The roles of cannabinoid and dopamine receptor systems in neural emotional learning circuits: implications for schizophrenia and addiction. Cellular and Molecular Life Sciences 63:1597–1613 Available at: http://link.springer.com/10.1007/s00018-006-6027-5 [Accessed February 27, 2021].

Leibowitz SF, Hammer NJ, Chang K (1981) Hypothalamic paraventricular nucleus lesions produce overeating and obesity in the rat. Physiology and Behavior 27:1031–1040.

Lévénès C, Daniel H, Soubrié P, Crépel F (1998) Cannabinoids decrease excitatory synaptic transmission and impair long-term depression in rat cerebellar Purkinje cells. The Journal of Physiology 510:867–879 Available at: http://doi.wiley.com/10.1111/j.1469-7793.1998.867bj.x [Accessed February 27, 2021].

Lim CT, Kola B, Feltrin D, Perez-Tilve D, Tschöp MH, Grossman AB, Korbonits M (2013) Ghrelin and cannabinoids require the ghrelin receptor to affect cellular energy

metabolism. Available at: http://dx.doi.org/10.1016/j.mce.2012.11.007 [Accessed June 10, 2021].

Lindemann L, Jaeschke G, Michalon A, Vieira E, Honer M, Spooren W, Porter R, Hartung T, Kolczewski S, Büttelmann B, Flament C, Diener C, Fischer C, Gatti S, Prinssen EP, Parrott N, Hoffmann G, Wettstein JG (2011) CTEP: a novel, potent, long-acting, and orally bioavailable metabotropic glutamate receptor 5 inhibitor. The Journal of pharmacology and experimental therapeutics 339:474–486 Available at: http://www.ncbi.nlm.nih.gov/pubmed/10381773 [Accessed July 10, 2021].

Llorente-Berzal A, Terzian ALB, di Marzo V, Micale V, Viveros MP, Wotjak CT (2015) 2-AG promotes the expression of conditioned fear via cannabinoid receptor type 1 on GABAergic neurons. Psychopharmacology 232:2811–2825 Available at: http://link.springer.com/10.1007/s00213-015-3917-y [Accessed March 6, 2021].

Long JZ, Li W, Booker L, Burston JJ, Kinsey SG, Schlosburg JE, Pavón FJ, Serrano AM, Selley DE, Parsons LH, Lichtman AH, Cravatt BF (2009) Selective blockade of 2-arachidonoylglycerol hydrolysis produces cannabinoid behavioral effects. Nature Chemical Biology 5:37–44 Available at: http://www.nature.com/articles/nchembio.129 [Accessed June 16, 2021].

Lopez Trinidad LM, Martinez R, Kapravelou G, Galisteo M, Aranda P, Porres JM, Lopez-Jurado M (2021) Caloric restriction, physical exercise, and CB1 receptor blockade as an efficient combined strategy for bodyweight control and cardiometabolic status improvement in male rats. Scientific Reports 11:4286 Available at: http://www.nature.com/articles/s41598-021-83709-9 [Accessed May 23, 2021].

Lowe MR, Levine AS (2005) Eating Motives and the Controversy over Dieting: Eating Less Than Needed versus Less Than Wanted. Obesity Research 13:797–806 Available at: http://doi.wiley.com/10.1038/oby.2005.90 [Accessed June 20, 2021].

Lutz B, Marsicano G, Maldonado R, Hillard CJ (2015) The endocannabinoid system in guarding against fear, anxiety and stress. Nature Reviews Neuroscience 16:705–718 Available at: http://www.nature.com/articles/nrn4036 [Accessed March 6, 2021].

Madisen L, Zwingman TA, Sunkin SM, Oh SW, Zariwala HA, Gu H, Ng LL, Palmiter RD, Hawrylycz MJ, Jones AR, Lein ES, Zeng H (2010) A robust and high-throughput Cre reporting and characterization system for the whole mouse brain. Nature Neuroscience 13:133–140 Available at: http://www.nature.com/articles/nn.2467 [Accessed June 23, 2021].

Maejima Y, Yokota S, Nishimori K, Shimomura K (2018) The Anorexigenic Neural Pathways of Oxytocin and Their Clinical Implication. Neuroendocrinology 107:91–104 Available at: http://www.ncbi.nlm.nih.gov/pubmed/29660735 [Accessed June 23, 2021].

Maneuf YP, Brotchie JM (1997) Paradoxical action of the cannabinoid WIN 55,212-2 in stimulated and basal cyclic AMP accumulation in rat globus pallidus slices. British Journal of Pharmacology 120:1397–1398 Available at: http://doi.wiley.com/10.1038/sj.bjp.0701101 [Accessed February 27, 2021].

Manvich DF, Webster KA, Foster SL, Farrell MS, Ritchie JC, Porter JH, Weinshenker D (2018) The DREADD agonist clozapine N-oxide (CNO) is reverse-metabolized to clozapine and produces clozapine-like interoceptive stimulus effects in rats and mice. Scientific Reports 8:3840 Available at: http://www.nature.com/articles/s41598-018-22116-z [Accessed July 10, 2021].

Marsicano G, Goodenough S, Monory K, Hermann H, Eder M, Cannich A, Azad SC, Cascio MG, Gutiérrez SO, van der Stelt M, López-Rodríguez ML, Casanova E, Schütz G, Zieglgänsberger W, di Marzo V, Behl C, Lutz B (2003) CB1 Cannabinoid Receptors and On-Demand Defense Against Excitotoxicity. Science 302:84 LP – 88 Available at: http://science.sciencemag.org/content/302/5642/84.abstract.

Marsicano G, Kuner R (2008) Anatomical Distribution of Receptors, Ligands and Enzymes in the Brain and in the Spinal Cord: Circuitries and Neurochemistry. In: Cannabinoids and the Brain, pp 161–201. Boston, MA: Springer US. Available at: http://link.springer.com/10.1007/978-0-387-74349-3_10 [Accessed February 27, 2021].

Marsicano G, Lutz B (1999) Expression of the cannabinoid receptor CB1 in distinct neuronal subpopulations in the adult mouse forebrain. European Journal of Neuroscience 11:4213–4225 Available at: http://doi.wiley.com/10.1046/j.1460-9568.1999.00847.x [Accessed January 17, 2021].

Marsicano G, Wotjak CT, Azad SC, Bisogno T, Rammes G, Cascio MG, Hermann H, Tang J, Hofmann C, Zieglgänsberger W, di Marzo V, Lutz B (2002) The endogenous cannabinoid system controls extinction of aversive memories. Nature 418:530–534 Available at: http://www.nature.com/articles/nature00839 [Accessed January 17, 2021].

Mathre MLynn (1997) Cannabis in medical practice: a legal, historical, and pharmacological overview of the therapeutic use of marijuana. McFarland & Co. Available at: https://books.google.de/books/about/Cannabis_in_Medical_Practice.html?id=1AWGDhIOvk0C&redir_esc=y [Accessed January 17, 2021].

Matsuda LA, Lolait SJ, Brownstein MJ, Young AC, Bonner TI (1990) Structure of a cannabinoid receptor and functional expression of the cloned cDNA. Nature 346:561–564 Available at: http://www.nature.com/articles/346561a0 [Accessed January 17, 2021].

Mayo LM, Asratian A, Lindé J, Holm L, Nätt D, Augier G, Stensson N, Vecchiarelli HA, Balsevich G, Aukema RJ, Ghafouri B, Spagnolo PA, Lee FS, Hill MN, Heilig M (2020) Protective effects of elevated anandamide on stress and fear-related behaviors: translational evidence from humans and mice. Molecular Psychiatry 25:993–1005 Available at: http://www.nature.com/articles/s41380-018-0215-1 [Accessed March 6, 2021].

Mechoulam R, Ben-Shabat S, Hanus L, Ligumsky M, Kaminski NE, Schatz AR, Gopher A, Almog S, Martin BR, Compton DR, Pertwee RG, Griffin G, Bayewitch M, Barg J, Vogel Z (1995) Identification of an endogenous 2-monoglyceride, present in canine gut, that binds to cannabinoid receptors. Biochemical Pharmacology 50:83–90 Available at: https://www.sciencedirect.com/science/article/pii/000629529500109D?via%3Dihub [Accessed January 17, 2021].

Mela DJ (2001) Determinants of Food Choice: Relationships with Obesity and Weight Control. Obesity Research 9:249S-255S Available at: http://doi.wiley.com/10.1038/oby.2001.127 [Accessed June 20, 2021].

Metna-Laurent M, Mondésir M, Grel A, Vallée M, Piazza P (2017) Cannabinoid-Induced Tetrad in Mice. Current Protocols in Neuroscience 80:9.59.1-9.59.10 Available at: https://onlinelibrary.wiley.com/doi/10.1002/cpns.31 [Accessed June 20, 2021].

Metna-Laurent M, Soria-Gómez E, Verrier D, Conforzi M, Jégo P, Lafenêtre P, Marsicano G (2012) Bimodal Control of Fear-Coping Strategies by CB1 Cannabinoid Receptors. The Journal of Neuroscience 32:7109 LP – 7118 Available at: http://www.jneurosci.org/content/32/21/7109.abstract.

Micale V, di Marzo V, Sulcova A, Wotjak CT, Drago F (2013) Endocannabinoid system and mood disorders: Priming a target for new therapies. Pharmacology & Therapeutics 138:18–37 Available at: https://www.sciencedirect.com/science/article/pii/S0163725812002409?via%3Dihub [Accessed February 27, 2021].

Mlekusch W, Truppe W, Beyer W, Paletta B (1975) The effect of hunger on free fatty acid and corticosterone plasma levels in rats. Experientia 31:1135–1137 Available at: http://link.springer.com/10.1007/BF02326753 [Accessed June 23, 2021].

Monory K et al. (2006) The Endocannabinoid System Controls Key Epileptogenic Circuits in the Hippocampus. Neuron 51:455–466 Available at: https://www.sciencedirect.com/science/article/pii/S0896627306005460?via%3Dihub [Accessed July 10, 2021].

Monory K, Blaudzun H, Massa F, Kaiser N, Lemberger T, Schütz G, Wotjak CT, Lutz B, Marsicano G (2007) Genetic Dissection of Behavioural and Autonomic Effects of Δ9-Tetrahydrocannabinol in Mice Nestler E, ed. PLoS Biology 5:e269 Available at: https://dx.plos.org/10.1371/journal.pbio.0050269 [Accessed June 5, 2021].

Monteleone P, Matias I, Martiadis V, de Petrocellis L, Maj M, di Marzo V (2005) Blood Levels of the Endocannabinoid Anandamide are Increased in Anorexia Nervosa and in Binge-Eating Disorder, but not in Bulimia Nervosa. Neuropsychopharmacology 30:1216–1221 Available at: http://www.nature.com/articles/1300695 [Accessed February 27, 2021].

Moreira FA, Aguiar DC, Terzian ALB, Guimarães FS, Wotjak CT (2012) Cannabinoid type 1 receptors and transient receptor potential vanilloid type 1 channels in fear and anxiety—two sides of one coin? Neuroscience 204:186–192 Available at: https://www.sciencedirect.com/science/article/pii/S0306452211009882 [Accessed June 20, 2021].

Morena M, Aukema RJ, Leitl KD, Rashid AJ, Vecchiarelli HA, Josselyn SA, Hill MN (2019) Upregulation of Anandamide Hydrolysis in the Basolateral Complex of Amygdala Reduces Fear Memory Expression and Indices of Stress and Anxiety. The Journal of neuroscience: the official journal of the Society for Neuroscience 39:1275–1292 Available at: http://www.ncbi.nlm.nih.gov/pubmed/30573646 [Accessed March 6, 2021].

Mukhopadhyay S, Shim J-Y, Assi A-A, Norford D, Howlett AC (2002) CB1 cannabinoid receptor-G protein association: a possible mechanism for differential signaling. Chemistry and Physics of Lipids 121:91–109 Available at: https://www.sciencedirect.com/science/article/pii/S0009308402001536?via%3Dihub [Accessed February 27, 2021].

Munro S, Thomas KL, Abu-Shaar M (1993) Molecular characterization of a peripheral receptor for cannabinoids. Nature 365:61–65 Available at: http://www.nature.com/articles/365061a0 [Accessed January 17, 2021].

Myers MG, Olson DP (2012) Central nervous system control of metabolism. Nature 491:357–363 Available at: https://www.nature.com/articles/nature11705 [Accessed June 13, 2021].

Niphakis MJ, Cognetta AB, Chang JW, Buczynski MW, Parsons LH, Byrne F, Burston JJ, Chapman V, Cravatt BF (2013) Evaluation of NHS Carbamates as a Potent and Selective Class of Endocannabinoid Hydrolase Inhibitors. ACS Chemical Neuroscience 4:1322–1332 Available at: https://pubs.acs.org/doi/10.1021/cn400116z [Accessed June 18, 2021].

Nogueras-Ortiz C, Yudowski GA (2016) The Multiple Waves of Cannabinoid 1 Receptor Signaling. Molecular pharmacology 90:620–626 Available at: http://www.ncbi.nlm.nih.gov/pubmed/27338082 [Accessed February 27, 2021].

Nüsken K-D, Jarz H (2010) Steuerung von Appetit, Hunger und Sättigung. In: Klinische Ernährungsmedizin, pp 33–45. Vienna: Springer Vienna. Available at: http://link.springer.com/10.1007/978-3-211-88900-8_3 [Accessed June 20, 2021].

Ogasawara D et al. (2016) Rapid and profound rewiring of brain lipid signaling networks by acute diacylglycerol lipase inhibition. Proceedings of the National Academy of

Sciences of the United States of America 113:26–33 Available at: http://www.ncbi.nlm.nih.gov/pubmed/26668358 [Accessed June 27, 2021].

Ohno-Shosaku T, Shosaku J, Tsubokawa H, Kano M (2002) Cooperative endocannabinoid production by neuronal depolarization and group I metabotropic glutamate receptor activation. European Journal of Neuroscience 15:953–961 Available at: http://doi.wiley.com/10.1046/j.1460-9568.2002.01929.x [Accessed June 10, 2021].

Paria BC, Das SK, Dey SK (1995) The preimplantation mouse embryo is a target for cannabinoid ligand-receptor signaling. Proceedings of the National Academy of Sciences of the United States of America 92:9460–9464 Available at: http://www.ncbi.nlm.nih.gov/pubmed/7568154 [Accessed February 27, 2021].

Patel S, Hill MN, Cheer JF, Wotjak CT, Holmes A (2017) The endocannabinoid system as a target for novel anxiolytic drugs. Neuroscience & Biobehavioral Reviews 76:56–66 Available at: https://www.sciencedirect.com/science/article/pii/S0149763416304699?via%3Dihub [Accessed March 6, 2021].

Perry RJ, Resch JM, Douglass AM, Madara JC, Rabin-Court A, Kucukdereli H, Wu C, Song JD, Lowell BB, Shulman GI (2019) Leptin's hunger-suppressing effects are mediated by the hypothalamic-pituitary-adrenocortical axis in rodents. Proceedings of the National Academy of Sciences of the United States of America 116:13670–13679 Available at: http://www.ncbi.nlm.nih.gov/pubmed/31213533 [Accessed June 23, 2021].

Philibert P, Leprieur E, Zenaty D, Thibaud E, Polak M, Frances A-M, Lespinasse J, Raingeard I, Servant N, Audran F, Paris F, Sultan C (2010) Steroidogenic factor-1 (SF-1) gene mutation as a frequent cause of primary amenorrhea in 46,XY female adolescents with low testosterone concentration. Reproductive Biology and Endocrinology 8:28 Available at: http://rbej.biomedcentral.com/articles/10.1186/1477-7827-8-28 [Accessed July 10, 2021].

Piazza PV, Cota D, Marsicano G (2017) The CB1 Receptor as the Cornerstone of Exostasis. Neuron 93:1252–1274.

Piomelli D (2003) The molecular logic of endocannabinoid signalling. Nature Reviews Neuroscience 4:873–884 Available at: http://www.nature.com/articles/nrn1247 [Accessed June 14, 2021].

Piomelli D (2020) Next Stop for Fatty Acid Amide Hydrolase Inhibitors, the Clinic? Biological Psychiatry 87:485–486 Available at: https://www.sciencedirect.com/science/article/abs/pii/S000632231931889X?via%3Dihub [Accessed March 6, 2021].

Piomelli D, Tarzia G, Duranti A, Tontini A, Mor M, Compton TR, Dasse O, Monaghan EP, Parrott JA, Putman D (2006) Pharmacological Profile of the Selective FAAH Inhibitor KDS-4103 (URB597). CNS Drug Reviews 12:21–38 Available at: https://onlinelibrary.wiley.com/doi/10.1111/j.1527-3458.2006.00021.x [Accessed July 10, 2021].

Pollington Stephen (2000) Leechcraft: early English charms, plant lore, and healing. Anglo-Saxon Books. Available at: https://books.google.de/books?id=3jhqAAAAMAAJ&hl=de&source=gbs_book_other_versions_r&cad=4 [Accessed January 17, 2021].

Quarta C, Cota D (2020) Anti-obesity therapy with peripheral CB1 blockers: from promise to safe(?) practice. International Journal of Obesity 44:2179–2193 Available at: http://www.nature.com/articles/s41366-020-0577-8 [Accessed July 27, 2021].

Refojo D et al. (2011) Glutamatergic and dopaminergic neurons mediate anxiogenic and anxiolytic effects of CRHR1. Science (New York, NY) 333:1903–1907 Available at: http://www.ncbi.nlm.nih.gov/pubmed/21885734 [Accessed June 15, 2021].

Rinaldi-Carmona M, Barth F, Héaulme M, Shire D, Calandra B, Congy C, Martinez S, Maruani J, Néliat G, Caput D, Ferrara P, Soubrié P, Brelière JC, le Fur G (1994) SR141716A, a potent and selective antagonist of the brain cannabinoid receptor. FEBS Letters 350:240–244 Available at: http://doi.wiley.com/10.1016/0014-5793%2894%2900773-X [Accessed January 17, 2021].

Robin LM et al. (2018) Astroglial CB1 Receptors Determine Synaptic D-Serine Availability to Enable Recognition Memory. Neuron 98:935-944.e5 Available at: https://www.sciencedirect.com/science/article/pii/S0896627318303696?via%3Dihub [Accessed June 14, 2021].

Rodríguez EM, Blázquez JL, Guerra M (2010) The design of barriers in the hypothalamus allows the median eminence and the arcuate nucleus to enjoy private milieus: The former opens to the portal blood and the latter to the cerebrospinal fluid. Peptides 31:757–776.

Ross CA, Margolis RL (2019) Research Domain Criteria: Strengths, Weaknesses, and Potential Alternatives for Future Psychiatric Research. Molecular Neuropsychiatry 5:218–236 Available at: http://www.ncbi.nlm.nih.gov/pubmed/31768375 [Accessed June 14, 2021].

Ryan PJ, Ross SI, Campos CA, Derkach VA, Palmiter RD (2017) Oxytocin-receptor-expressing neurons in the parabrachial nucleus regulate fluid intake. Nature Neuroscience 20:1722–1733 Available at: http://www.nature.com/articles/s41593-017-0014-z [Accessed June 23, 2021].

Saario SM, Savinainen JR, Laitinen JT, Järvinen T, Niemi R (2004) Monoglyceride lipase-like enzymatic activity is responsible for hydrolysis of 2-arachidonoylglycerol in rat cerebellar membranes. Biochemical Pharmacology 67:1381–1387 Available at: https://www.sciencedirect.com/science/article/pii/S0006295203009420?via%3Dihub [Accessed June 16, 2021].

Sartori SB, Singewald N (2019) Novel pharmacological targets in drug development for the treatment of anxiety and anxiety-related disorders. Pharmacology & Therapeutics 204:107402 Available at: https://www.sciencedirect.com/science/article/pii/S0163725819301512?via%3Dihub [Accessed March 6, 2021].

Sbarski B, Akirav I (2018) Chronic exposure to cannabinoids before an emotional trauma may have negative effects on emotional function. European Neuropsychopharmacology 28:955–969 Available at: https://www.sciencedirect.com/science/article/pii/S0924977X18301238?via%3Dihub [Accessed March 6, 2021].

Sbarski B, Akirav I (2020) Cannabinoids as therapeutics for PTSD. Pharmacology & Therapeutics 211:107551 Available at: https://www.sciencedirect.com/science/article/abs/pii/S0163725820300796?via%3Dihub [Accessed June 17, 2021].

Schalk-Hihi C et al. (2011) Crystal structure of a soluble form of human monoglyceride lipase in complex with an inhibitor at 1.35 Å resolution. Protein Science 20:670–683 Available at: http://doi.wiley.com/10.1002/pro.596 [Accessed June 16, 2021].

Schneider U, Leweke F, Mueller-Vahl K, Emrich H (1998) Cannabinoid/Anandamide System and Schizophrenia: Is there Evidence for Association? Pharmacopsychiatry 31:110–113 Available at: http://www.thieme-connect.de/DOI/DOI?10.1055/s-2007-979355 [Accessed February 27, 2021].

Schreiber JR, Hsueh AJW, Baulieu EE (1983) Binding of the anti-progestin ru-486 to rat ovary steroid receptors. Contraception 28:77–85 Available at: https://www.sciencedirect.com/science/article/pii/S0010782483800080?via%3Dihub [Accessed July 10, 2021].

Segev A, Korem N, Mizrachi Zer-Aviv T, Abush H, Lange R, Sauber G, Hillard CJ, Akirav I (2018) Role of endocannabinoids in the hippocampus and amygdala in emotional memory and plasticity. Neuropsychopharmacology: official publication of the American College of Neuropsychopharmacology 43:2017–2027 Available at: http://www.ncbi.nlm.nih.gov/pubmed/29977073 [Accessed March 6, 2021].

Sharma TD (1972) Clinical observations of patients who used tetra-hydro cannabinol (T.H.C.) intravenously. Behavioral Neuropsychiatry 4:17–19.

Shen M, Piser TM, Seybold VS, Thayer SA (1996) Cannabinoid receptor agonists inhibit glutamatergic synaptic transmission in rat hippocampal cultures. The Journal of neuroscience: the official journal of the Society for Neuroscience 16:4322–4334 Available at: http://www.ncbi.nlm.nih.gov/pubmed/8699243 [Accessed February 27, 2021].

Shimizu N, Oomura Y, Plata-Salamán CR, Morimoto M (1987) Hyperphagia and obesity in rats with bilateral ibotenic acid-induced lesions of the ventromedial hypothalamic nucleus. Brain Research 416:153–156.

Simon P (2012) History, pharmakology and therapeutic application of Cannabis sativa and its compounds.

Sink KS, McLaughlin PJ, Wood JAT, Brown C, Fan P, Vemuri VK, Pang Y, Olzewska T, Thakur GA, Makriyannis A, Parker LA, Salamone JD (2008) The Novel Cannabinoid CB1 Receptor Neutral Antagonist AM4113 Suppresses Food Intake and Food-Reinforced Behavior but Does not Induce Signs of Nausea in Rats. Neuropsychopharmacology 33:946–955 Available at: http://www.nature.com/articles/1301476 [Accessed July 27, 2021].

Sofia RD, Barry H (1974) Acute and chronic effects of δ9-tetrahydrocannabinol on food intake by rats. Psychopharmacologia 39:213–222 Available at: http://link.springer.com/10.1007/BF00421028 [Accessed June 20, 2021].

Soria-Gómez, E., Bellocchio, L., Reguero, L., Lepousez, G., Martin, C., Bendahmane, M., … Marsicano, G. (2014). The endocannabinoid system controls food intake via olfactory processes. Nature Neuroscience, 17(3), 407–415. https://doi.org/10.1038/nn.3647

Stella N, Schweitzer P, Piomelli D (1997) A second endogenous cannabinoid that modulates long-term potentiation. Nature 388:773–778 Available at: http://www.nature.com/articles/42015 [Accessed June 18, 2021].

Stepan J et al. (2021) Hippo-Released WWC1 Primes Ampa Receptor Regulatory Complexes for Hippocampal Learning. SSRN Electronic Journal Available at: https://www.ssrn.com/abstract=3831460 [Accessed June 6, 2021].

Sternson SM, Shepherd GM, Friedman JM (2005) Topographic mapping of VMH-arcuate nucleus microcircuits and their reorganization by fasting. Available at: http://www.nature.com/natureneuroscience [Accessed June 22, 2021].

Sugiura T, Kodaka T, Nakane S, Miyashita T, Kondo S, Suhara Y, Takayama H, Waku K, Seki C, Baba N, Ishima Y (1999) Evidence That the Cannabinoid CB1 Receptor Is a 2-Arachidonoylglycerol Receptor: STRUCTURE-ACTIVITY RELATIONSHIP OF 2-ARACHIDONOYLGLYCEROL, ETHER-LINKED ANALOGUES, AND RELATED COMPOUNDS. Journal of Biological Chemistry 274:2794–2801 Available at: https://www.sciencedirect.com/science/article/pii/S0021925819880560 [Accessed February 28, 2021].

Sugiura T, Kondo S, Sukagawa A, Nakane S, Shinoda A, Itoh K, Yamashita A, Waku K (1995a) 2-Arachidonoylgylcerol: A Possible Endogenous Cannabinoid Receptor Ligand in Brain. Biochemical and Biophysical Research Communications 215:89–97 Available at:

https://www.sciencedirect.com/science/article/pii/S0006291X85724370?via%3Dihub [Accessed January 17, 2021].

Sugiura T, Kondo S, Sukagawa A, Nakane S, Shinoda A, Itoh K, Yamashita A, Waku K (1995b) 2-Arachidonoylgylcerol: A Possible Endogenous Cannabinoid Receptor Ligand in Brain. Biochemical and Biophysical Research Communications 215:89–97 Available at: https://www.sciencedirect.com/science/article/pii/S0006291X85724370?via%3Dihub [Accessed January 17, 2021].

Timper K, Brüning JC (2017) Hypothalamic circuits regulating appetite and energy homeostasis: pathways to obesity. Disease Models & Mechanisms 10:679–689 Available at: https://journals.biologists.com/dmm/article/10/6/679/2413/Hypothalamic-circuits-regulating-appetite-and [Accessed June 13, 2021].

Tong Q, Ye C-P, Jones JE, Elmquist JK, Lowell BB (2008) Synaptic release of GABA by AgRP neurons is required for normal regulation of energy balance. Nature Neuroscience 11:998–1000 Available at: http://www.nature.com/articles/nn.2167 [Accessed June 23, 2021].

Touriño C, Oveisi F, Lockney J, Piomelli D, Maldonado R (2010) FAAH deficiency promotes energy storage and enhances the motivation for food. International Journal of Obesity 34:557–568 Available at: http://www.nature.com/articles/ijo2009262 [Accessed June 21, 2021].

Trojniar W, Wise RA (1991) Facilitory effect of Δ9-tetrahydrocannabinol on hypothalamically induced feeding. Psychopharmacology 103:172–176.

Tschöp M, Smiley DL, Heiman ML (2000) Ghrelin induces adiposity in rodents. Nature 407:908–913 Available at: http://www.nature.com/articles/35038090 [Accessed June 17, 2021].

Tucci S, Halford J, Harrold J, Kirkham T (2006) Therapeutic Potential of Targeting the Endocannabinoids: Implications for the Treatment of Obesity, Metabolic Syndrome, Drug Abuse and Smoking Cessation. Current Medicinal Chemistry 13:2669–2680.

Valassi E, Scacchi M, Cavagnini F (2008) Neuroendocrine control of food intake. Nutrition, Metabolism and Cardiovascular Diseases 18:158–168 Available at: https://www.sciencedirect.com/science/article/abs/pii/S0939475307001329?via%3Dihub [Accessed June 27, 2021].

van Gaal LF, Rissanen AM, Scheen AJ, Ziegler O, Rössner S (2005) Effects of the cannabinoid-1 receptor blocker rimonabant on weight reduction and cardiovascular risk factors in overweight patients: 1-year experience from the RIO-Europe study. The Lancet 365:1389–1397 Available at: https://www.sciencedirect.com/science/article/pii/S014067360566374X?via%3Dihub [Accessed May 23, 2021].

Viskaitis P, Irvine EE, Smith MA, Choudhury AI, Alvarez-Curto E, Glegola JA, Hardy DG, Pedroni SMA, Paiva Pessoa MR, Fernando ABP, Katsouri L, Sardini A, Ungless MA, Milligan G, Withers DJ (2017) Modulation of SF1 Neuron Activity Coordinately Regulates Both Feeding Behavior and Associated Emotional States. Cell Reports 21:3559–3572 Available at: https://www.sciencedirect.com/science/article/pii/S2211124717317564?via%3Dihub [Accessed June 22, 2021].

Volk DW, Lewis DA (2016) The Role of Endocannabinoid Signaling in Cortical Inhibitory Neuron Dysfunction in Schizophrenia. Biological Psychiatry 79:595–603 Available at: https://www.sciencedirect.com/science/article/pii/S0006322315005211?via%3Dihub [Accessed February 27, 2021].

von Esenbeck N, Ludwig TF, Ebermaier CH (1830) Handbuch der medicinisch-pharmaceutischen Botanik. Arnz, Düsseldorf.

Wagner K v, Hartmann J, Mangold K, Wang X-D, Labermaier C, Liebl C, Wolf M, Gassen NC, Holsboer F, Rein T, Müller MB, Schmidt M v (2013) Behavioral/Cognitive Homer1 Mediates Acute Stress-Induced Cognitive Deficits in the Dorsal Hippocampus. Available at: https://www.jneurosci.org/content/jneuro/33/9/3857.full.pdf [Accessed May 24, 2021].

Wagner K v, Marinescu D, Hartmann J, Wang X-D, Labermaier C, Scharf SH, Liebl C, Uhr M, Holsboer F, Müller MB, Schmidt M v (2012) Differences in FKBP51 Regulation Following Chronic Social Defeat Stress Correlate with Individual Stress Sensitivity: Influence of Paroxetine Treatment. Neuropsychopharmacology 37:2797–2808 Available at: http://www.nature.com/articles/npp2012150 [Accessed May 24, 2021].

Walter H (2017) Research Domain Criteria (RDoC). Der Nervenarzt 88:538–548 Available at: http://link.springer.com/10.1007/s00115-017-0284-4 [Accessed June 14, 2021].

Wang L, Chen IZ, Lin D (2015) Collateral Pathways from the Ventromedial Hypothalamus Mediate Defensive Behaviors. Neuron 85:1344–1358.

Waterson MJ, Horvath TL (2015) Neuronal Regulation of Energy Homeostasis: Beyond the Hypothalamus and Feeding. Cell Metabolism 22:962–970.

Wellman M, Abizaid A (2015) Growth Hormone Secretagogue Receptor Dimers: A New Pharmacological Target. eneuro 2:ENEURO.0053-14.2015 Available at: https://www.eneuro.org/lookup/doi/10.1523/ENEURO.0053-14.2015 [Accessed June 19, 2021].

Wilker S, Pfeiffer A, Elbert T, Ovuga E, Karabatsiakis A, Krumbholz A, Thieme D, Schelling G, Kolassa I-T (2016) Endocannabinoid concentrations in hair are associated with PTSD symptom severity. Psychoneuroendocrinology 67:198–206 Available at: https://www.sciencedirect.com/science/article/pii/S0306453016300403?via%3Dihub [Accessed June 17, 2021].

Wu D-F, Yang L-Q, Goschke A, Stumm R, Brandenburg L-O, Liang Y-J, Höllt V, Koch T (2008) Role of receptor internalization in the agonist-induced desensitization of cannabinoid type 1 receptors. Journal of Neurochemistry 104:1132–1143 Available at: http://doi.wiley.com/10.1111/j.1471-4159.2007.05063.x [Accessed March 1, 2021].

Yücel M et al. (2019) A transdiagnostic dimensional approach towards a neuropsychological assessment for addiction: an international Delphi consensus study. Addiction 114:1095–1109 Available at: http://doi.wiley.com/10.1111/add.14424 [Accessed June 14, 2021].

Ziegler LM von, Floriou-Servou A, Waag R, Gupta RR das, Sturman O, Gapp K, Maat CA, Kockmann T, Lin H-Y, Duss SN, Privitera M, Hinte L, Meyenn F von, Zeilhofer HU, Germain P-L, Bohacek J (2021) Molecular roadmap of the healthy stress response in the mouse hippocampus. bioRxiv:2021.03.26.436970 Available at: https://www.biorxiv.org/content/10.1101/2021.03.26.436970v1 [Accessed June 16, 2021].

Zigman JM, Jones JE, Lee CE, Saper CB, Elmquist JK (2006) Expression of ghrelin receptor mRNA in the rat and the mouse brain. The Journal of Comparative Neurology 494:528–548 Available at: http://doi.wiley.com/10.1002/cne.20823 [Accessed June 19, 2021].

Zimmer A, Zimmer AM, Hohmann AG, Herkenham M, Bonner TI (1999) Increased mortality, hypoactivity, and hypoalgesia in cannabinoid CB1 receptor knockout mice. Proceedings of the National Academy of Sciences of the United States of America 96:5780–5785 Available at: http://www.ncbi.nlm.nih.gov/pubmed/10318961 [Accessed July 8, 2021].

Zittel TT, Glatzle J, Müller M, Kreis ME, Raybould HE, Becker HD, Jehle EC (2002) Total gastrectomy severely alters the central regulation of food intake in rats. Annals of surgery 236:166–176 Available at: http://www.ncbi.nlm.nih.gov/pubmed/12170021 [Accessed June 27, 2021].

ACKNOWLEDGMENTS

My thesis contains several contributions by a variety of colleagues and (later) friends. I am thankful to all of them (listed under contributions) and appreciated the enormous support.

Nonetheless, I wish to express my greatest gratitude to Carsten Wotjak. Next to endless fruitful project discussions and direct thesis support, I was awarded with a tremendous degree of autonomy in various aspects. Coupled with nearly unlimited support, I was teached not only in scientific project management, but supervision and teaching, science-diplomacy and politics, budgeting, and the policy of the steady hand. I am grateful for many opportunities, trust, and motivating moments. Not to forget, it is an honor to close the door behind me.

I want to thank Beat Lutz for attending my TAC and supporting me with (project)-advises whenever needed. Laura Busse contributed with valuable social- and project input during my TAC meetings. I highly appreciate her willingness to supervise my doctoral thesis.

Regular visits in the offices of Jan Deussing and Chris Turck helped me with several different concerns and I appreciated and benefited of his open-door policy a lot.

Special thanks to Robert Neuner (†2020), supporting with a variety of technical and mental support and Rainer Stoffel for backing me up with his tremendous assistance. Many thanks to Ilka Schießler-Gäbler (GA), Dietlinde Schöffend and Madlehna Riaz (controlling), Jael Wohlert (travel expenses), Dejan Hulic, Stefan Huber and Dominic Böhm (purchase dept.) and, especially Silvia Graf – great administrative support by a motivated team remains as essential part of science and its daily life.

Next to great scientific input and support, I am thankful to have the chance to work with Nils Gassen, Tim Ebert, Rainer Stoffel, Simon Chang, Paul Kaplick, Julien Diene, Rosa Hüttl, Fabian Stamp, Bozo Novidar, Thomas Bajaj, Alec Dick, Lea Brix, Marg Springer, Ulli Schmidt, Philipp Sämann, Caro Eggert and Lea Bartmann. Special thank comes to my office team, in particular Julia Ruat, who made the day-to-day PhD life in the lab more than endurable. I further thank family and friends understanding long evenings/weekends in the lab.